CALCULATIONS OF MAGNETIC VARIATIONS ASSOCIATED WITH INTERNAL OCEAN WAVES

by

H.T. BEAL

B.Sc., University of Victoria, 1968

A THESIS SUBMITTED IN PARTIAL FULFILLMENT

OF THE REQUIREMENTS FOR THE DEGREE OF

MASTER OF SCIENCE

in the Department

of

Physics

We accept this thesis as conforming

to the required standard

[redacted]

Accepted for the Faculty of Graduate Studies

[redacted]

May 13, 1970

April, 1970

ABSTRACT

Supervisor: Dr. J.T. Weaver

In this thesis calculations are obtained for the magnetic field induced by internal waves of periods in the range 1 min--30 min. Solutions for the induced magnetic (and electric) field are derived for a two-layer ocean of finite depth. The results show that the magnitude of the magnetic field associated with internal waves is, in general, less than that induced by the shorter period surface-waves. However, under suitable conditions the magnetic field can become quite appreciable. For instance, an internal wave of amplitude 2 m and period 4 min, located at a depth of 100 m below the sea surface, induces a field of 0.1 γ at 50 m above and below the surface. A similar wave of only 1.5 min period induces the same field at a depth of 100 m below the surface.

[redacted]

TABLE OF CONTENTS

ACKNOWLEDGEMENTS

The author wishes to express his sincere gratitude to Dr. J.T. Weaver for his support and help during this study.

The author also wishes to thank Miss B. Mar for her careful typing of the thesis.

Financial support from the National Research Council of Canada is gratefully acknowledged.

LIST OF FIGURES

CHAPTER 1

INTRODUCTION

1.1 Purpose of the thesis

Sea water is a reasonably good electrical conductor. Consequently, any motion of sea water across the ever present Earth's magnetic field lines induces electric currents within the sea, as originally predicted by Faraday in 1832 (see Hutchins, 1952).

The purpose of this thesis is to discuss the nature of the magnetic field associated with the induced currents generated by subsurface undulations between water layers of different density. These undulations are commonly referred to as internal waves. It is believed that this study will be helpful for the proper interpretation of the measurements of geomagnetic variations taken at sea. Specifically, it is important to understand the nature of this type of "wave noise" before attempting to interpret signals detected at sea, by floating, submerged or airborne magnetometers.

1.2 Summary of previous investigations of the magnetic variations associated with ocean waves

To view this study in its proper perspective, it is necessary to give a brief historical survey of previous studies of the electromagnetic field associated with ordinary surface sea waves. It was established both theoretically and experimentally that surface waves do indeed give appreciable " wave noise " detectable by both submarine and airborne magnetometers. One may, therefore, speculate on the possibility of internal waves having significant electromagnetic effects.

The problem of determing the electric currents induced by ocean waves was considered in some detail by Longuet-Higgins et al. (1954). Crews and Futterman (1962) first calculated the magnetic field above the sea surface arising from currents induced by wind driven waves. They concluded, for example, that a sea-state 5 (1.2 m - 1.8 m wave amplitude) was necessary to give a field of 0.1 γ (the gamma, γ, is a measure of the magnetic flux density in the emu system frequently used in geomagnetism, defined by 1 $\gamma = 10^{-5}$ G or in MKS units 1 γ = 1 nT) at an altitude of 30.5 m. The corresponding calculations for the field below the sea surface were given by Warburton and Caminiti (1964). A sea-state 6 (1.8 m - 3.0 m wave amplitude) was found necessary to give the same field at a depth of 95 m for a 100 m wave. In the above two papers, the magnetic field was obtained by integrating the contributions of all the induced current elements, a procedure which led to some rather cumbersome integrals. However, Weaver (1965) found a much more elegant approach in

which the exact solutions for the magnetic field, both above and within the sea, are simply obtained by solving the differential equations for the magnetic vector directly and applying the usual electromagnetic boundary conditions at the sea surface. Furthermore, his paper showed the importance of ocean swell in generating significant magnetic fields. For instance, an ocean swell of 20 sec period and only 10 cm amplitude induces a magnetic field of 0.2 γ at a depth of 100 m below the surface and a field of 0.1 γ at an altitude of 50 m above the sea. This important fact seems to have been overlooked by Crews and Futterman and by Warburton and Caminiti, for they restricted their discussion to short-period waves. Measurements corroborating Weaver's theoretical results were made by Baker and Graefe (1968) using an airborne magnetometer and by Maclure et al. (1964) using a magnetometer suspended beneath the ocean surface from a buoy. In addition, Weaver pointed out that his approach could easily be extended to give the field for a sea of finite depth (useful in situations where long-period waves are present in shallow waters). This calculation was undertaken by Woods (1965). His results show, however, that little generality is lost by assuming the ocean to be of infinite depth. Nevertheless, Woods' results are helpful in interpreting magnetic signals recorded at the sea bottom. For example, Wynn (1967) obtained good agreement between his recorded magnetic variations, arising from surface waves, at the sea floor and the predicted wave-induced field by applying the theoretical results obtained by Woods (see also Fraser, 1966).

Weaver's study was extended to include the electromagnetic field induced by very long-period ocean waves, Larsen (1970). The model

used by Larsen included a layer of conducting sediments just below the sea floor and further down a conducting mantle. In all cases it was found that the effect of bottom sediments was essentially negligible, but the conducting mantle influenced the electromagnetic field in the frequency range of 1 to 10 cycles per hour for very deep oceans (i.e. 5000 m). For the above frequency range and a wave amplitude of 20 cm the induced magnetic field components were found to be of order 1.5 γ for very deep oceans and of order 0.7 γ for shallow oceans (i.e. 200 m).

Another possibility is whether or not artificially generated gravity waves may induce a time-varying magnetic field of importance. To this end, Weaver and Woods (1965) examined the electromagnetic field of a pressure impulse in a conducting fluid (a moving impulse of this type is the simplest way of describing the so called Kelvin wake of a ship). In addition to the familiar Kelvin wake, however, a ship may produce internal waves, especially if a large discontinuity of density exists just below the sea surface. In such a situation there is also the strong possibility of the presence of naturally occuring internal waves. To estimate the magnetic field associated with such internal waves, Weaver (1966), using a simple two layer ocean of constant electrical conductivity everywhere, found that for a thin upper layer (4 m) an internal wave (amplitude 1 m and of 500 m length) produced a corresponding magnetic signal of about 0.02γ at an altitude of 30 m above the sea surface.

For an ocean having a constant electrical conductivity every-

where and composed of many layers of varying density Larsen (1966), also reported by Cox et al. (1970), found the magnitude of the magnetic field components to be of order 0.1 γ for an internal wave of tidal frequency. However, Larsen evaluated the electromagnetic field components only at the sea floor.

1.3 Description of thesis

In this thesis we choose to examine the magnetic field induced, both above and within a two layer ocean of finite depth, by an internal wave located at the boundary separating the two superposed fluid layers each having a different density and conductivity. This particular model was chosen for three reasons:

(i) It is a reasonably good description of internal waves occuring naturally within the sea and has the advantage of yielding exact solutions of a relatively simple form.

(ii) A finite bottom was chosen to examine the behaviour of the field in shallow waters.

(iii) The model provides an opportunity to study the behaviour of the wave-induced field when the conductivity of the two fluid layers is changed. In both of the two previous papers this effect has not been considered.

We begin in Chapter 2 by giving some background information concerning internal waves; as to their origin, wavelength, period, amplitude and occurence. In Chapter 3 we develop the linearized field equations and boundary conditions necessary for an exact analysis of the problem and point out the limitations imposed by the linearized theory. The general solution for the internal wave-induced magnetic field is obtained in Chapter 4 and, in addition, some useful approximate solutions have been derived from the general solution. Also, the complete solution for the magnetic field arising from a surface wave in the two layer ocean is

presented. The results are discussed, in detail, in Chapter 5.

The results show that the electromagnetic field generated by internal waves, in general, of much smaller magnitude than the field induced by surface waves. However, it is shown that under certain conditions, appreciable " magnetic noise " from internal waves can occur within the sea, and just above the surface.

CHAPTER 2

A BACKGROUND DISCUSSION OF INTERNAL WAVES

2.1 Introduction

In such a non-homogeneous element as the sea, undulations exist between subsurface water layers of varying density which are commonly called internal waves.

Internal waves exist in all oceans and most bays and lakes, and vary widely in amplitude and period. Internal waves have slower speeds than surface waves (ordinary ocean waves) but the amplitude may be much greater. The simplest type of internal wave is shown in Figure 1, where the maximum displacement occurs at the boundary between a homogeneous top layer and the more dense lower layer. The surface displacement caused by the internal wave motion has been greatly exaggerated in relation to the internal wave amplitude as shown in Figure 1.

The theory of internal waves was first developed in 1847 by Stokes (Lamb, 1932) for two superposed fluids. Since internal waves are present at each boundary, it follows that in a stratified ocean (i.e. an ocean composed of many superposed layers of varying density) a great number of internal waves may be present simultaneously. Furthermore, if the density varies continuously with depth, as is the case in nature, an infinite number of internal waves may occur with the maximum vertical displacement in the region of steepest density gradient. Wave motion in a stratified fluid (with or without density discontinuities) has been treated theoretically by Yih (1960). Usually a two or three-layered ocean model is con-

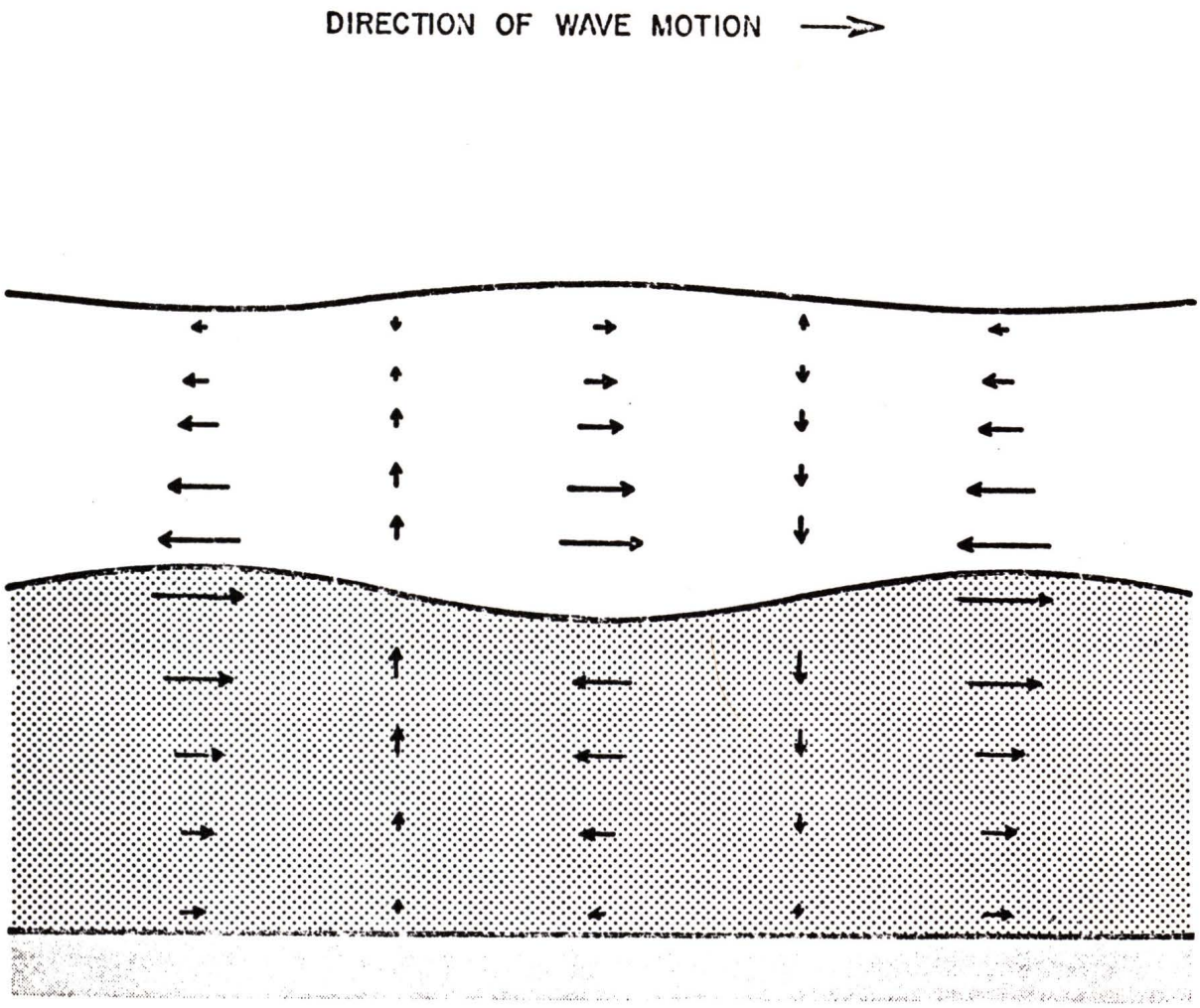

Fig. 1. A schematic representation of an internal wave at the boundary between two fluids of different densities. The arrows indicate the magnitude and the instantaneous direction of the fluid particle velocities.

sidered to examine a property of internal waves or their interaction with beaches, sound waves and so forth.

The exact causes of internal waves are not yet firmly established, but are thought to be of varied origin.

2.2 The density distribution

We shall now discuss, very generally, the main factors which influence the vertical density distribution within the sea. From this brief discussion, it may be seen that the ocean is naturally stratified, hence internal waves may occur frequently.

The density of seawater continuously increases by about 0.0045 g/cm^3 for every 1000 m increase in depth, to a maximum value of approximately 1.07 g/cm^3 (Fairbridge, 1966). While in such an ocean where the density is solely a function of pressure no internal waves can exist, energy may still be transmitted by acoustic waves. However, the density also depends on the temperature and salinity (total concentration of dissolved salts, expressed in parts per thousand by weight) of seawater. The density gradients are thus linked to temperature and salinity gradients. Relatively steep gradients of temperature (thermocline) and salinity (halocline) are quite common and normally coincide, see Figure 2. The relationship between density, salinity, temperature and the electrical conductivity is shown in Figure 3.

Roughly the sea may be divided into four layers, separated by three transition regions where the density changes relatively quickly. The change in density is mainly due to the differences in temperature. The three thermoclines are, in order of descending depth, the diurnal, seasonal and main thermocline. The diurnal thermocline has a depth between 6 m to 10 m with a corresponding temperature change of 1 to 2 $^{\circ}C$ across it. The main cause is the daily heating effects of the sun.

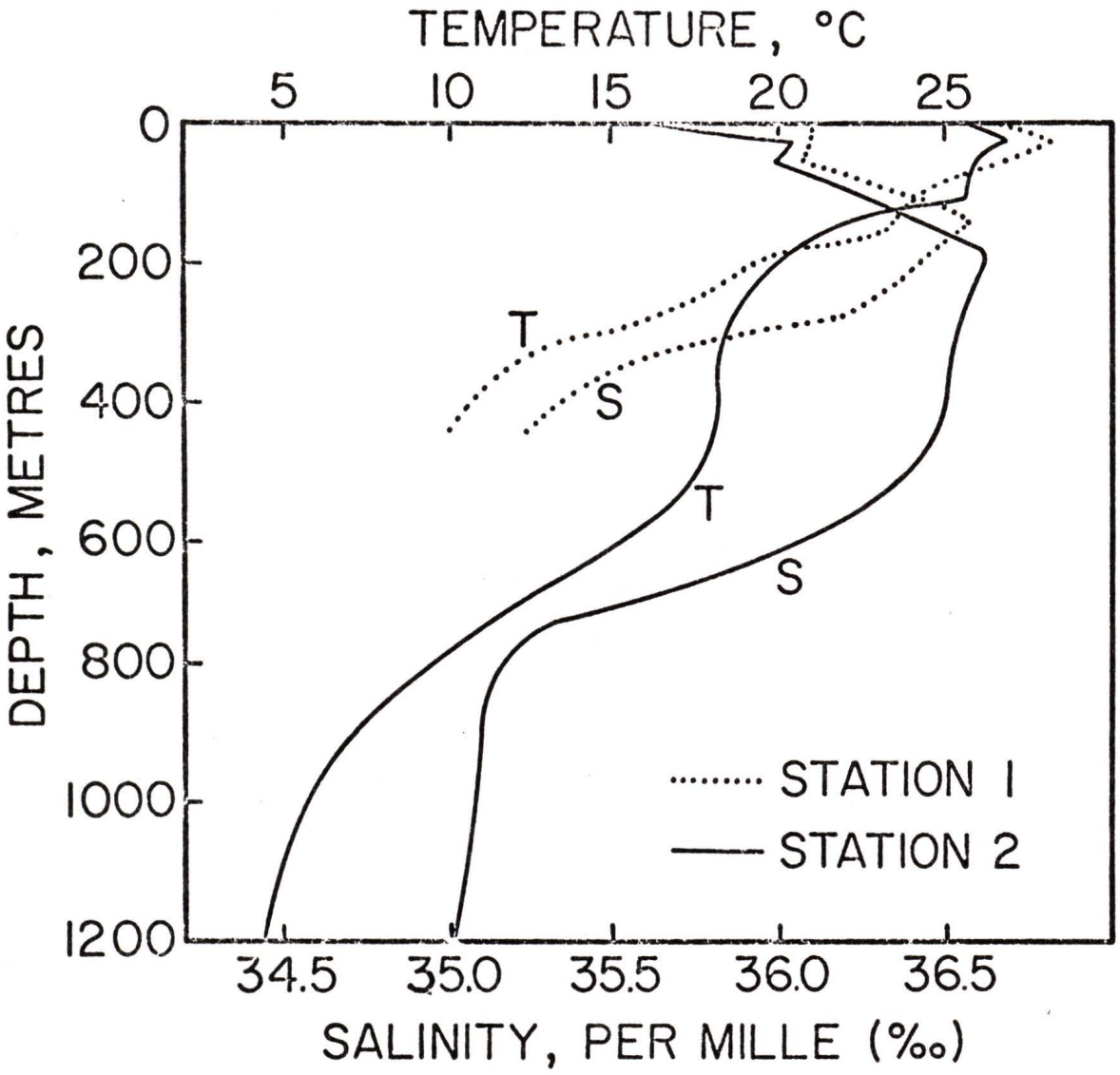

Fig. 2. Temperature and salinity at two stations off Onslow Bay plotted against depth (after Sverdrup et al., 1942).

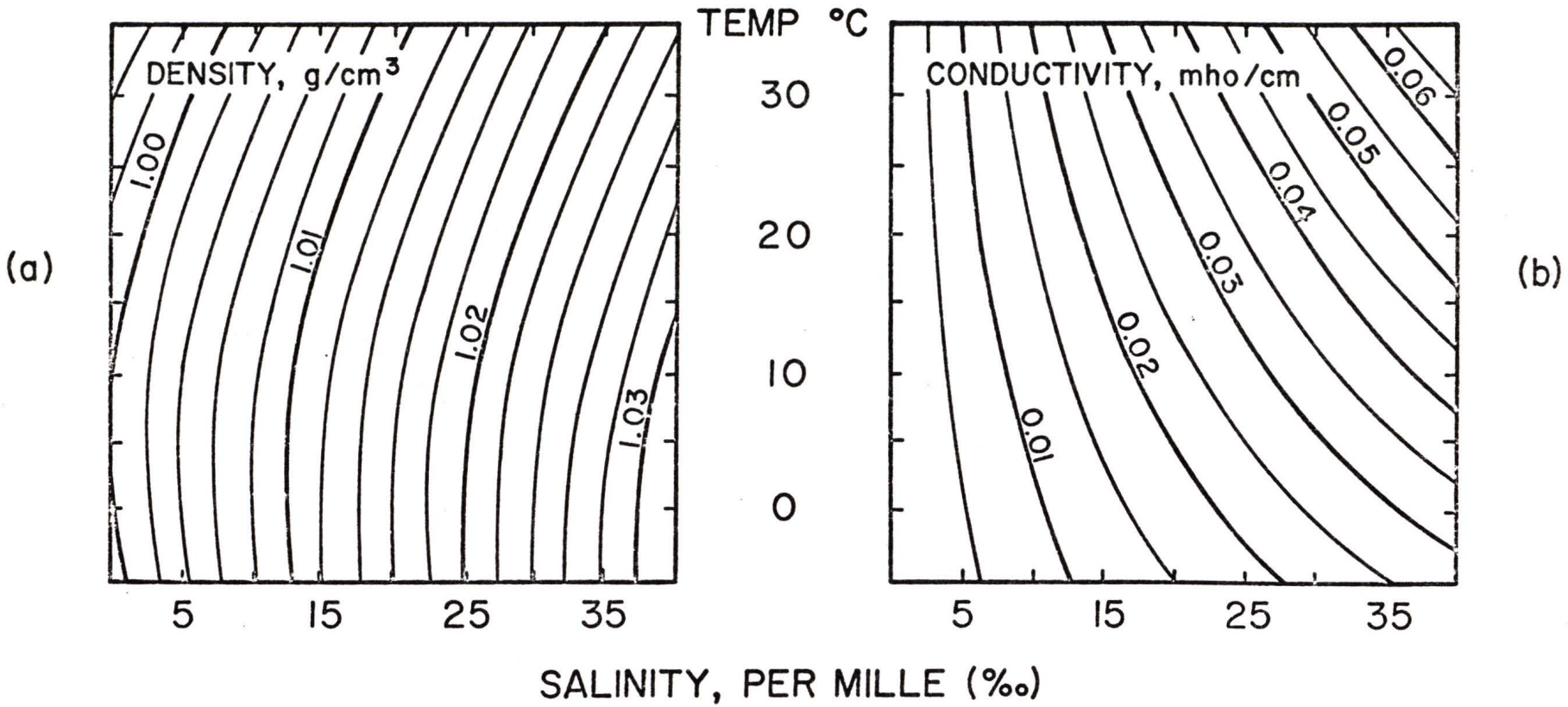

Fig. 3. Temperature-salinity diagrams for sea water at 1 atm pressure: (a) density (Knudsen, 1963), (b) conductivity (Thomas et al., 1963).

Prolonged heating gives rise to the seasonal thermocline, which is most clearly marked towards the end of the summer months. It has as much as a 5 to 10° C temperature change across the transition region at a depth between 50m to 100 m. Finally, the main thermocline, separating the deep ocean waters from the upper water masses, lies somewhere between 300 m and 1000 m with a temperature difference of 10 to 20° C across it. Moving towards the colder latitudes, this temperature distribution gradually disappears and the sea tends to one constant temperature.

In addition, local meteorological conditions, the vicinity of land masses and subsurface currents may also greatly influence the distribution of density within the sea. For instance, Parker (1968) observed a homogeneous surface layer up to 100 m thick, apparently due to a cold air outbreak over the Gulf of Mexico. The density may be decreased by the addition of melt-water from ice or run-off from land. In the Arctic waters and near the mouths of some Norwegian fiords a thin top layer of nearly fresh water is formed by this process. This situation gave rise to the " dead water " phenomenon (Ekman, 1904). It was observed at times that vessels moving in these waters behaved very sluggishly. Ekman established that slowly moving vessels created internal waves at the surface of density discontinuity, so that the energy otherwise used for propulsion now went into the generation of internal waves. Excess precipitation and heating in equatorial regions often produces a homogeneous surface layer with a well defined lower boundary, especially after the surface layer has been well stirred by wind action (Munk and Anderson, 1948). When a surface layer of density greater then the water mass below

is formed (e.g. in regions where evaporation is dominant), an instability is formed. If this condition persists then the heavier water must sink until it encounters water of equal density. This gives rise to vertical convection currents which may form a new homogeneous layer after they have been active some time. Subsurface currents can sometimes cause a denser layer of sea water to overlie a less dense layer, and again vertical convection currents can result. The vertical currents may well have been responsible for the stratification observed by Tait and Howe (1968) midway between Cape St. Vincent and Madeira. They found, at a depth between 1280 m and 1500 m, nine descrete temperature and salinity steps of the order of 0.25°C and 0.044°/oo, ranging in thickness from 15 m to 30 m.

Since temperature measurements are easily accomplished and the salinity gradient is usually much less than the temperature gradient, internal waves are usually observed by recording the temperature fluctuations caused by the periodic vertical displacements of the isotherms, Figure 4. However, care must be taken when interpreting temperature fluctuations because variations of temperature may also be caused by horizontal currents. (Helland-Hansen, 1930 and Voorhis and Perkins, 1966),

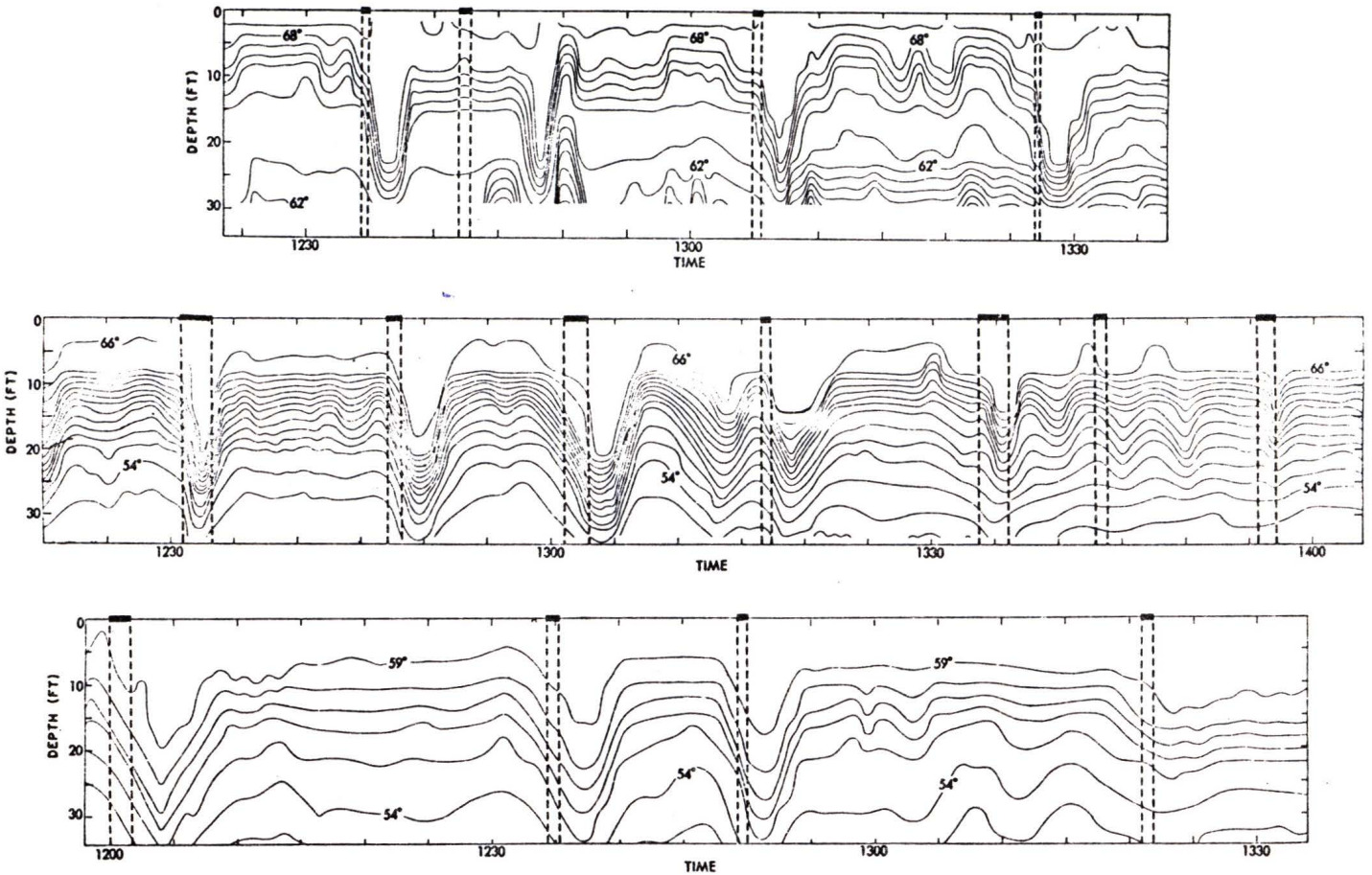

Fig. 4. Observed isotherms of internal wave motions. The most common location of the slicks is indicated by the heavy bars (LaFond, 1966).

2.3 Observed features of internal waves

Ekman (1904) first suggested that internal waves occurred in the sea. For the purposes of this thesis, we will be mainly concerned with the properties of short-period internal waves (i.e. periods from 1 sec to 30 min) for reasons given in sections 3.2 and 3.5. Observations of internal waves of tidal character (i.e. waves with periods ranging from hours to several days) up to 1956 have been summarized by Davis and Patterson (1956). Later observations have been obtained by Summers and Emery (1963), Rainer et al. (1967) and Zalkan (1969).

Valdez (1960) and Chindonova and Shulepov (1965) observed internal waves on their echo sounder records due to sound waves reflected off layers of small organisms undergoing periodic motion from the internal wave train. Chindonova and Shulepov observed 19 internal waves, taken in the Atlantic Ocean. Three of the waves occurred in the 100 m - 400 m depth range with amplitudes between 5 m to 50 m, all three waves had an apparent wavelength of 3200 m. Unfortunately, the true wavelength was not known since the direction and propagation rate of the waves was undetermined. These observations seem to indicate that large amplitude internal waves with relatively short periods are possible within the sea. Furthermore, large scale internal waves with relatively short periods have also been observed near Indonesia (Perry and Schimke, 1965). The maximum amplitude observed was 40 m with a wavelength of about 2000 m. This motion occurred between two nearly homogeneous layers (density 1.021 g/ cm^3 and temperature 28° C for the upper layer, and a density

1.026 g/cm^3 with a temperature of 14° C for the lower layer).

Visible evidence of the presence of internal waves is often given by sea-surface slicks. Slicks are long streaks or patches of relatively calm surface water surrounded by rippled water. They are formed by the rippled-damping action of a surface film of organic matter. The ability of films to dampen ripples varies radically with the degree of compation of the film molecules. Such compaction can be produced by wind stress or by a horizontally convergent flow produced by internal waves (Ewing, 1950). LaFond (1966) found that 10% of his observed internal waves had surface-slicks associated with them, and that in 85 out of 105 such cases, the slick was located between the crest and the trough of the internal waves (Figure 4). Slick-type phenomena have also been observed in the Georgia Strait and the mainland inlets of British Columbia. Pickard (1954) and Shand (1953) observed streaks which appeared to be associated with the internal wave motion having wavelengths of 900 m with periods of about 20 min. Shand noted that the speed of the internal wave was about 75 cm/sec. Later, Pickard (1961) recorded internal waves, approximately 4 m to 8 m below the surface, with amplitudes up to 5 m and periods from 1 - 4 min.

LaFond (1963) made a series of experiments on the characteristics of internal waves off San Diego in water 18 m deep. Average wave period, speed and amplitude observed were 7.3 min, 15 cm/sec and 0.85 m respectively. The thermocline was located at about 5 m below the surface. Again in the same area Armstrong and LaFond (1966) made further obser-

vations and found that the average period and amplitude was 7.2 min and 0.82 m respectively. Some of the internal waves had a period of 10 min with an amplitude of 2.5 m. Also near San Diego, Ufford (1947) measured two internal waves which had periods of 12 and 16 min, wavelengths of 130 m and 330 m, and amplitudes 1.52 m and 2.28 m. On the opposite coast Gaul (1961) observed internal waves near Hudson Canyon (off the coast of New York) in water 56 m deep. The internal waves had nominal periods of several minutes travelling at an average speed of 50 cm/sec. He also mentions that for purposes of a two-layer calculation the salinity, temperature and density could be taken to be 31.5 and 32.5°/oo, 20 and 10° C, 1.0225 and 1.0247 g/cm^3 for the upper and lower layer respectively. The thickness of the upper layer was approximately 20 m. While measuring undercurrents in the Equatorial Atlantic region, Metcalf et al. (1962) observed small scale structure on their records which they attributed to internal waves. The estimated velocity was 50 cm/sec, with a wavelength of 500 m and a period of 17 min. The average amplitude was 5 m with the maximum density gradient between 40 to 100 m below the surface. The average salinity was about 35.5°/oo with the temperature 27° C and 14° C just above and below the density gradient.

In summary, we note that the period and amplitude of internal waves usually differ appreciably from those commonly found in surface waves. For example, surface waves have periods in the 1 - 30 sec range with 50% of the waves having amplitudes less than 0.6 m and only 10% having amplitudes greater than 3 m (Kinsman, 1965), while internal waves generally have periods of the order of minutes and amplitudes greater

than 0.6 m. Furthermore, wavelengths of 250 m or more are common for internal waves, but large amplitude surface waves of this wavelength only occur during heavy gales. Most surface waves whose wavelengths are comparable to those of internal waves are ocean swells which usually have extremely small amplitudes.

2.4 Generation of internal waves

There are a number of different mechanisms available for the generation of internal waves. Most of these are due to natural causes, but their artificial production by ships has also been observed, by Ekman (1904). He showed experimentally that a vessel moving near the critical internal wave velocity (i.e. the velocity of waves for which the wavelength is large compared to the thickness of the surface layer) strongly excites internal waves, provided the keel depth is near the boundary of the density discontinuity. The internal wave system generated by a ship in a two layer ocean was theoretically investigated by Hudimac (1961).

Sources of natural origin include seismic disturbances on the ocean floor. Fedosenko and Cherkesov (1969) treated long and short waves on the free and division surface resulting from such disturbances. Again, just as surface waves can be developed by atmospheric pressure fluctuations, so can internal waves be generated by slowly varying atmospheric disturbances. However, these waves tend to have long periods and wavelengths corresponding to the scale of the slowly moving force (Proudman, 1953 and Krauss, 1959). Phillips (1966) mentions that under appropriate conditions, internal waves of significant amplitude can be developed this way. Another cause of internal waves is a strong shear, developed when two layers of different density flow in opposite directions. This unstable situation, at the common boundary, may be a source of growing internal waves as well as turbulence (Proudman, 1953 and Miles, 1961

and 1963). Pickard (1961), Metcalf et al. (1962) and, Perry and Schimke (1965) all attributed the observed internal waves to the strong shear flow. On the other hand, a weak shear has the effect of reducing the frequency and vertical scale of small scale internal wave motions (Phillips, 1966).

If the surface of density discontinuity lies near the ocean bottom, then bottom topography will effect the behaviour of internal waves (Sandstrom, 1966). Zeilon (1913) first demonstrated that long surface waves on passing over bottom irregularities (in a stratified ocean) can generate internal waves. For example, Proudman (1953) proved analytically that a long surface wave passing over a thin vertical barrier rising from the bottom and just reaching up to the surface of separation of the two layers may give rise to an internal wave. Furthermore, Zeilon (1934) demonstrated that the incidence of a surface tide upon the continental shelf (which often rises to the level of the density discontinuity) results in the production of internal waves. At the transition region between the deep and shallower water, the oscillatory fluid motion from the surface wave suddenly encounters the shallower bottom which results in a disturbance creating the internal wave. Rattray (1960) gave a simple analysis of this problem using a two layer ocean. He found that the internal wave behaved as a standing wave in the coastal region and that further offshore it was a progressive wave travelling seawards. Weigand et al. (1969) further found that long surface waves (i.e. wavelengths long compared with the shelf width) may also generate internal waves by this mechanism. In addition, frictional effects may decrease

the amplitude and change the character of the standing wave to that of a progressive wave propagating coastwards. Model studies gave favourable results with the theoretical predictions. Moreover, an undulating ocean floor with a current flowing over it can produce a train of standing waves in a stratified fluid (Long, 1953, 1954, and 1955). However, if the current is oscillatory (e.g. due to the presence of long or tidal waves), internal waves of a progressive nature can result.

Yet another mechanism arises from the interaction between surface and internal waves. The simplest situation occurs when the fluid motion due to a long surface wave, induces an internal wave at a density discontinuity beneath the surface. Cox and Sandstrom (1962) have analysed the coupling between long surface waves and internal waves in water of variable depth. On the other hand, when two surface waves interact at second order, a bounded disturbance results which may interact with an internal wave and cause amplification. A similar situation can occur when two internal waves interact and transfer energy into a third internal wave (Ball, 1964, Thorpe, 1966 and Phillips, 1966). Thorpe has indicated that under certain conditions internal waves could possibly be generated in this manner. Kenyon (1968) used oceanographic measurements to evaluate the energy transfer rates for the above two processes. Generally the energy transfer rates for mutual internal wave interactions are much larger than for the surface - internal wave interactions. Both interactions are strongest in highly stratified water whose depth is shallow compared with the wavelength.

In summary we see that the above mechanisms when combined with

the varied distributions of density within the sea, can produce complex internal wave motion. Consequently the induced electromagnetic effects arising from such motion of sea water, across the Earth's magnetic field lines can be very complicated. However, by assuming a reasonably simple mathematical model, we can obtain an explicit solution for the magnetic field induced by internal and surface waves, as is shown in the following chapter.

CHAPTER 3

THE FIELD EQUATIONS

3.1 The mathematical model

We shall investigate an ocean consisting of two homogeneous, incompressible fluid layers of different densities in a rectangular coordinate system. The z axis is directed downwards into the sea, with the plane $z = 0$ representing the mean free surface and $z = L$ the ocean floor. The plane $z = D$ divides the ocean into an upper and lower layer of densities ρ_1 and ρ_2 respectively. We assume that the ratio of the density in region $D < z < L$ to the density in region $0 < z < D$ is α (i.e. $\alpha = \rho_2/\rho_1 \geq 1$). The earth's atmosphere occupies the half space $z < 0$ and the earth's crust fills the space $z > L$.

A progressive harmonic internal wave causes the lower surface of density discontinuity to undergo harmonic oscillations of amplitude $|a_2|$, say, so that its equation is $z = D + \eta_2$ where η_2 is the instantaneous vertical displacement. The presence of the internal wave causes the mean free surface to undergo a similar harmonic motion of amplitude $|a_1|$ with the equation $z = \eta_1$ where η_1 is the instantaneous vertical surface displacement. The irrotational fluid motion resulting from the above displacements will be specified by velocity potentials ϕ_1 and ϕ_2 in regions $0 < z < D$ and $D < z < L$ respectively. The x axis is defined to be along the direction of wave propagation, and the y axis perpendicular to the wave profile to form a right-handed triad. Denote by $\underline{i}$, $\underline{j}$ and $\underline{k}$

the three unit vectors along the coordinate axes.

We assume that the earth's magnetic field $\underline{F}$ is constant everywhere. Thus the model will be two dimensional, all quantities being independent of the variable y. We may write

$$\underline{F} = F(\cos I \cos\theta\, \underline{i} - \cos I \sin\theta\, \underline{j} + \sin I\, \underline{k}) \quad (3.1.1)$$

where I is the angle of dip and θ is the eastward inclination of direction of wave propagation from the magnetic meridian. The mathematical model is illustrated in Figure 5.

The electromagnetic system of units (emu) will be used, so that the magnetic induction is identical with the magnetic field everywhere because air, seawater and the earth's crust all have very nearly the free space values of permeability. The electrical conductivity of seawater and the earth's crust is at least nine orders of magnitude greater than that of air, therefore, the electrical conductivity of air is set to zero (i.e. $\sigma_o = 0$).

In the following analysis we shall make use of a subscript j to denote to which layer of the model a quantity belongs. The subscript j has the values 0, 1, 2 and 3 designating the regions $z < 0$, $0 < z < D$, $D < z < L$ and $z > L$ respectively, this notation is in agreement with quantities already subscripted. When the values of j are not explicitly written out, it is understood that j ranges over all its allowed values. We must keep in mind that $\phi_o = \phi_3 = 0$ and $\sigma_o = 0$.

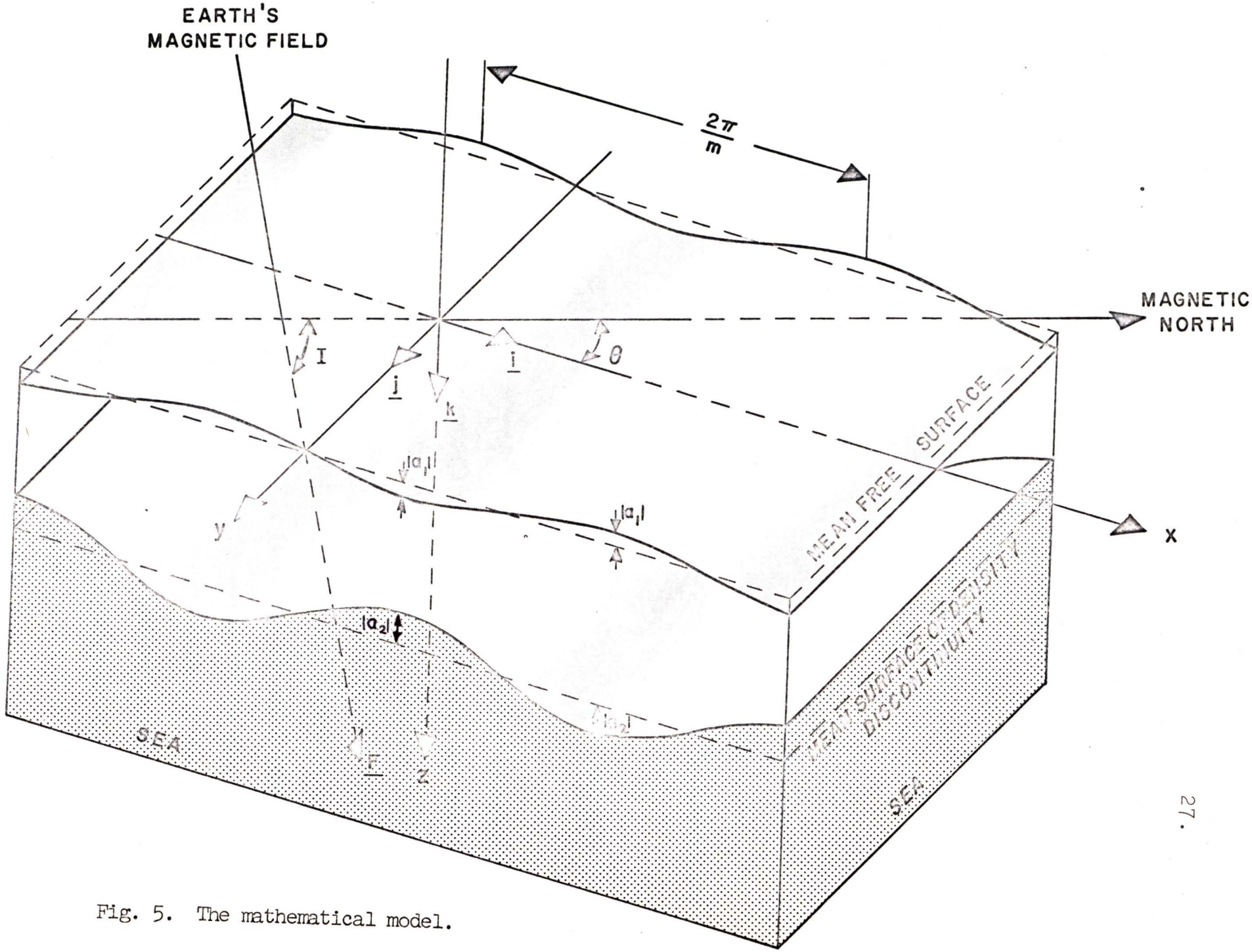

Fig. 5. The mathematical model.

3.2 The basic equations

The continuity equation expressing the conservation of mass of the fluid reduces to the Laplace equation

$$\nabla^2 \phi_j = 0 \quad , \quad j = 1, 2 \tag{3.2.1}$$

when the density ρ_j is constant.

We denote by p_j the excess pressure of the fluid above atmospheric pressure. This means, for instance, that at the surface $z = \eta_1$ the pressure is zero (i.e. $p_1 = 0$). The pressure p_j is given by Bernoulli's equation.

$$\partial \phi_j / \partial t + \tfrac{1}{2} (\nabla \phi_j)^2 - gz + p_j / \rho_j = c_j \quad , \quad j = 1, 2 \tag{3.2.2}$$

where g is the gravity field strength, and c_j is a constant of integration. The Coriolis force, due to the earth's rotation of period T_e, has been neglected. The ratio of the Coriolis force and the acceleration of the fluid particles caused by the wave motion with period T is proportional to $2T/T_e$, and this quantity is of order 10^{-2} for a wave period of about 1/2 hour. Thus the Coriolis force is only important for waves with periods of more than half an hour. We do not consider such waves in this thesis. Furthermore, the ratio of the electromagnetic body force and the force of gravity is proportional to $\sigma v F^2 / \rho g$ where σ and v are the conductivity of seawater and the fluid particle speed respectively (Longuet-Higgins et al., 1954). Taking F = 0.5 gauss, v = 50 cm/sec, $\sigma = 4 \times 10^{-11}$ emu, $\rho = 1.0$ g/cm^3 and $g = 1 \times 10^3$ cm/sec we find that the ratio is of order

5×10^{-13}. Thus the electromagnetic body force is entirely neglible for seawater.

The electric and magnetic vectors $\underline{E}_j$ and $\underline{H}_j$ respectively, due to the induction effect of the periodic fluid motion across the magnetic field lines, satisfy Maxwell's equations in the form

$$\text{CURL } \underline{E}_j = -\partial \underline{H}_j / \partial t \quad , \tag{3.2.3}$$

$$\text{CURL } \underline{H}_j = 4\pi \sigma_j \{ \underline{E}_j + \nabla \phi_j \times (\underline{F} + \underline{H}_j) \} + k_j \partial \underline{E}_j / c^2 \partial t \quad . \tag{3.2.4}$$

Here σ_j and k_j are the electrical conductivity and the dielectric constant respectively and c denotes the speed of light. Taking the divergence of (3.2.3) , we obtain

$$\text{div } \underline{H}_j = 0 \tag{3.2.5}$$

This result simplifies the identity

$$\text{CURL CURL } \underline{H}_j = \text{GRAD div } \underline{H}_j - \nabla^2 \underline{H}_j$$

to

$$\text{CURL CURL } \underline{H}_j = -\nabla^2 \underline{H}_j \quad . \tag{3.2.6}$$

Hence, by taking the curl of (3.2.4) and using (3.2.3) and (3.2.6), we obtain the differential equation satisfied by $\underline{H}_j$,

$$\nabla^2 \underline{H}_j = 4\pi\sigma_j \{ \partial \underline{H}_j/\partial t - \text{CURL}[\nabla\phi_j \times (\underline{F} + \underline{H}_j)] \}$$

$$+ k_j \partial^2 \underline{H}_j / c^2 \partial t^2 \quad . \qquad (3.2.7)$$

We expand the second term on the right hand side of (3.2.7) to give

$$\text{CURL}[\nabla\phi_j \times (\underline{F} + \underline{H}_j)] = \nabla\phi_j \, \text{div}(\underline{F} + \underline{H}_j) - (\underline{F} + \underline{H}_j)\nabla^2\phi_j$$

$$+ [(\underline{F} + \underline{H}_j)\cdot\nabla]\nabla\phi_j - [\nabla\phi_j \cdot \nabla](\underline{F} + \underline{H}_j) \, ,$$

which after substitution of(3.2.1) and (3.2.5) reduces to

$$\text{CURL}[\nabla\phi_j \times (\underline{F} + \underline{H}_j)] = [(\underline{F} + \underline{H}_j)\cdot\nabla]\nabla\phi_j - [\nabla\phi_j \cdot \nabla]\underline{H}_j \, .$$

Thus the differential equation (3.2.7) takes the form

$$\nabla^2 \underline{H}_j = 4\pi\sigma_j \{ \partial \underline{H}_j/\partial t - [(\underline{F} + \underline{H}_j)\cdot\nabla]\nabla\phi_j + [\nabla\phi_j \cdot \nabla]\underline{H}_j \}$$

$$+ k_j \partial^2 \underline{H}_j / c^2 \partial t^2 \quad . \qquad (3.2.8)$$

3.3 Linearization of the basic equation

It is postulated that ϕ_j may be expanded in the form

$$\phi_j = \epsilon \phi_j^{(1)} + O(\epsilon^2) \quad , \quad j = 1,2 \tag{3.3.1}$$

(Wehausen and Laitone, 1960) and where ϵ is a small non-dimensional parameter. As we shall see in section 4.6, ϵ is chosen to be the amplitude to wavelenght ratio of the fluid oscillations, and provided this is small the linearized theory will be valid. This is a natural condition since in practice it is unusual to meet waves of heights exceeding one tenth their wavelength (Sverdrup and Munk, 1947). We also assume that η_j, $\underline{H}_j$ and $\underline{E}_j$ may be expanded in powers of ϵ as follows

$$\eta_j = \eta_j^{(0)} + \epsilon \eta_j^{(1)} + O(\epsilon^2) \quad , \quad j = 1,2 \tag{3.3.2}$$

$$\underline{H}_j = \underline{H}_j^{(0)} + \epsilon \underline{H}_j^{(1)} + O(\epsilon^2) \quad , \tag{3.3.3}$$

$$\underline{E}_j = \underline{E}_j^{(0)} + \epsilon \underline{E}_j^{(1)} + O(\epsilon^2) \quad . \tag{3.3.4}$$

Substituting these expressions for $\underline{H}_j$ and ϕ_j into (3.2.8) and equating like powers of ϵ together with discarding terms $O(\epsilon^2)$, we find

that $\underline{H}_j^{(o)}$ and $\underline{H}_j^{(1)}$ satisfy respectively

$$\nabla^2 \underline{H}_j^{(o)} = (4\pi\sigma_j \partial/\partial t + k_j \partial^2/c^2\partial t^2)\, \underline{H}_j^{(o)} \,, \tag{3.3.5}$$

$$\nabla^2 \underline{H}_j^{(1)} = (4\pi\sigma_j \partial/\partial t + k_j \partial^2/c^2\partial t^2)\, \underline{H}_j^{(1)}$$

$$-4\pi\sigma_j \{[(\underline{F} + \underline{H}_j^{(o)})\cdot\nabla]\nabla\phi_j^{(1)} - [\nabla\phi_j^{(1)}\cdot\nabla]\underline{H}_j^{(o)}\} \,. \tag{3.3.6}$$

3.4 Boundary conditions

The pertinent boundary conditions in this model are of both fluid dynamical and electromagnetic nature.

From fluid dynamics it is required that

(a) the pressure is continuous across a surface of density discontinuity; and

(b) any fluid particle which is on a boundary surface must remain on it.

The electromagnetic boundary conditions we shall use are

(c) that the magnetic field is continuous across a surface of discontinuity (because in this problem the magnetic induction and the magnetic field are identical) and that the tangential electric field is likewise continuous; and

(d) the magnetic field vector must vanish at infinity.

The constants c_1 and c_2 appearing in (3.2.2) are evaluated by considering the special case of a fluid completely at rest (i.e. $\phi_j = \eta_j = 0$) and applying boundary condition (a). This gives $p_1 = 0$ at $z = 0$ so that (3.2.2) shows that $c_1 = 0$. Similarly at $z = D$, boundary condition (a) requires that $p_1 = p_2$, thus we find that $c_2 = (\rho_1/\rho_2 - 1)gD$.

Returning to a fluid in motion, we may expand the term $\partial \phi_1 / \partial t$ evaluated at $z = \eta_1$ as a Taylor series about $z = 0$, to give

$$[\partial\phi_1/\partial t]_{z=\eta_1} = [\partial\phi_1/\partial t]_{z=0} + (\eta_1/1!)[\partial^2\phi_1/\partial z\partial t]_{z=0} + \cdots .$$

Substituting in this expansion the expressions for ϕ_1 and η_1 as defined by (3.3.1) and (3.3.2) respectively, we then obtain

$$[\partial\phi_1/\partial t]_{z=\eta_1} = \epsilon[\partial\phi_1^{(1)}/\partial t + \eta_1^{(0)}\partial^2\phi_1^{(1)}/\partial z\partial t]_{z=0} + O(\epsilon^2) .$$

This can, in turn, be substituted in equation (3.2.2), evaluated at $z = \eta_1$. Boundary condition (a) again requires that $p_1 = 0$, whence it follows that

$$\epsilon[\partial\phi_1^{(1)}/\partial t + \eta_1^{(0)}\partial^2\phi_1^{(1)}/\partial z\partial t]_{z=0} - g[\eta_1^{(0)} + \epsilon\eta_1^{(1)}] + O(\epsilon^2) = 0 .$$

Here we have again expanded η_1 and ϕ_1 according to (3.3.2) and (3.3.1) respectively. Equating like powers of ϵ we obtain, after discarding terms $O(\epsilon^2)$,

$$\eta_1^{(0)} = 0 \quad ,$$

$$[\partial\phi_1^{(1)}/\partial t]_{z=0} - g\eta_1^{(1)} = 0 \quad . \qquad (3.4.1)$$

The boundary condition (a) applied at $z = D + \eta_2$ requires $p_1 = p_2$ there, where by Bernoulli's equation (3.2.2) with $j = 1$

$$[p_1]_{z=D+\eta_2} = \rho_1 g(D+\eta_2) - \rho_1[\partial\phi_1/\partial t + \tfrac{1}{2}(\nabla\phi_1)^2]_{z=D+\eta_2}$$

and with $j = 2$

$$[P_2]_{z=D+\eta_2} = \rho_2 g(D+\eta_2) - \rho_2[\partial\phi_2/\partial t + \tfrac{1}{2}(\nabla\phi_2)^2]_{z=D+\eta_2} + \rho_2(\rho_1/\rho_2 - 1)gD .$$

Equating the two expressions, we obtain

$$(\rho_2-\rho_1)g\eta_2 = [\rho_2\partial\phi_2/\partial t - \rho_1\partial\phi_1/\partial t + \tfrac{1}{2}\rho_2(\nabla\phi_2)^2 - \tfrac{1}{2}\rho_1(\nabla\phi_1)^2]_{z=D+\eta_2} .$$

Expanding the partial derivatives about $z = D$, i.e.

$$[\partial\phi_{1,2}/\partial t]_{z=D+\eta_2} = [\partial\phi_{1,2}/\partial t]_{z=D} + (\eta_2/1!)[\partial^2\phi_{1,2}/\partial z\partial t]_{z=D} + \cdots .$$

Then substitute this into the previous equation and using the expansions (3.3.1) and (3.3.2) for $\phi_{1,2}$ and η_2 respectively we now have

$$(\rho_2-\rho_1)[\eta_2^{(0)} + \epsilon\eta_2^{(1)}]g = \epsilon[(\partial/\partial t + \eta_2^{(0)}\partial^2/\partial z\partial t)(\rho_2\phi_2^{(1)} - \rho_1\phi_1^{(1)})]_{z=D}$$

where terms of order ϵ^2 have been discarded. Equating coefficients of powers of ϵ, we obtain

$$\eta_2^{(0)} = 0 ,$$

$$(\rho_2-\rho_1)g\eta_2^{(1)} = [\partial(\rho_2\phi_2^{(1)} - \rho_1\phi_1^{(1)})/\partial t]_{z=D} . \qquad (3.4.2)$$

We now consider boundary condition (b). Let the equation of a boundary surface be $S(x,z,t) = 0$. This equation may be regarded as describing the position of the fluid particles lying on the surface and the boundary condition requires these particles to remain on the surface. Thus the total rate of change of position of such particles relative to the surface must vanish, i.e.

$$dS/dt = 0 .$$

Expanding the total derivative of S, we arrive at

$$\partial S/\partial t + (\partial S/\partial x)(dx/dt) + (\partial S/\partial z)(dz/dt) = 0 \qquad (3.4.3)$$

where dx/dt and dz/dt are respectively the x and z components of the velocity of the surface particles, i.e. $dx/dt = [\partial \phi_j/\partial x]_{S=0}$ and $dz/dt = [\partial \phi_j/\partial z]_{S=0}$. The equations of the three boundary surfaces are;

$$S_1 \equiv z - \eta_1 = 0 ,$$

$$S_2 \equiv z - (D + \eta_2) = 0 ,$$

$$S_3 \equiv z - L = 0 .$$

Putting $S = S_1$ in (3.4.3) we obtain

$$\partial \eta_1/\partial t + (\partial \eta_1/\partial x)[\partial \phi_1/\partial x]_{z=\eta_1} - [\partial \phi_1/\partial z]_{z=\eta_1} = 0 .$$

Similarly, when $S = S_2$ we have the two equations

$$\partial\eta_2/\partial t + (\partial\eta_2/\partial x)\left[\partial\phi_1/\partial x\right]_{z=D+\eta_2} - \left[\partial\phi_1/\partial z\right]_{z=D+\eta_2} = 0 ,$$

$$\partial\eta_2/\partial t + (\partial\eta_2/\partial x)\left[\partial\phi_2/\partial x\right]_{z=D+\eta_2} - \left[\partial\phi_2/\partial z\right]_{z=D+\eta_2} = 0 ,$$

since (3.4.3) applies both just above and below the surface $S_2 = 0$. Finally, when $S = S_3$, we have

$$\left[\partial\phi_2/\partial z\right]_{z=L} = 0 .$$

When $\eta_{1,2}$ and $\phi_{1,2}$ are replaced by their expansions (3.3.2) and (3.3.1) respectively, the above four equations become

$$\epsilon\partial\eta_1^{(1)}/\partial t - \epsilon\left[\partial\phi_1^{(1)}/\partial z\right]_{z=\eta_1} + O(\epsilon^2) = 0 ,$$

$$\epsilon\partial\eta_2^{(1)}/\partial t - \epsilon\left[\partial\phi_1^{(1)}/\partial z\right]_{z=D+\eta_2} + O(\epsilon^2) = 0 ,$$

$$\epsilon\partial\eta_2^{(1)}/\partial t - \epsilon\left[\partial\phi_2^{(1)}/\partial z\right]_{z=D+\eta_2} + O(\epsilon^2) = 0 ,$$

$$\epsilon\left[\partial\phi_2^{(1)}/\partial z\right]_{z=L} + O(\epsilon^2) = 0 .$$

The terms $\partial\phi_{1,2}^{(1)}/\partial z$ are expanded about the undisturbed surfaces $z = 0$ and $z = D$ in exactly the same way that we expanded $\partial\phi_{1,2}/\partial z$ previously. If these terms are then substituted into the above equations and terms $O(\epsilon^2)$ discarded, then we arrive at, the linear boundary conditions

$$\left[\partial\phi_1^{(i)}/\partial z\right]_{z=0} = \partial\eta_1^{(i)}/\partial t \quad , \tag{3.4.4}$$

$$\left[\partial\phi_1^{(i)}/\partial z\right]_{z=D} = \partial\eta_2^{(i)}/\partial t \quad , \tag{3.4.5}$$

$$\left[\partial\phi_2^{(i)}/\partial z\right]_{z=D} = \partial\eta_2^{(i)}/\partial t \quad , \tag{3.4.6}$$

$$\left[\partial\phi_2^{(i)}/\partial z\right]_{z=L} = 0 \quad . \tag{3.4.7}$$

Furthermore the electromagnetic boundary condition (c) demands that

$$\left[\underline{H}_0 - \underline{H}_1\right]_{z=\eta_1} = 0 \quad ,$$

$$\left[\underline{H}_1 - \underline{H}_2\right]_{z=D+\eta_2} = 0 \quad ,$$

$$\left[\underline{H}_2 - \underline{H}_3\right]_{z=L} = 0 \quad .$$

Expansion of the magnetic vectors as a Taylor series about the surfaces z = 0 and z = D yields

$$\left[\underline{H}_0 - \underline{H}_1\right]_{z=0} + (\eta_1/1!)\left[\partial(\underline{H}_0 - \underline{H}_1)/\partial z\right]_{z=0} + \cdots = 0 \quad ,$$

$$\left[\underline{H}_1 - \underline{H}_2\right]_{z=D} + (\eta_2/1!)\left[\partial(\underline{H}_1 - \underline{H}_2)/\partial z\right]_{z=D} + \cdots = 0 \quad .$$

We now substitute the expansions (3.3.2) and (3.3.3) for η_j and $\underline{H}_j$ respectively in the above three equations and after equating like powers of ε obtain

$$[\underline{H}_0^{(0)} - \underline{H}_1^{(0)}]_{z=0} = 0 \quad , \tag{3.4.8}$$

$$[\underline{H}_1^{(0)} - \underline{H}_2^{(0)}]_{z=D} = 0 \quad , \tag{3.4.9}$$

$$[\underline{H}_2^{(0)} - \underline{H}_3^{(0)}]_{z=L} = 0 \quad , \tag{3.4.10}$$

$$[\underline{H}_0^{(1)} - \underline{H}_1^{(1)}]_{z=0} + \eta_1^{(1)}[\partial(\underline{H}_0^{(0)} - \underline{H}_1^{(0)})/\partial z]_{z=0} = 0 \quad , \tag{3.4.11}$$

$$[\underline{H}_1^{(1)} - \underline{H}_2^{(1)}]_{z=D} + \eta_2^{(1)}[\partial(\underline{H}_1^{(0)} - \underline{H}_2^{(0)})/\partial z]_{z=D} = 0 \quad , \tag{3.4.12}$$

$$[\underline{H}_2^{(1)} - \underline{H}_3^{(1)}]_{z=L} = 0 \quad . \tag{3.4.13}$$

Boundary condition (c) also requires that

$$\underline{n}_1 \times [\underline{E}_0 - \underline{E}_1]_{z=\eta_1} = 0 \quad ,$$

$$\underline{n}_2 \times [\underline{E}_1 - \underline{E}_2]_{z=D+\eta_2} = 0 \quad ,$$

$$\underline{k} \times [\underline{E}_2 - \underline{E}_3]_{z=L} = 0$$

where $\underline{n}_1$ and $\underline{n}_2$ are unit vectors normal to the surfaces $z = \eta_1$ and $z = D + \eta_2$ respectively. Let us denote by ζ the angle of slope measured from the horizontal of the wave

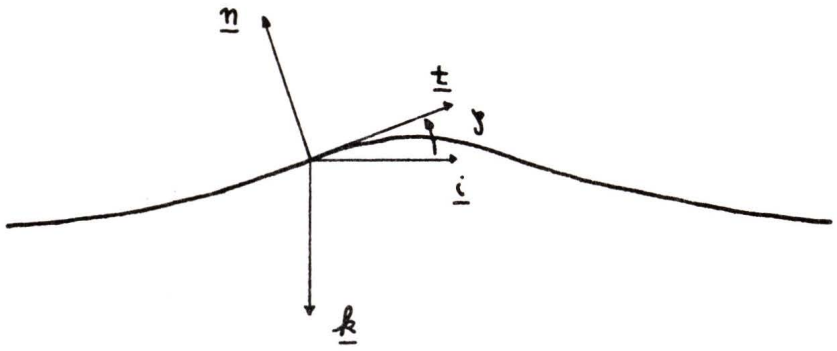

Fig. 6. Orientation of the unit vectors.

profile at a general point on a surface of discontinuity as shown in Figure 6. The unit tangent vector $\underline{t}$ at this point is clearly given by $\underline{t} = \underline{i} \cos\zeta - \underline{k} \sin\zeta$. It follows that the unit normal vector $\underline{n}$, being perpendicular to $\underline{t}$, is

$$\underline{n} = -\underline{i}\sin\zeta - \underline{k}\cos\zeta = -(\underline{i}\tan\zeta + \underline{k})(1+\tan^2\zeta)^{-\frac{1}{2}} .$$

On the surface $z = \eta_1$, $\tan\zeta = -\partial\eta_1/\partial x$, and on $z = D + \eta_2$, $\tan\zeta = -\partial\eta_2/\partial x$, the negative sign arising because η_j is measured positively downwards, i.e. in the direction of $\underline{k}$. Hence the above three boundary conditions become

$$(\underline{i}\,\partial\eta_1/\partial x - \underline{k}) \times [\underline{E}_0 - \underline{E}_1]_{z=\eta_1} = 0 ,$$

$$(\underline{i}\,\partial\eta_2/\partial x - \underline{k}) \times [\underline{E}_1 - \underline{E}_2]_{z=D+\eta_2} = 0 ,$$

$$\underline{k} \times [\underline{E}_2 - \underline{E}_3]_{z=L} = 0 .$$

Expanding the boundary values of the electric field vectors as a Taylor series about the undisturbed surfaces z = 0 and z = D, we obtain

$$(\underline{i}\,\partial\eta_1/\partial x - \underline{k}) \times [(\underline{E}_0 - \underline{E}_1) + (\eta_1/1!)\partial(\underline{E}_0 - \underline{E}_1)/\partial z + \cdots]_{z=0} = 0,$$

$$(\underline{i}\,\partial\eta_2/\partial x - \underline{k}) \times [(\underline{E}_1 - \underline{E}_2) + (\eta_2/1!)\partial(\underline{E}_1 - \underline{E}_2)/\partial z + \cdots]_{z=D} = 0.$$

Substituting the expansions (3.3.2) and (3.3.4) for η_j and $\underline{E}_j$ respectively into the y component of the above three cross products, we arrive at the following boundary conditions

$$[(\underline{E}_0^{(o)} - \underline{E}_1^{(o)})_x]_{z=0} = 0, \tag{3.4.14}$$

$$[(\underline{E}_1^{(o)} - \underline{E}_2^{(o)})_x]_{z=D} = 0, \tag{3.4.15}$$

$$[(\underline{E}_2^{(o)} - \underline{E}_3^{(o)})_x]_{z=L} = 0, \tag{3.4.16}$$

$$[(\underline{E}_0^{(1)} - \underline{E}_1^{(1)})_x + \eta_1^{(1)}\partial(\underline{E}_0^{(o)} - \underline{E}_1^{(o)})_z/\partial z + (\underline{E}_0^{(o)} - \underline{E}_1^{(o)})_z\,\partial\eta_1^{(1)}/\partial x]_{z=0} = 0, \tag{3.4.17}$$

$$[(\underline{E}_1^{(1)} - \underline{E}_2^{(1)})_x + \eta_2^{(1)}\partial(\underline{E}_1^{(o)} - \underline{E}_2^{(o)})_z/\partial z + (\underline{E}_1^{(o)} - \underline{E}_2^{(o)})_z\,\partial\eta_2^{(1)}/\partial x]_{z=D} = 0, \tag{3.4.18}$$

$$[(\underline{E}_2^{(1)} - \underline{E}_3^{(1)})_x]_{z=L} = 0. \tag{3.4.19}$$

Here we have equated like powers of ε and discarded terms of second and higher order in ε.

3.5 Further simplification of the basic equations and boundary conditions

Since we are dealing with a periodic wave, propagating in the positive x direction, the vertical displacements about the mean free boundaries must be of the form

$$\eta_j^{(k)} = -i a_j^{(k)} \exp(i\omega t - imx) \quad , \quad j = 1, 2 \qquad (3.5.1)$$

where $i = (-1)^{1/2}$, $|a_j^{(k)}|$ the wave amplitude ($a_j^{(k)}$ is complex), ω the ocean wave angular frequency and m the ocean wave number (i.e. $m = 2\pi/\lambda$ where λ is the wavelength). The index k, here, refers to the k^{th} term in the expansion (3.3.2) for η_j. It is understood, of course, that the real part of (3.5.1) and all subsequent expressions is to be taken. Since particles lying on the surface undergo harmonic oscillations as well, we may assume that all the fluid particles within the ocean undergo a similar motion, i.e. that the velocity potential takes the form

$$\phi_j^{(k)} = \varphi_j^{(k)}(z) \exp(i\omega t - imx) \quad , \quad j = 1, 2 \; . \qquad (3.5.2)$$

The induced electromagnetic field resulting from this fluid motion will clearly have a similar dependence on x and t, i.e. we can write

$$\underline{H}_j^{(k)} = \underline{h}_j^{(k)}(z) \exp(i\omega t - imx) \quad , \qquad (3.5.3)$$

$$\underline{E}_j^{(k)} = \underline{e}_j^{(k)}(z)\exp(i\omega t - imx) \quad . \tag{3.5.4}$$

With this simplification we note that the operators $\partial/\partial t$ and $\partial/\partial x$ correspond to multiplication by $i\omega$ and $-im$ respectively. For example, (3.2.5) now takes the simple form

$$im(\underline{h}_j^{(k)})_x = d(\underline{h}_j^{(k)})_z/dz \quad . \tag{3.5.5}$$

We now direct our attention to the differential equation (3.3.5) for $\underline{H}_j^{(o)}$. Upon substitution of (3.5.3) with k = 0 into (3.3.5) ,we have

$$d^2\underline{h}_j^{(o)}/dz^2 = (m^2 + i4\pi\sigma_j\omega - k_j\omega^2/c^2)\,\underline{h}_j^{(o)}$$

whose solution for the z component everywhere is

$$\begin{aligned}
(\underline{h}_0^{(o)})_z &= A_z^{(o)}\exp(f_0 z) \quad , \\
(\underline{h}_1^{(o)})_z &= B_z^{(o)}\exp(f_1 z) + C_z^{(o)}\exp(-f_1 z) \quad , \\
(\underline{h}_2^{(o)})_z &= D_z^{(o)}\exp(f_2 z) + E_z^{(o)}\exp(-f_2 z) \quad , \\
(\underline{h}_3^{(o)})_z &= F_z^{(o)}\exp(-f_3 z)
\end{aligned} \tag{3.5.6}$$

where

$$f_j = (m^2 + i4\pi\sigma_j\omega - k_j\omega^2/c^2)^{\frac{1}{2}}$$

and in accordance with boundary condition (d) the field vanishes in air and the earth's crust as z approaches infinity. The boundary conditions (3.4.8) and (3.4.10), together with relation (3.5.3), require $(\underline{h}_j^{(o)})_z$ and $(\underline{h}_j^{(o)})_x$ to be continuous across the boundaries. The latter condition, by virtue of (3.5.5), is equivalent to $d(\underline{h}_j^{(o)})_z/dz$ being continuous across each boundary. Applying the above conditions to the solution for $(\underline{h}_j^{(o)})_z$, we obtain

$$A_z^{(o)} - B_z^{(o)} - C_z^{(o)} = 0 ,$$

$$f_o A_z^{(o)} - f_1 B_z^{(o)} + f_1 C_z^{(o)} = 0 ,$$

$$B_z^{(o)} e^{f_1 D} + C_z^{(o)} e^{-f_1 D} - D_z^{(o)} e^{f_2 D} - E_z^{(o)} e^{-f_2 D} = 0 ,$$

$$f_1 B_z^{(o)} e^{f_1 D} - f_1 C_z^{(o)} e^{-f_1 D} - f_2 D_z^{(o)} e^{f_2 D} + f_2 E_z^{(o)} e^{-f_2 D} = 0 ,$$

$$D_z^{(o)} e^{f_2 L} + E_z^{(o)} e^{-f_2 L} - F_z^{(o)} e^{-f_3 L} = 0 ,$$

$$f_2 D_z^{(o)} e^{f_2 L} - f_2 E_z^{(o)} e^{-f_2 L} + f_3 F_z^{(o)} e^{-f_3 L} = 0 .$$

This system of six homogeneous equations in six unknowns possesses only the trivial solution, $A_z^{(o)} = \ldots = F_z^{(o)} = 0$. A nontrivial solution would require that the determinant of the coefficient matrix vanish, thereby implying a relationship between f_0 , f_1, f_2 and f_3 which is physically impossible since ω, σ_j and k_j are independent.

Therefore, we may conclude that

$$(\underline{h}_j^{(o)})_z = 0$$

and, by (3.5.5),

$$(\underline{h}_j^{(o)})_x = 0 \quad .$$

The solution for $(\underline{h}_j^{(o)})_y$ is clearly similar to that obtained for $(\underline{h}_j^{(o)})_z$ in (3.5.6). However, after substitution from (3.5.3), we see that the boundary conditions (3.4.8) to (3.4.10) require $(\underline{h}_j^{(o)})_y$ to be continuous across each of the three boundaries. Three additional conditions are needed to determine explicitly all six constants in the solution.

Solving for $\underline{E}$ in equation (3.2.4), we obtain

$$\underline{E}_j = (4\pi\sigma_j + ik_j\omega/c^2)^{-1}\{\text{curl } \underline{H}_j - 4\pi\sigma_j[\nabla\phi_j \times (\underline{F} + \underline{H}_j)]\} \quad .$$

Substituting the expansions (3.3.1), (3.3.3) and (3.3.4) for ϕ_j, $\underline{H}_j$ and $\underline{E}_j$ respectively into the above equation and, as usual, equating like powers of ε while discarding terms $O(\varepsilon^2)$, we arrive at

$$\underline{E}_j^{(o)} = (4\pi\sigma_j + ik_j\omega/c^2)^{-1}\,\text{curl } \underline{H}_j^{(o)} \quad , \tag{3.5.7}$$

$$\underline{E}_j^{(1)} = (4\pi\sigma_j + ik_j\omega/c^2)^{-1}\{\text{curl}\,\underline{H}_j^{(1)} - 4\pi\sigma_j[\nabla\phi_j^{(1)} \times (\underline{F} + \underline{H}_j)]\} \quad . \tag{3.5.8}$$

When (3.5.7) is used in conjunction with the boundary conditions (3.4.14) to (3.4.16) we find that the expression

$(4\pi\sigma_j + ik_j\omega/c^2)^{-1} d(\underline{h}_j^{(o)})_y/dz$ must be continuous across each boundary. This condition yields the three extra conditions required to determine the constants in the solution for $(\underline{h}_j^{(o)})_y$. In fact, we again obtain six homogeneous equations in six unknowns which, by the same argument as before, can possess only the trivial solution, from which it follows that $(\underline{h}_j^{(o)})_y = 0$. We have now shown that all components of $\underline{h}_j^{(o)}$ vanish, and we may therefore conclude that

$$\underline{H}_j^{(o)} = \underline{E}_j^{(o)} = 0$$

the latter result following by (3.5.7).

We shall now consider the differential equation (3.3.6) for $\underline{H}_j^{(1)}$, whose y component is

$$d^2(\underline{h}_j^{(1)})_y/dz^2 = m^2(1 + i4\pi\sigma_j\omega/m^2 - k_j\omega^2/m^2c^2)(\underline{h}_j^{(1)})_y .$$

First, we note that the approximation

$$k_j\omega^2/m^2c^2 \ll \begin{cases} 4\pi\sigma_j\omega/m^2 & (j \neq 0) \\ 1 & (j = 0) \end{cases} \qquad (3.5.9)$$

is valid under all conditions encountered in this problem. Certainly (3.5.9) must always hold in air ($j = 0$, $\sigma_o = 0$, $k_o = 1$) since $(\omega/m)/c$, the ratio of the wave speed to the speed of light, is clearly much less than unity for all wave speeds. In the sea ($\sigma_{1,2} = 4 \times 10^{-11}$ emu, $k_{1,2} = 80$) and the earth's crust ($\sigma_3 = 1 \times 10^{-14}$ emu, $k_3 = 10$), the approximation is well satisfied for all ocean wave periods greater

than 10^{-4} seconds. As we shall not consider waves of periods less than one second in this problem (because such periods are associated with capillary waves, which on account of their small amplitude and wavelength produce no significant magnetic field), we are completely justified in using (3.5.9). This approximation is, of course, equivalent to neglecting displacement currents everywhere. It follows that we may write

$$d^2(\underline{h}_j^{(1)})_y/dz^2 = m^2(1 + i4\pi\sigma_j\omega/m^2)(\underline{h}_j^{(1)})_y \ .$$

Furthermore, putting the expansions (3.3.3) and (3.3.4) into the y component of (3.2.3) and equating the like powers of ε again, we obtain a relation between the y component of the magnetic field and the x and z components of the electric field, viz:

$$d(\underline{e}_o^{(1)})_x/dz + im(\underline{e}_o^{(1)})_z = -i\omega(\underline{h}_o^{(1)})_y \ .$$

Taking the divergence of (3.5.8) and using the identity div curl $\equiv$ 0, we obtain

$$im(\underline{e}_o^{(1)})_x = d(\underline{e}_o^{(1)})_z/dz \ ,$$

which when substituted in the above equation yields

$$[d^2/dz^2 - m^2](\underline{e}_o^{(1)})_z = m\omega(\underline{h}_o^{(1)})_y \ . \qquad (3.5.10)$$

Replacing the term $(\underline{h}_o^{(1)})_y$ by means of

$$(\underline{e}_o^{(1)})_z = -(mc^2/\omega)(\underline{h}_o^{(1)})_y \quad ,$$

obtained by taking the z component of (3.5.8) with j = 0 we arrive at

$$[d^2/dz^2 - m^2(1 - \omega^2/m^2c^2)](\underline{e}_o^{(1)})_z = 0 \quad .$$

Comparing this result with the previous differential equation (3.5.10), we first note that the additional term ω^2/m^2c^2 arises from $(\underline{h}_o^{(1)})_y$. However, by approximation (3.5.9), the above equation reduces to

$$[d^2/dz^2 - m^2](\underline{e}_o^{(1)})_z = 0 \quad .$$

For this equation to be consistent with (3.5.10), we must have

$$(\underline{h}_o^{(1)})_y = 0 \quad .$$

Of course, $(\underline{h}_o^{(1)})_y$, only vanishes because of the approximation (3.5.9). What we have actually shown, is that $(\underline{h}_o^{(1)})_y$ is of the same order as the magnetic fields produced by displacement currents and is therefore negligibly small in this problem.

The complete solution for $(\underline{h}_j^{(1)})_y$ is thus of the form

$$(\underline{h}_o^{(1)})_y = 0 \quad ,$$

$$(\underline{h}_1^{(1)})_y = B_y^{(1)} \exp(m g_1 z) + C_y^{(1)} \exp(-m g_1 z) \quad ,$$

$$(\underline{h}_2^{(1)})_y = D_y^{(1)} \exp(m g_2 z) + E_y^{(1)} \exp(-m g_2 z) \quad ,$$

$$(\underline{h}_3^{(1)})_y = F_y^{(1)} \exp(-m g_3 z)$$

where

$$g_j = (1 + i 4\pi \sigma_j \omega / m^2)^{\frac{1}{2}}$$

and $(\underline{h}_3^{(1)})_y$ vanishes as z approaches infinity as demanded by boundary condition (d). Boundary conditions (3.4.11) to (3.4.13) require that $(\underline{h}_j^{(1)})_y$ is continuous across each of the three boundaries. Two additional conditions are still required to determine all five constants in the above solution. Taking the x component of (3.5.8) and using the approximation (3.5.9) in the first factor, we have

$$(\underline{E}_j^{(1)})_x = -\partial(\underline{H}_j^{(1)})_y / 4\pi\sigma_j \partial z + (\underline{F})_y \partial \phi_j^{(1)} / \partial z \quad , \quad j = 1,2,3 \; .$$

By substituting for $(\underline{E}_j^{(1)})_x$ in boundary conditions (3.4.18) and (3.4.19), the two extra conditions are easily found to be

$$[d(\sigma_2 \underline{h}_1^{(1)} - \sigma_1 \underline{h}_2^{(1)})_y / dz]_{z=D} = 0 \quad ,$$

$$[d(\sigma_3 \underline{h}_2^{(1)} - \sigma_2 \underline{h}_3^{(1)})_y / dz]_{z=L} = 0 \quad .$$

Here we used the fluid dynamical conditions (3.4.5) to (3.4.7) and relation (3.5.3). From the above conditions, we obtain five homogeneous equations in five unknowns which, by the same argument as before, can again possess only the trivial solution. Therefore we conclude that the y component of $\underline{h}_j^{(1)}$ vanishes everywhere, i.e.

$$(\underline{H}_d^{(1)})_y = 0 \quad .$$

3.6 Statement of the final equations and boundary conditions

The induced magnetic field is now of the form

$$\underline{H}_j^{(i)} = \underline{i}\,(\underline{H}_j^{(i)})_x + \underline{k}\,(\underline{H}_j^{(i)})_z \qquad (3.6.1)$$

where, by (3.5.3),

$$(\underline{H}_j^{(i)})_{x,z} = (\underline{h}_j^{(i)})_{x,z} \exp(i\omega t - imx) \,. \qquad (3.6.2)$$

Fortunately, from (3.5.5), we also have that

$$(\underline{h}_j^{(i)})_x = d(\underline{h}_j^{(i)})_z / im\,dz \,. \qquad (3.6.3)$$

Thus it is only necessary to solve for the z component which satisfies the differential equation

$$d^2(\underline{h}_j^{(i)})_z/dz^2 = m^2 g_j^2 (\underline{h}_j^{(i)})_z + 4\pi\sigma_j (im F_x - F_z\, d/dz)\, d\psi_j^{(i)}/dz \qquad (3.6.4)$$

where, as before,

$$g_j = (1 + i\,4\pi\sigma_j \omega/m^2)^{\frac{1}{2}} \,. \qquad (3.6.5)$$

The terms F_x and F_z denote the x and z components of the earth's magnetic field vector $\underline{F}$ respectively. Here (3.6.4) has been found by taking the z component of (3.3.6), using relations (3.5.2) and (3.5.3), and the first factor on the right hand side of the resultant equation was reduced, by approximation (3.5.9), to its present

form $m^2 q_j^2$. The boundary conditions (3.4.11) to (3.4.13) governing the differential equation (3.6.4) are, by (3.6.3), equivalent to the following set of conditions:

$$\left[(\underline{h}_0^{(1)} - \underline{h}_1^{(1)})_z \right]_{z=0} = 0 \quad , \tag{3.6.6}$$

$$\left[(\underline{h}_1^{(1)} - \underline{h}_2^{(1)})_z \right]_{z=D} = 0 \quad , \tag{3.6.7}$$

$$\left[(\underline{h}_2^{(1)} - \underline{h}_3^{(1)})_z \right]_{z=L} = 0 \quad , \tag{3.6.8}$$

$$\left[d(\underline{h}_0^{(1)} - \underline{h}_1^{(1)})_z / dz \right]_{z=0} = 0 \quad , \tag{3.6.9}$$

$$\left[d(\underline{h}_1^{(1)} - \underline{h}_2^{(1)})_z / dz \right]_{z=D} = 0 \quad , \tag{3.6.10}$$

$$\left[d(\underline{h}_2^{(1)} - \underline{h}_3^{(1)})_z / dz \right]_{z=L} = 0 \quad . \tag{3.6.11}$$

Prior to solving (3.6.4), it is clear that an expression for the velocity potential,

$$\phi_j^{(1)} = \psi_j^{(1)} \exp(i\omega t - imx) \quad , \tag{3.6.12}$$

is needed. The expression (3.6.12) must satisfy the Laplace equation (3.2.1) in the form

$$(d^2/dz^2 - m^2)\, \psi_j^{(1)} = 0 \tag{3.6.13}$$

Substituting (3.6.12) into the fluid dynamical boundary conditions (3.4.1), (3.4.2) and (3.4.4) to (3.4.7), together with (from (3.5.1) with k = 1)

$$\eta_j^{(1)} = -i a_j^{(1)} \exp(i\omega t - i m x) , \tag{3.6.14}$$

we obtain respectively:

$$[\psi_1^{(1)}]_{z=0} = -a_1^{(1)} g/\omega , \tag{3.6.15}$$

$$[\rho_2 \psi_2^{(1)} - \rho_1 \psi_1^{(1)}]_{z=D} = -a_2^{(1)} (\rho_2 - \rho_1) g/\omega , \tag{3.6.16}$$

$$[d\psi_1^{(1)}/dz]_{z=0} = a_1^{(1)} \omega , \tag{3.6.17}$$

$$[d\psi_1^{(1)}/dz]_{z=D} = a_2^{(1)} \omega , \tag{3.6.18}$$

$$[d\psi_2^{(1)}/dz]_{z=D} = a_2^{(1)} \omega , \tag{3.6.19}$$

$$[d\psi_2^{(1)}/dz]_{z=L} = 0 . \tag{3.6.20}$$

In the next chapter we shall devote our attention to solving the above equations. Since they involve only first order quantities, we may henceforth delete all superscripts (1) without introducing any ambiguity.

CHAPTER 4

THE INDUCED MAGNETIC FIELD

4.1 The velocity potential

Solutions for the velocity potential of a two layer fluid are developed in many texts on Hydrodynamics (e.g. Lamb, 1932 and Milne-Thomson, 1968). However, we shall derive the solutions anew here for completeness.

The solution of equation (3.6.13) with $j = 1$ is

$$\Psi_1 = M_1 \cosh(mz) + N_1 \sinh(mz) \qquad (4.1.1)$$

and with $j = 2$

$$\Psi_2 = M_2 \cosh[m(L-z)] \qquad (4.1.2)$$

since ψ_2 must satisfy condition (3.6.20). Substituting expression (4.1.1) into the conditions (3.6.15) and (3.6.17), we obtain respectively

$$M_1 = -a_1 g/\omega \quad , \qquad (4.1.3)$$

$$N_1 = a_1 \omega/m \quad . \qquad (4.1.4)$$

By substituting for ψ_2 in (3.6.19) from (4.1.2), the remaining constant M_2 is readily found to be,

$$M_2 = -a_2 \omega/m \sinh[m(L-D)] \quad . \qquad (4.1.5)$$

Equating conditions (3.6.18) and (3.6.19), we have

$$\left[d(\psi_1 - \psi_2)/dz \right]_{z=D} = 0 \quad .$$

Upon substitution of expressions (4.1.1) to (4.1.5) into the above condition, we immediately arrive at the ratio of the internal to surface wave amplitude, viz

$$a_2/a_1 = (P - b)\cosh(mD)/P \tag{4.1.6}$$

where

$$P = \omega^2/gm \quad , \tag{4.1.7}$$

$$b = \tanh(mD) \quad , \tag{4.1.8}$$

$$c = \tanh\left[m(L-D)\right] \quad . \tag{4.1.9}$$

We note that even though a_1 and a_2 are complex, their ratio as given by (4.1.6) is real.

Furthermore, using expressions (4.1.1) to (4.1.9) in conjunction with the last fluid dynamical condition (3.6.16), we obtain

$$(\alpha + bc)P^2 - \alpha(b+c)P + (\alpha - 1)bc = 0 \quad .$$

The two solutions, of course, are

$$P_{\pm} = \left\{\alpha(b+c) \pm \left[\alpha^2(b+c)^2 - 4bc(\alpha-1)(\alpha+bc)\right]^{\frac{1}{2}}\right\}/2(\alpha+bc). \tag{4.1.10}$$

This expression will always give a real and positive value for $P_{\pm}$ since $\alpha \geq 1$, $0 \leq b \leq 1$ and $0 \leq c \leq 1$. Therefore, two possible frequencies for a wave exist for a given wavelength.

The above quadratic equation in P may be rewritten, so as to take the form

$$(\alpha + bc)(P-b)^2 + d(P-b) - (1-b^2)bc = 0$$

where

$$d = 2b^2c + \alpha(b-c) .$$

The solution clearly is

$$P_{\pm} - b = \{-d \pm [d^2 + 4bc(1-b^2)(\alpha+bc)]^{\frac{1}{2}}\}/2(\alpha+bc),$$

from which it is easily seen that $(P_+ - b) \geq 0$ and $(P_- - b) \leq 0$ under all possible conditions. Hence by (4.1.6), we see that

$$a_2/a_1 \geq 0 \quad (\text{i.e. } a_2/a_1 = |a_2/a_1|) ,$$

when the P_+ root is used. For the P_- root, we have

$$a_2/a_1 \leq 0 \quad (\text{i.e. } a_2/a_1 = |a_2/a_1| e^{i\pi}) .$$

Thus the ratio of η_2 and η_1 for each of the roots P_+ and P_- is respectively

$$\eta_2/\eta_1 = |a_2/a_1| ,$$

$$\eta_2/\eta_1 = |a_2/a_1| e^{i\pi} .$$

When an internal wave is generated, it will induce a surface wave at the air-sea interface, such that the crests (troughs) of the surface wave overlie the troughs (crests) of the internal wave as shown in Figure 1. Thus the waves are out of phase by π radians and must propagate with a frequency given by P_- . The above situation may be reversed, i.e. it is possible for a surface wave to cause an internal wave at the boundary of the density discontinuity such that the crests (troughs) of the internal wave lie directly below the crests (troughs) of the surface wave. The waves are, therefore, in phase and must propagate with a frequency given by P_+ . For example, when $\alpha = 1$ (constant density) the expression (4.1.10) gives $P_+ = \tanh(mL)$ and $P_- = 0$. Since no internal wave is possible in a sea where the density is the same everywhere, we know that the non-vanishing solution must describe a surface wave, thus confirming that P_+ is indeed associated with surface waves and P_- with internal waves.

4.2 The general solution for the magnetic field

In this section we shall denote derivatives with respect to the variable z by the prime symbol in the usual manner. Thus the differential equation (3.6.4) may be conveniently rewritten in the form

$$(\underline{h}_j'')_z = m^2 q_j^2 (\underline{h}_j)_z + m^2(1-q_j^2)\, G_j(z) \tag{4.2.1}$$

where

$$\begin{aligned} G_j(z) &= i\omega^{-1}(im F_x \psi_j' - F_z \psi_j''), \\ G_0 &= G_3 = 0 \end{aligned} \tag{4.2.2}$$

When $j = 1,2$, we also note that $G_j''(z) = m^2 G_j(z)$ because the functional dependence of G_j on z is always of the form $\exp(\pm mz)$. The solution of (4.2.1) is clearly

$$(\underline{h}_0)_z = A_0 \exp(mz)$$

$$(\underline{h}_1)_z = A_1 \exp(mq_1 z) + B_1 \exp(-mq_1 z) + G_1(z), \tag{4.2.3}$$

$$(\underline{h}_2)_z = A_2 \exp(mq_2 z) + B_2 \exp(-mq_2 z) + G_2(z),$$

$$(\underline{h}_3)_z = A_3 \exp(-mq_3 z)$$

where $(\underline{h}_0)_z \to 0$ as $z \to -\infty$, and $(\underline{h}_3)_z \to 0$ as $z \to +\infty$ as is required by boundary condition (d). We also note that $q_0 = 1$ since $\sigma_0 = 0$. The complete solution for $(\underline{h}_j)_x$ is now immediately obtainable from (4.2.3) by means of (3.6.3).

Application of the conditions (3.6.6) and (3.6.9) to the solution (4.2.3), yields

$$A_o = A_1 + B_1 + G_1(o) ,$$

$$mA_o = mg_1 A_1 - mg_1 B_1 + G_1'(o) ,$$

whence

$$A_1 = Q_1^+ A_o - W_1^+ , \tag{4.2.4}$$

$$B_1 = Q_1^- A_o - W_1^- \tag{4.2.5}$$

where

$$Q_1^\pm = (g_1 \pm 1)/2g_1 , \tag{4.2.6}$$

$$W_1^\pm = [mg_1 G_1(o) \pm G_1'(o)]/2mg_1 . \tag{4.2.7}$$

Similarly conditions (3.6.8) and (3.6.11), give

$$A_3 e^{-mg_3 L} = A_2 e^{mg_2 L} + B_2 e^{-mg_2 L} + G_2(L) ,$$

$$-mg_3 A_3 e^{-mg_3 L} = mg_2 A_2 e^{mg_2 L} - mg_2 B_2 e^{-mg_2 L} + G_2'(L) ,$$

leading to

$$A_2 = [\, Q_2^- A_3 e^{-m\mathcal{g}_3 L} - W_2^+ \,] \exp(-m\mathcal{g}_2 L) \quad , \tag{4.2.8}$$

$$B_2 = [\, Q_2^+ A_3 e^{-m\mathcal{g}_3 L} - W_2^- \,] \exp(m\mathcal{g}_2 L) \tag{4.2.9}$$

where

$$Q_2^{\pm} = (\mathcal{g}_2 \pm \mathcal{g}_3)/2\mathcal{g}_2 \quad , \tag{4.2.10}$$

$$W_2^{\pm} = [m\mathcal{g}_2 G_2(L) \pm G_2'(L)]/2m\mathcal{g}_2 \quad . \tag{4.2.11}$$

The remaining two conditions, (3.6.7) and (3.6.10), yield

$$A_1 e^{m\mathcal{g}_1 D} + B_1 e^{-m\mathcal{g}_1 D} = A_2 e^{m\mathcal{g}_2 D} + B_2 e^{-m\mathcal{g}_2 D} + G_2(D) - G_1(D) \, ,$$

$$m\mathcal{g}_1 A_1 e^{m\mathcal{g}_1 D} - m\mathcal{g}_1 B_1 e^{-m\mathcal{g}_1 D} = m\mathcal{g}_2 A_2 e^{m\mathcal{g}_2 D} - m\mathcal{g}_2 B_2 e^{-m\mathcal{g}_2 D} + G_2'(D) - G_1'(D) \, .$$

These equations can be written in the form

$$Q_3^+ A_1 e^{m\mathcal{g}_1 D} + Q_3^- B_1 e^{-m\mathcal{g}_1 D} = A_2 e^{m\mathcal{g}_2 D} + W_3^+ \, , \tag{4.2.12}$$

$$Q_3^- A_1 e^{m\mathcal{g}_1 D} + Q_3^+ B_1 e^{-m\mathcal{g}_1 D} = B_2 e^{-m\mathcal{g}_2 D} + W_3^- \tag{4.2.13}$$

where

$$Q_3^{\pm} = (g_2 \pm g_1)/2g_2 \quad , \tag{4.2.14}$$

$$W_3^{\pm} = (mg_2[G_2(D) - G_1(D)] \pm [G_2'(D) - G_1'(D)])/2mg_2 \quad . \tag{4.2.15}$$

Substituting (4.2.4), (4,2,8), (4.2.5) and (4.2.9) for $A_{1,2}$ and $B_{1,2}$ respectively into equations (4.2.12) and (4.2.13), we arrive at two equations in two unknowns, viz:

$$Q_3^+(Q_1^+A_o - W_1^+)e^{mg_1D} + Q_3^-(Q_1^-A_o - W_1^-)e^{-mg_1D} =$$

$$[Q_2^-A_3e^{-mg_3L} - W_2^+]\exp(mg_2D - mg_2L) + W_3^+$$

and

$$Q_3^-(Q_1^+A_o - W_1^+)e^{mg_1D} + Q_3^+(Q_1^-A_o - W_1^-)e^{-mg_1D} =$$

$$[Q_2^+A_3e^{-mg_3L} - W_2^-]\exp(mg_2L - mg_2D) + W_3^- \quad .$$

We now define

$$b_1 = Q_1^+Q_3^+ + Q_1^-Q_3^- \exp(-2mg_1D) \quad , \tag{4.2.16}$$

$$b_2 = Q_1^+Q_3^- + Q_1^-Q_3^+ \exp(-2mg_1D) \quad , \tag{4.2.17}$$

$$C_1 = \{ W_3^+ - W_2^+ \exp[-m\mu_2(L-D)] \} \exp(-m\mu_1 D)$$

$$+ Q_3^+ W_1^+ + Q_3^- W_1^- \exp(-2m\mu_1 D) \ , \qquad (4.2.18)$$

$$C_2 = \{ W_3^- \exp[-m\mu_2(L-D)] - W_2^- \} \exp(-m\mu_1 D)$$

$$+ \{ Q_3^- W_1^+ + Q_3^+ W_1^- \exp(-2m\mu_1 D) \} \exp[-m\mu_2(L-D)] \qquad (4.2.19)$$

so that, the previous two equations become

$$A_0 b_1 - A_3 Q_2^- \exp[-m\mu_2(L-D) - m\mu_1 D - m\mu_3 L] = C_1 \ ,$$

$$A_0 b_2 \exp[-m\mu_2(L-D)] - A_3 Q_2^+ \exp[-m\mu_1 D - m\mu_3 L] = C_2 \ .$$

The constants A_0 and A_3 are clearly given by

$$A_0 = \Delta^{-1} \{ Q_2^- C_2 \exp[-m\mu_2(L-D)] - Q_2^+ C_1 \} \qquad (4.2.20)$$

and

$$A_3 = \Delta^{-1} \{ b_1 C_2 - b_2 C_1 \exp[-m\mu_2(L-D)] \} \exp[m\mu_1 D + m\mu_3 L] \qquad (4.2.21)$$

where

$$\Delta = Q_2^- b_2 \exp[-2m\mu_2(L-D)] - Q_2^+ b_1 \ . \qquad (4.2.22)$$

Substituting for $c_{1,2}$ and $b_{1,2}$ in the constants A_0 and A_3, we obtain

$$A_o = \Delta^{-1}\{(Q_2^+ W_2^+ - Q_2^- W_2^-)\exp[-mg_2(L-D) - mg_1 D]$$

$$+ Q_2^-[Q_3^- W_1^+ + (W_3^- + Q_3^+ W_1^- e^{-mg_1 D})e^{-mg_1 D}]\exp[-2mg_2(L-D)]$$

$$- Q_2^+[Q_3^+ W_1^+ + (W_3^+ + Q_3^- W_1^- e^{-mg_1 D})e^{-mg_1 D}]\} \qquad (4.2.23)$$

and

$$A_3 = \Delta^{-1}\{-W_2^-(Q_1^+ Q_3^+ + Q_1^- Q_3^- e^{-2mg_1 D})$$

$$+ [W_2^+(Q_1^+ Q_3^- + Q_1^- Q_3^+ e^{-2mg_1 D})\exp[-mg_2(L-D)]$$

$$- Q_1^-(Q_3^+ W_3^+ - Q_3^- W_3^-)\exp[-2mg_1 D]$$

$$- (g_1/g_2)(Q_1^- W_1^+ - Q_1^+ W_1^-)\exp(-mg_1 D)$$

$$- Q_1^+(Q_3^- W_3^+ - Q_3^+ W_3^-)]\exp[-mg_2(L-D)]\}e^{mg_3 L} \qquad (4.2.24)$$

Replacing the constants A_0 and A_3, by the expressions (4.2.23) and (4.2.24) in equations (4.2.4), (4.2.5), (4.2.8) and (4.2.9) respectively, we obtain after some lengthy algebra

$$A_1 = \Delta^{-1}\{ Q_1^+ [Q_2^+ W_2^+ - Q_2^- W_2^-] \exp[-m g_2 (L-D)]$$

$$- Q_2^+ [Q_1^+ W_3^+ - Q_3^- (Q_1^- W_1^+ - Q_1^+ W_1^-) e^{-m g_1 D}]$$

$$+ Q_2^- [Q_1^+ W_3^- - Q_3^+ (Q_1^- W_1^+ - Q_1^+ W_1^-) e^{-m g_1 D}] \cdot$$

$$\cdot \exp[-2 m g_2 (L-D)] \} e^{-m g_1 D} , \qquad (4.2.25)$$

$$B_1 = \Delta^{-1}\{ Q_1^- [Q_2^+ W_2^+ - Q_2^- W_2^-] \exp[-m g_2 (L-D) - m g_1 D]$$

$$+ Q_2^- [Q_3^- (Q_1^- W_1^+ - Q_1^+ W_1^-) + Q_1^- W_3^- e^{-m g_1 D}] \exp[-2 m g_2 (L-D)]$$

$$- Q_2^+ [Q_3^+ (Q_1^- W_1^+ - Q_1^+ W_1^-) + Q_1^- W_3^+ e^{-m g_1 D}] \} , \qquad (4.2.26)$$

$$A_2 = \Delta^{-1}\{ (Q_2^+ W_2^+ - Q_2^- W_2^-)(Q_1^+ Q_3^+ + Q_1^- Q_3^- e^{-2 m g_1 D})$$

$$- Q_2^- [\{ Q_1^- (Q_3^+ W_3^+ - Q_3^- W_3^-) e^{-m g_1 D}$$

$$+ (g_1 / g_2)(Q_1^- W_1^+ - Q_1^+ W_1^-) \} e^{-m g_1 D}$$

$$+Q_1^+(Q_3^-W_3^+ - Q_3^+W_3^-)]\exp[-m\gamma_2(L-D)]\}\, e^{-m\gamma_2 L} \qquad (4.2.27)$$

and

$$B_2 = \Delta^{-1}\{(Q_2^+W_2^+ - Q_2^-W_2^-)(Q_1^+Q_3^- + Q_1^-Q_3^+ e^{-2m\gamma_1 D})\exp[-m\gamma_2(L-D)]$$

$$- Q_2^+[\{Q_1^-(Q_3^+W_3^+ - Q_3^-W_3^-)e^{-m\gamma_1 D}$$

$$+(\gamma_1/\gamma_2)(Q_1^-W_1^+ - Q_1^+W_1^-)\}e^{-m\gamma_1 D}$$

$$+Q_1^+(Q_3^-W_3^+ - Q_3^+W_3^-)]\}\, e^{m\gamma_2 D} \,. \qquad (4.2.28)$$

We have established the general form of the solution in terms of the six constants A_0, A_1, A_2, A_3, B_1 and B_2 defined in this section. In this solution, the explicit form of $G_{1,2}(z)$ and $W^{\pm}_{1,2,3}$ determines whether the solution represents the magnetic field due to a surface or internal wave. When $G_{1,2}(z)$ and $W^{\pm}_{1,2,3}$ are expressed in terms of a_1 and P_+, the solutions give the magnetic field arising from a surface wave of amplitude $|a_1|$, whereas when they are expressed in terms of a_2 and P_-, the field is that of an internal wave of amplitude $|a_2|$. The magnetic field corresponding to each of the above two situations will be obtained in the following two sections.

4.3 The magnetic field induced by an internal wave

We shall now determine the magnetic field arising from an internal wave. The frequency of propagation of the wave will be obtained from P_-, by equation (4.1.10). All the terms $G_{1,2}(z)$ and $W^{\pm}_{1,2,3}$ in the general solution will be expressed in terms of the internal wave amplitude a_2 and P_-.

After substitution for $\psi_{1,2}$ from (4.1.1) and (4.1.2) respectively, equation (4.2.2) becomes

$$G_1(z) = -\tfrac{1}{2}m^2\omega^{-1}\{(F_x + iF_z)(N_1+M_1)e^{mz}_{+} (F_x - iF_z)(N_1-M_1)e^{-mz}\},$$

$$G_2(z) = \tfrac{1}{2}m^2\omega^{-1}M_2\{(F_x - iF_z)e^{m(L-z)}_{-} (F_x + iF_z)e^{-m(L-z)}\}.$$

Replacing the constants $M_{1,2}$ and N_1 by (4.1.3), (4.1.5) and (4.1.4) respectively, the above equations take the form

$$G_1(z) = \tfrac{1}{2}a_1P_-^{-1}mF\{(1-P_-)(C+iS)e^{mz}_{-} (1+P_-)(C-iS)e^{-mz}\} \tag{4.3.1}$$

and

$$G_2(z) = -\tfrac{1}{2}a_2mF\{(C-iS)e^{m(L-z)}_{-} (C+iS)e^{-m(L-z)}\}/\sinh[m(L-D)]$$

where $F_x = FC$, $F_z = FS$, $C = \cos I \cos\theta$ and $S = \sin I$. Changing a_1 to a_2, by (4.1.6), we obtain after some manipulation the following expressions

$$G_1(z) = a_2 m F U_1^-(z) \exp[-m(D-z)] ,$$

$$G_1'(z) = a_2 m^2 F U_1^+(z) \exp[-m(D-z)] ,$$

$$G_2(z) = -a_2 m F U_2^-(z) \exp[-m(z-D)] , \qquad (4.3.2)$$

$$G_2'(z) = a_2 m^2 F U_2^+(z) \exp[-m(z-D)]$$

where we have put

$$U_1^{\pm}(z) = \{(1-\underline{P})(C+iS) \pm (1+\underline{P})(C-iS)e^{-2mz}\}\{(\underline{P}-1)+(\underline{P}+1)e^{-2mD}\}^{-1},$$

$$U_2^{\pm}(z) = \{(C-iS) \pm (C+iS)e^{-2m(L-z)}\}\{1 - e^{-2m(L-D)}\}^{-1} . \qquad (4.3.3)$$

In conjunction with (4.3.2) and (4.3.3), the expressions (4.2.7), (4.2.11) and (4.2.15) may be rewritten as

$$W_1^{\pm} = \pm a_2 m F V_1^{\pm} \exp(-mD) ,$$

$$W_2^{\pm} = \pm a_2 m F V_2^{\pm} \exp[-m(L-D)] , \qquad (4.3.4)$$

$$W_3^{\pm} = \pm a_2 m F \delta_o V_2^{\pm}$$

where

$$V_1^{\pm} = \{C(1 \mp g_1 \underline{P}) \pm iS(g_1 \mp \underline{P})\}/g_1\{(\underline{P}_- 1)_+ (\underline{P}_+ 1)e^{-2mD}\} , \tag{4.3.5}$$

$$V_2^{\pm} = (C \pm iSg_2)/g_2\{1 - e^{-2m(L-D)}\}$$

and

$$\delta_o = \{(\underline{P}_- 1)_+ (\underline{P}_+ 1)e^{-2mL}\}/\{(\underline{P}_- 1)_+ (\underline{P}_+ 1)e^{-2mD}\} \tag{4.3.6}$$

The six constants, defined by expressions (4.2.23) to (4.2.28), may be written as follows, by using (4.3.4) and (4.3.5),

$$A_o = a_2 m F \bar{A}_o \exp[-mD] ,$$

$$A_1 = a_2 m F \bar{A}_1 \exp[-mg_1 D] ,$$

$$B_1 = a_2 m F \bar{B}_1 \exp[-mD] , \tag{4.3.7}$$

$$A_2 = a_2 m F \bar{A}_2 \exp[-m(L-D) - mg_2 L] ,$$

$$B_2 = a_2 m F \bar{B}_2 \exp[mg_2 D] ,$$

$$A_3 = a_2 m F \bar{A}_3 \exp[mg_3 L - m(L-D)]$$

where

$$\bar{A}_o = \Delta^{-1}\{\delta_2 \exp[-m(q_2+1)(L-D) - m(q_1-1)D]$$

$$+Q_2^-(Q_3^-V_1^+ - \{\delta_o V_2^- + Q_3^+ V_1^- \exp[-m(q_1+1)D]\}\cdot$$

$$\cdot \exp[-m(q_1-1)D])\exp[-2mq_2(L-D)] - Q_2^+(Q_3^+V_1^+$$

$$+\{\delta_o V_2^+ - Q_3^- V_1^- \exp[-m(q_1+1)D]\}\exp[-m(q_1-1)D])\}, \quad (4.3.8)$$

$$\bar{A}_1 = \Delta^{-1}\{Q_1^+\delta_2 \exp[-m(q_2+1)(L-D)]$$

$$-Q_2^-(Q_1^+\delta_o V_2^- + Q_3^+\delta_1 \exp[-m(q_1+1)D])\exp[-2mq_2(L-D)]$$

$$-Q_2^+(Q_1^+\delta_o V_2^+ + Q_3^-\delta_1 \exp[-m(q_1+1)D])\}, \quad (4.3.9)$$

$$\bar{B}_1 = \Delta^{-1}\{Q_1^-\delta_2 \exp[-m(q_2+1)(L-D) - m(q_1-1)D]$$

$$+Q_2^-(Q_3^-\delta_1 - Q_1^-\delta_o V_2^- \exp[-m(q_1-1)D])\exp[-2mq_2(L-D)]$$

$$-Q_2^+(Q_3^+\delta_1 + Q_1^-\delta_o V_2^+ \exp[-m(q_1-1)D])\}, \quad (4.3.10)$$

$$\bar{A}_2 = \Delta^{-1}\{\delta_2 b_1 - Q_2^-[\{Q_1^-\delta_3^+\delta_0 \exp[-m(g_1-D)]$$
$$+ (g_1/g_2)\delta_1\}\exp[-m(g_1+1)D]$$
$$+ Q_1^+\delta_3^-\delta_0]\exp[-m(g_2-1)(L-D)]\}\ , \qquad (4.3.11)$$

$$\bar{B}_2 = \Delta^{-1}\{\delta_2 b_2 \exp[-m(g_2+1)(L-D)]$$
$$- Q_2^+[\{Q_1^-\delta_3^+\delta_0 \exp[-m(g_1-1)D] + (g_1/g_2)\delta_1\}\cdot$$
$$\cdot\exp[-m(g_1+1)D] + Q_1^+\delta_3^-\delta_0]\}\ , \qquad (4.3.12)$$

$$\bar{A}_3 = \Delta^{-1}\{V_2^- b_1 + (V_2^+ b_2 \exp[-m(g_2+1)(L-D)]$$
$$- Q_1^-\delta_3^+\delta_0 \exp[-2mg_1D] - (g_1/g_2)\delta_1 \exp[-m(g_1+1)D]$$
$$- Q_1^+\delta_3^-\delta_0)\exp[-m(g_2-1)(L-D)]\}\ ; \qquad (4.3.13)$$

and,

$$\delta_1 = (P_- + 1)(C - iS)/g\{(P_- - 1) + (P_- + 1)e^{-2mD}\}\ ,$$
$$\delta_2 = (C + iSg_3)/g_2\{1 - \exp[-2m(L-D)]\}\ ,$$
$$\delta_3^{\pm} = (C \pm iSg_1)/g_2\{1 - \exp[-2m(L-D)]\}\ . \qquad (4.3.14)$$

With the help of (4.3.7) and (3.6.3), the amplitudes $(\underline{h}_j)_{x,z}$ of the magnetic field $\underline{H}_j$ are expressed as follows

$$(\underline{h}_0)_x = -ia_2 m F \bar{A}_0 \exp[m(z-D)] ,$$

$$(\underline{h}_0)_z = a_2 m F \bar{A}_0 \exp[m(z-D)] ,$$

$$(\underline{h}_1)_x = -ia_2 m F \{ g_1 \bar{A}_1 \exp[-m(g_1-1)(D-z)] - g_1 \bar{B}_1 \cdot$$

$$\cdot \exp[-m(g_1+1)z] + U_1^+(z) \} \exp[-m(D-z)] ,$$

$$(\underline{h}_1)_z = a_2 m F \{ \bar{A}_1 \exp[-m(g_1-1)(D-z)] + \bar{B}_1 \cdot$$

$$\cdot \exp[-m(g_1+1)z] + U_1^-(z) \} \exp[-m(D-z)] ,$$

$$(\underline{h}_2)_x = -ia_2 m F \{ g_2 \bar{A}_2 \exp[-m(g_2+1)(L-z)] - g_2 \bar{B}_2 \cdot$$

$$\cdot \exp[-m(g_2-1)(z-D)] + U_2^+(z) \} \exp[-m(z-D)] , \quad (4.3.15)$$

$$(\underline{h}_2)_z = a_2 m F \{ \bar{A}_2 \exp[-m(g_2+1)(L-z)] + \bar{B}_2 \cdot$$

$$\cdot \exp[-m(g_2-1)(z-D)] - U_2^-(z) \} \exp[-m(z-D)] ,$$

$$(\underline{h}_3)_x = ia_2 m F g_3 \bar{A}_3 \exp[-m g_3 (z-L) - m(L-D)] ,$$

$$(\underline{h}_3)_z = a_2 m F \bar{A}_3 \exp[-m g_3 (z-L) - m(L-D)] .$$

The above solution completely describes the magnetic field induced by an internal wave of amplitude a_2 and ocean wave number m.

4.4 The magnetic field induced by a surface wave

Turning to the magnetic field produced by a surface wave in a two layer ocean, we note that the field should now be expressed in terms of the surface wave amplitude a_1 with its corresponding frequency obtained from P_+ .

Changing a_2 to a_1, by (4.1.6), and letting P_- be P_+ now, the expressions (4.3.2) and (4.3.4) take the form

$$
\begin{aligned}
G_1(z) &= (a_1 m F/2P_+)\,\tilde{U}_1^-(z)\, e^{-mz} \quad , \\
G_1'(z) &= (a_1 m^2 F/2P_+)\,\tilde{U}_1^+(z)\, e^{-mz} \quad , \\
G_2(z) &= -(a_1 m F/2P_+)\,\tilde{U}_2^-(z)\, e^{-mz} \quad , \\
G_2'(z) &= (a_1 m^2 F/2P_+)\,\tilde{U}_2^+(z)\, e^{-mz} \quad , \\
W_1^{\pm} &= \pm (a_1 m F/2P_+)\,\tilde{V}_1^{\pm} \quad , \\
W_2^{\pm} &= \pm (a_1 m F/2P_+)\,\gamma_0\,\tilde{V}_2^{\pm}\, e^{-mL} \quad , \\
W_3^{\pm} &= \pm (a_1 m F/2P_+)\,\gamma_1 V_2^{\pm}\, \exp[-2m(L-D)-mD] \quad ,
\end{aligned}
\tag{4.4.1}
$$

where

$$
\tilde{U}_1^{\pm}(z) = (1-P_+)(C+iS)\, e^{2mz} \pm (1+P_+)(C-iS) \quad ,
$$

$$\tilde{U}_2^{\pm}(\bar{z}) = \gamma_o \{ (C - iS) \pm (C + iS) \exp[-2m(L-\bar{z})] \} ,$$

(4.4.2)

$$\tilde{V}_1^{\pm} = \{ C(1 \mp \beta_1 P_+) \pm iS(\beta_1 \mp P_+) \} / \beta_1 ,$$

$$\tilde{V}_2^{\pm} = (C \pm iS\beta_2) / \beta_2$$

and

$$\gamma_o = \{ (P_+ - 1) e^{2mD} + (P_+ + 1) \} / \{ 1 - \exp[-2m(L-D)] \} ,$$

(4.4.3)

$$\gamma_1 = \{ (P_+ - 1) e^{2mL} + (P_+ + 1) \} / \{ 1 - \exp[-2m(L-D)] \} .$$

In conjunction with the expressions (4.4.1) and (4.4.2), the six constants defined by (4.2.23) to (4.2.28) become after some algebra

$$A_o = (a_1 mF / 2P_+) \tilde{A}_o ,$$

$$A_1 = (a_1 mF / 2P_+) \tilde{A}_1 \exp[-m(\beta_1 + 1)D] ,$$

$$B_1 = (a_1 mF / 2P_+) \tilde{B}_1 , \qquad (4.4.4)$$

$$A_2 = (a_1 mF / 2P_+) \tilde{A}_2 \exp[-m(\beta_1 + 1)L] ,$$

$$B_2 = (a_1 mF / 2P_+) \tilde{B}_2 ,$$

$$A_3 = (a_1 mF / 2P_+) \tilde{A}_3 \exp[m(\beta_3 - 1)L]$$

where

$$\tilde{A}_o = \Delta^{-1}\{\tilde{V}_1^-(Q_2^+Q_3^- \exp[-2mg_1D] - Q_2^-Q_3^+ \exp[-2mg_2L + 2m(g_2-g_1)D]) - \gamma_1(Q_2^+\tilde{V}_2^+ + Q_2^-\tilde{V}_2^- \exp[-2mg_2(L-D)])\cdot \exp[-2mL - m(g_1-1)D] + \gamma_0\gamma_3 \exp[-m(g_2+1)L + m(g_2-g_1)D] - \tilde{V}_1^+(Q_2^+Q_3^+ - Q_2^-Q_3^- \exp[-2mg_2(L-D)])\}, \quad (4.4.5)$$

$$\tilde{A}_1 = \Delta^{-1}\{(Q_1^+\gamma_0\gamma_3 - Q_2^-Q_3^+\gamma_2 \exp[-m(g_2-1)L + m(g_2-g_1)D])\cdot \exp[-m(g_2+1)(L-D)] - Q_1^+\gamma_1(Q_2^+\tilde{V}_2^+ + Q_2^-\tilde{V}_2^- \exp[-2mg_2(L-D)])\cdot \exp[-2m(L-D)] + Q_2^+\gamma_2Q_3^- \exp[-m(g_1-1)D]\}, \quad (4.4.6)$$

$$\tilde{B}_1 = \Delta^{-1}\{Q_2^-(Q_3^-\gamma_2 \exp[-2mg_2(L-D)] - Q_1^-\gamma_1\tilde{V}_2^- \exp[-m(g_1+1)D - 2m(g_2+1)(L-D)]) - Q_2^+(Q_3^+\gamma_2 + Q_1^-\gamma_1\tilde{V}_2^+ \exp[-2m(L-D) - m(g_1+1)D]) + Q_1^-\gamma_0\gamma_3 \exp[-m(g_2+1)L + m(g_2-g_1)D]\}, \quad (4.4.7)$$

$$\tilde{A}_2 = \Delta^{-1}\{(\gamma_0\gamma_3b_1) - Q_2^-(\gamma_2[g_1/g_2] \exp[-m(g_2-1)L + m(g_2-g_1)D]$$

$$+\gamma_1(\varphi_1^+\gamma_4^- + \varphi_1^-\gamma_4^+ \exp[-2m\xi_1 D])\exp[-m(\xi_2+1)(L-D)])\}\ , \quad (4.4.8)$$

$$\tilde{B}_2 = \Delta^{-1}\{(\gamma_0\gamma_3\varphi_1^-\varphi_3^+ \exp[-m(\xi_2+1)L + m(\xi_2-\xi_1)D] - \varphi_2^+(\xi_1/\xi_2)\gamma_2)\cdot$$
$$\cdot\exp[m(\xi_2-\xi_1)D] + (\gamma_0\gamma_3\varphi_1^+\varphi_3^- \exp[-m(\xi_2-1)(L-D)] - \varphi_2^+\gamma_1\cdot$$
$$\cdot\{\varphi_1^+\gamma_4^- + \varphi_1^-\gamma_4^+ \exp[-2m\xi_1 D]\})\exp[-2m(L-D)+m(\xi_2-1)D]\}, \quad (4.4.9)$$

$$\tilde{A}_3 = \Delta^{-1}\{\gamma_0\tilde{V}_2^- b_1 + (\gamma_0\varphi_1^-\varphi_3^+\tilde{V}_2^+ \exp[-m(\xi_2+1)L + m(\xi_2-\xi_1)D]$$
$$-(\xi_1/\xi_2)\gamma_2)\exp[-m(\xi_2-1)L + m(\xi_2-\xi_1)D]$$
$$+(\gamma_0\varphi_1^+\varphi_3^-\tilde{V}_2^+ \exp[-m(\xi_2-1)(L-D)] - \gamma_1\{\varphi_1^+\gamma_4^-$$
$$+\varphi_1^-\gamma_4^+ \exp[-2m\xi_1 D]\})\exp[-m(\xi_2+1)(L-D)]\}\ . \quad (4.4.10)$$

Here we have defined

$$\gamma_2 = (P_+ + 1)(C - iS)/\xi_1\ ,$$
$$\gamma_3 = (C + iS\xi_3)/\xi_2\ , \quad (4.4.11)$$
$$\gamma_4^{\pm} = (C \pm iS\xi_1)/\xi_2\ .$$

Therefore, substituting (4.4.1) and (4.4.4) into the general solution (4.2.3), we arrive at

$$(\underline{h}_o)_x = -i(a_1 mF/2P_+)\tilde{A}_o \exp[mz] \ ,$$

$$(\underline{h}_o)_z = (a_1 mF/2P_+)\tilde{A}_o \exp[mz] \ ,$$

$$(\underline{h}_1)_x = -i(a_1 mF/2P_+)\{g_1\tilde{A}_1 \exp[-m(g_1+1)(D-z)]$$

$$-g_1\tilde{B}_1 \exp[-m(g_1-1)z] + \tilde{U}_1^+(z)\}\exp[-mz] \ ,$$

$$(\underline{h}_1)_z = (a_1 mF/2P_+)\{\tilde{A}_1 \exp[-m(g_1+1)(D-z)]$$

$$+\tilde{B}_1 \exp[-m(g_1-1)z] + \tilde{U}_1^-(z)\}\exp[-mz] \ ,$$

(4.4.12)

$$(\underline{h}_2)_x = -i(a_1 mF/2P_+)\{g_2\tilde{A}_2 \exp[-m(g_2+1)(L-z)]$$

$$-g_2\tilde{B}_2 \exp[-m(g_2-1)z] + \tilde{U}_2^+(z)\}\exp[-mz] \ ,$$

$$(\underline{h}_2)_z = (a_1 mF/2P_+)\{\tilde{A}_2 \exp[-m(g_2+1)(L-z)]$$

$$+\tilde{B}_2 \exp[-m(g_2-1)z] - \tilde{U}_2^-(z)\}\exp[-mz] \ ,$$

$$(\underline{h}_3)_x = ig_3(a_1 mF/2P_+)\tilde{A}_3 \exp[-mg_3(z-L) - mL] \ ,$$

$$(\underline{h}_3)_z = (a_1 mF/2P_+)\tilde{A}_3 \exp[-mg_3(z-L) - mL] \ .$$

These equations everywhere describe the magnetic field induced by a surface wave, for a two layer ocean.

4.5 Special cases

The results (4.3.15) and (4.4.12) are the exact solutions to the problem, but are cumbersome to examine analytically. It is possible, however, to obtain the solutions of the magnetic field in a simple form for two special cases. The first case treats surface waves only, and we will show that the solutions reduce to those obtained by a direct solution of the simple surface wave model (Weaver, 1965), thereby providing a useful check on the validity of the general solution obtained here. The second case describes the simplest possible model involving an internal wave.

(a) We now consider an ordinary surface wave over an infinitely deep ocean with respect to the wavelength (i.e. $mL >> 1$). Furthermore, the density and the electrical conductivity of the sea are assumed to have everywhere the constant value ρ and σ respectively, i.e. $\rho_1 = \rho_2 = \rho$ and $\sigma_1 = \sigma_2 = \sigma$. Thus no induced wave is present since $\alpha = 1$.

Equation (4.1.10), with $\alpha = 1$, becomes

$$P_+ = \tanh (mL). \qquad (4.5.1)$$

As the depth to wavelength ratio is large, the frequency of propagation of the surface wave is

$$P_+ = \omega^2/gm = 1 \quad , \qquad (4.5.2)$$

by (4.5.1). Since $\sigma_1 = \sigma_2 = \sigma$, it is clear that $q_1 = q_2 = q$ now, from this we see that $Q_3^+ = 1$ and $Q_3^- = 0$. Substituting (4.5.1) into

(4.4.3), we readily find $\gamma_0 = 2$ and $\gamma_1 = 0$. In conjunction with the above simplifications, we may establish from (4.4.2)

$$\tilde{U}_1^{\pm} \exp[-mz] = \pm 2(C - iS) \exp[-mz] ,$$

$$\tilde{U}_2^{\pm} \exp[-mz] = 2(C - iS) \exp[-mz] , \qquad (4.5.3)$$

$$\tilde{V}_1^{\pm} = \{ C(1 \mp g) \pm iS(g \mp 1) \} / g$$

and, from (4.2.22)

$$\Delta = - Q_1^+ Q_2^+ . \qquad (4.5.4)$$

Therefore, remembering that the ratio mL >> 1, the constants defined by (4.4.5) to (4.4.10) take the simple form

$$\tilde{A}_0 = \tilde{V}_1^+ / Q_1^+ ,$$

$$\tilde{B}_1 = \tilde{B}_2 = \gamma_2 / Q_1^+ , \qquad (4.5.5)$$

$$\tilde{A}_1 = \tilde{A}_2 = \tilde{A}_3 = 0$$

where

$$\gamma_2 = 2(C - iS)/g .$$

Here the constants $A_{1,2,3}$ have been set to zero since when substituted into the solution (4.4.12) each term involving one of these constants is at least of the order of exp(-mL). Substitution of (4.5.3) and (4.5.5) into the solution (4.4.12), yields

$$(\underline{h}_o)_x = -ia_1 mF(C-iS)(1-q)(1+q)^{-1}\exp(mz),$$

$$(\underline{h}_o)_z = a_1 mF(C-iS)(1-q)(1+q)^{-1}\exp(mz),$$

$$(\underline{h})_x = ia_1 mF(C-iS)\{2q(1+q)^{-1}\exp[-m(q-1)z]-1\}e^{-mz}, \tag{4.5.6}$$

$$(\underline{h})_z = a_1 mF(C-iS)\{2(1+q)^{-1}\exp[-m(q-1)z]-1\}e^{-mz}.$$

We note that $(\underline{h}_3)_x = (\underline{h}_3)_z = 0$. Previously, the ocean was divided into two layers with corresponding solutions for each layer. However, by assuming the same density and conductivity throughout the ocean the distinction between the two layers disappeared. Consequently, the two solutions for the layers became identical, i.e. $(\underline{h}_1)_x = (\underline{h}_2)_x = (\underline{h})_x$ and $(\underline{h})_z = (\underline{h}_1)_z = (\underline{h}_2)_z$.

The result (4.5.6), describing the magnetic field induced by a surface wave of amplitude $|a_1|$, may be simplified by noting that

$$q = (1+i\beta)^{\frac{1}{2}} = 1 + i\beta/2 + O(\beta^2)$$

where

$$\beta = 4\pi\sigma\omega/m^2 .$$

Thus the terms involving q may be approximated. This is possible since β is at most of order 10^{-1} for a surface wave of one minute

period, while at shorter periods typical of surface waves β becomes much smaller. The term $\exp(-1/2\beta mz)$ in (4.5.6) may also be approximated by the first two terms of its Taylor expansion, provided $1/2\beta mz$ is less than unity. Thus expansion of the terms involving β in (4.5.6), while neglecting terms $0(\beta^2)$, yields the approximate solution

$$
\begin{aligned}
(\underline{h}_o)_x &= -\pi a_1 \sigma F (g/m)^{\frac{1}{2}} (c - iS) \exp(mz) \ , \\
(\underline{h}_o)_z &= -i\pi a_1 \sigma F (g/m)^{\frac{1}{2}} (c - iS) \exp(mz) \ , \\
(\underline{h})_x &= \pi a_1 \sigma F (g/m)^{\frac{1}{2}} (c - iS)(2mz - 1) \exp(-mz) \ , \\
(\underline{h})_z &= -i\pi a_1 \sigma F (g/m)^{\frac{1}{2}} (c - iS)(2mz + 1) \exp(-mz) \ .
\end{aligned}
\qquad (4.5.7)
$$

Here we have substituted for β and used (4.5.2). Apart from an arbitrary phase factor-1, the solutions (4.5.6) and (4.5.7) agree with those obtained by Weaver (1965), who has treated this case in detail.

(b) Next, we will examine the special case of an internal wave whose wavelength is negligible when compared with the depth of the lower fluid layer (i.e. $m(L-D) \gg 1$). As before, we assume that the sea has a constant electrical conductivity σ everywhere (i.e. $\sigma_1 = \sigma_2 = \sigma$). The propagation frequency will be given by P_-, from (4.1.10)

$$
P_- = \omega^2/gm = (\alpha - 1) b / (\alpha + b) \qquad (4.5.8)
$$

where $c = \tanh[m(L-D)]$ has been approximated by unity since $m(L-D) \gg 1$.

Because $\sigma_1 = \sigma_2 = \sigma$, it follows that we may put $q_1 = q_2 = q$, thus $Q_3^+ = 1$ and $Q_3^- = 0$. Using (4.5.8), we immediately find

$$(P_- - 1) + (P_- + 1)\, e^{-2mD} = -2P_-/(\alpha - 1) \quad . \tag{4.5.9}$$

The six constants, defined by expressions (4.3.8) to (4.3.13), become with the help of the above relations

$$\begin{aligned}
\bar{A}_0 &= [(\alpha-1)/(1+g)P_-]\{(Cg + iS)P_- - (C + iSg)\cdot \\
&\qquad \cdot(1 - [1-P_-]\exp[-m(g-1)D])\}, \\
\bar{A}_1 &= (\alpha-1)(1-P_-)(C + iSg)/2g_- \quad , \\
\bar{B}_1 &= [(\alpha-1)/2gP_-(1+g)]\{(g-1)(1-P_-)(C + iSg)\cdot \\
&\qquad \cdot\exp[-m(g-1)D] - 2g(1+P_-)(C - iS)\} \quad , \\
\bar{B}_2 &= [(\alpha-1)/2gP_-(1+g)]\{(1+g)(1-P_-)(C - iSg) + [(g-1)(1-P_-)\cdot \\
&\qquad \cdot(C+iSg)\exp[-m(g-1)D] - 2g(1+P_-)(C-iS)]\exp[-m(g+1)D]\}, \\
\bar{A}_2 &= \bar{A}_3 = 0 \quad .
\end{aligned} \tag{4.5.10}$$

Here the constants $\bar{A}_{2,3}$ have been set to zero, since in the general solution (4.3.15) they will form terms of order exp [-m(L-D)]. Furthermore, the expressions for $U^{\pm}_{1,2}(z)$, from (4.3.3), take the form

$$U_1^{\pm}(z) = -[(\alpha-1)/2P_-]\{(1-P_-)(C+iS) \pm (1+P_-)(C-iS)e^{-2mz}\}, \tag{4.5.11}$$

$$U_2^{\pm}(z)\exp[-m(z-D)] = (C-iS)\exp[-m(z-D)] \quad .$$

Substituting (4.5.10) and (4.5.11) into the general solution (4.3.15), we obtain the magnetic field induced by an internal wave. The resultant solution is still rather cumbersome. However, the formulas for the induced field above the ocean are relatively simple compared with those for the field below the surface. Moreover, we will simplify the solution for the field above the ocean even further so as to check our result against that obtained by a direct solution of the simple internal wave model (Weaver, 1966). To examine the field above the ocean, we assume that the internal wave lies close to the surface (i.e. the depth of the boundary of density discontinuity D is small compared with 1/m). The propagation frequency will now be

$$P = \omega^2/gm = (\alpha - 1)mD/\alpha \quad , \tag{4.5.12}$$

obtained by expanding $b = \tanh(mD)$ in (4.5.8) and discarding terms $O(m^2D^2)$. Hence, using (4.5.10) and (4.5.12), we obtain

$$\bar{A}_o = (i\beta/4)\{(C - iS)(\alpha - 1) - (C + iS)\alpha\} \quad .$$

Here, as in the previous case, the terms containing q in $\bar{A}_o$ have been expanded in terms of β (of order 10^{-3} or less for typical conditions) and, terms $O(\beta^2)$ and $O(\beta mD)$ have been neglected. Substituting the above expression into (4.3.15) and expanding $\exp(-mD)$ we immediately obtain

$$(\underline{h}_o)_z = i(\underline{h}_o)_x \quad , \tag{4.5.13}$$

$$(\underline{h}_o)_x = -\pi a_2 \sigma F\{C + iS(2\alpha - 1)\}\{gD(1 - 1/\alpha)\}^{\frac{1}{2}} e^{mz} \quad .$$

Here we have substituted for β and, again, discarded terms $O(\beta mD)$. Thus (4.5.13) completely describes, in air, the induced field from an internal wave of amplitude $|\, a_2 \,|$. This solution was first obtained by Weaver (1966).

Since, measurements of the magnetic variations within the sea are also made, it is of interest to obtain a simple expression for the solutions near the internal wave itself. This is more easily accomplished if we first assume that the wavelength is very small compared with the depth of the internal density discontinuity, i.e. $mD \gg 1$. This effectively removes any influence that the free surface has on the solutions. With this approximation the propagation frequency is now

$$P_- = \omega^2/gm = (\alpha - 1)/(\alpha + 1) \qquad (4.5.14)$$

obtained from (4.5.8) with $b = 1$. From the above result, it is clear that

$$(\alpha-1)(1-P_-)/2P_- = 1 \quad . \qquad (4.5.15)$$

In conjunction with the above assumption, (4.5.14) and (4.5.15), expressions (4.5.10) and (4.5.11) become

$$\bar{A}_1 = (C + iS_g)/g \quad ,$$

$$\bar{B}_2 = (C - iS_g)/g \quad ,$$

$$\bar{A}_o = \bar{B}_1 = \bar{A}_2 = \bar{A}_3 = 0 \quad ,$$

$$U_1^{\pm}(z)\exp[-m(D-z)] = -(C+iS)\exp[-m(D-z)] \quad ,$$

$$U_2^{\pm}(z)\exp[-m(z-D)] = (C-iS)\exp[-m(z-D)] \quad .$$

The constants $\bar{A}_o$ and $\bar{B}_1$ have been set to zero since in the solution (4.3.15) they will form terms of order exp(-mD). After substituting the above five expressions into (4.3.15), we then expand the expressions containing q in powers of β and neglect all terms $0(\beta^2)$. Terms of the form $\exp|\pm i\beta m(D-z)|$ are present in the solution; these can also be approximated by the first two terms of their Taylor expansion if $1/2\beta m|D-z|$ is less than unity. The approximate solutions for the induced field directly above and below the internal wave are now

$$\begin{aligned}
(\underline{h}_1)_x &= \bar{a}_2\{Cm\bar{z} + iS(1+m\bar{z})\}\exp[m\bar{z}] \quad , \\
(\underline{h}_1)_z &= -\bar{a}_2\{Sm\bar{z} + iC(1-m\bar{z})\}\exp[m\bar{z}] \quad , \\
(\underline{h}_2)_x &= \bar{a}_2\{Cm\bar{z} + iS(1-m\bar{z})\}\exp[-m\bar{z}] \quad , \\
(\underline{h}_2)_z &= -\bar{a}_2\{Sm\bar{z} + iC(1+m\bar{z})\}\exp[-m\bar{z}]
\end{aligned} \qquad (4.5.16)$$

where

$$\bar{z} = z - D \quad ,$$

$$\bar{a}_2 = 2\pi a_2 \sigma F\{(\alpha-1)g/(\alpha+1)m\}^{\frac{1}{2}} \quad .$$

4.6 The expansion parameter

It is now possible to see precisely how the expansion parameter ε should be chosen. Let us use the inverse wave number as our scale of length, and denote by primes the distance measured in these units (e.g. $\eta_j' = \eta_j m$, $x' = xm$). We can also define a non-dimensional velocity potential ϕ_j' and magnetic field H_j' by the expressions

$$\phi_j' = (m^2/\omega)\,\phi_j \quad ,$$

$$H_j' = H_j / F$$

where F is the Earth's magnetic field strength. Substituting (4.1.1) into the expressions for ϕ_j' with $j = 1$ and then (4.1.2) into ϕ_j' with $j = 2$, we obtain respectively

$$\phi_1' = a_1' \{ \sinh(z') - P^{-1}\cosh(z') \} \exp(i\omega t - ix')$$

and

$$\phi_2' = -a_2' \{ \cosh(L'-z') / \sinh(L'-D') \} \exp(i\omega t - ix') .$$

Note that P is a non-dimensional quantity. Since we originally defined ε to be a non-dimensional parameter such that the velocity potential was of the form

$$\epsilon\phi_j + O(\epsilon^2) \quad ,$$

we see immediately that for surface waves a suitable choice for ε is

$$\epsilon = |a_1'| \quad .$$

Since

$$|a_2'| = |a_2'/a_1'|\,\epsilon < \epsilon \quad ,$$

we note that both ϕ_1' and ϕ_2' are now of the required form. If, on the other hand, we are considering internal waves, we choose

$$\epsilon = |a_2'|$$

and then

$$|a_1'| = |a_1'/a_2'|\,\epsilon < \epsilon \quad .$$

We now have

$$\eta_{1,2}' = -i\,a_{1,2}'\exp(i\omega t - ix') \quad ,$$

hence $\eta_{1,2}'$ is of the order of ε also, as required by the theory in chapter three. Furthermore, because of the factor $a_{1,2}'F$ in front of the solutions (4.3.15) and (4.4.12), the magnetic field H_j' is of the order of ε also.

Thus the linearized theory is valid provided that the amplitude-wavelength ratio of the surface or internal waves is small (i.e. $\varepsilon \ll 1$). This condition imposes a severe restriction on the allowed amplitudes of the waves, but for wavelengths of practical interest in this study the linearized theory will be entirely adequate.

4.7 The induced electric field associated with surface and internal ocean waves

We have restricted this study to the induced magnetic field. However, with very little difficulty the induced electric field can be obtained from the solutions in this chapter.

Substituting the expansions (3.3.3) and (3.3.4) for $\underline{H}_j$ and $\underline{E}_j$ respectively into the equations (3.2.3) and (3.2.4), we obtain (with superscripts (1) omitted)

$$\text{curl } \underline{E}_j = -\partial \underline{H}_j / \partial t \quad , \tag{4.7.1}$$

$$\text{curl } \underline{H}_j = (4\pi\sigma_j + k_j \partial / c^2 \partial t)\, \underline{E}_j + 4\pi\sigma_j (\nabla \phi_j \times \underline{F}) \quad . \tag{4.7.2}$$

Here we have neglected all terms $0(\varepsilon^2)$. Taking the divergence of (4.7.2), we have

$$(4\pi\sigma_j + k_j \partial / c^2 \partial t)\, \text{div } \underline{E}_j = 0 \quad . \tag{4.7.3}$$

Replacement of $\underline{E}_j$ in (4.7.3) by (3.5.4), yields

$$(\underline{e}_j)_x = d(\underline{e}_j)_z / im\, dz \quad . \tag{4.7.4}$$

Taking the y component of (4.7.1) and using (3.5.3), (3.5.4) and (4.7.4), we arrive at the differential equation

$$[\, d^2/dz^2 - m^2 \,] (\underline{e}_j)_z = 0 \quad . \tag{4.7.5}$$

Here, we made use of the result $(\underline{H}_j)_y = 0$ obtained in section 3.5. The solutions of (4.7.5) for $j = 0$ and $j = 3$ are clearly of the form

$$(\underline{e}_0)_z = A \exp(mz) \quad ,$$

$$(\underline{e}_3)_z = B \exp(-mz) \quad , \tag{4.7.6}$$

respectively, since the electric field must vanish at infinity both within the air and the ocean bed. Within the ocean, the component $(\underline{e}_j)_z$ can be obtained directly by taking the z component of (4.7.2) in conjunction with (3.5.2), (3.5.3), (3.5.4) and the approximation (3.5.9). Thus we obtain with little difficulty

$$(\underline{e}_j)_z = im\psi_j F_y \quad , \quad j = 1,2 \; . \tag{4.7.7}$$

To evaluate the constants A and B in (4.7.6), we may use the expressions (3.4.17) and (3.4.19) which state that the x component of the electric field is continuous across the undisturbed surfaces $z = 0$ and $z = L$. But by (4.7.4), this is equivalent to demanding that $d(\underline{e}_j)_z/dz$ shall be continuous across these two surfaces. Application of this boundary condition to (4.7.6) and (4.7.7), yields

$$A = i\,(d\psi_1/dz)_{z=0}\, F_y$$

and

$$B = -i(d\psi_2/dz)_{z=L} F_y \exp(mL) = 0 \qquad (4.7.8)$$

since there can be no fluid motion normal to the ocean floor. Taking the z component of (4.7.1), we obtain

$$(\underline{e}_j)_y = (\omega/m)(\underline{h}_j)_z \qquad (4.7.9)$$

In summary we see that the components of the electric field are given everywhere by

$$(\underline{e}_j)_x = \begin{cases} (d\psi_1/dz)_{z=0} F_y \exp(mz) & j = 0 \\ (d\psi_j/dz)\ F_y & j = 1,2 \\ 0 & j = 3 \end{cases} \qquad (4.7.10)$$

$$(\underline{e}_j)_y = (\omega/m)(\underline{h}_j)_z \qquad j = 0,1,2,3$$

$$(\underline{e}_j)_z = \begin{cases} i(d\psi_1/dz)_{z=0} F_y \exp(mz) & j = 0 \\ im\psi_j F_y & j = 1,2 \\ 0 & j = 3 \end{cases}$$

Here the x component of the field was found by (4.7.4). The above expressions give the induced electric field everywhere for a surface or internal ocean wave in a two layer ocean. The exact form of the solutions can be found by substituting the appropriate expressions for the velocity potential and the z component of the induced magnetic field.

The principal component of the induced electric field is, of course in the y - direction. It is simply related to the vertical magnetic field by the formula (4.7.10).

CHAPTER 5

DISCUSSION OF MAGNETIC VARIATIONS INDUCED BY INTERNAL OCEAN WAVES

5.1 Introduction

It was pointed out in Chapter 1 that the magnetic field generated by surface waves has already been described in some detail by Crews and Futterman, Warburton and Caminiti, Weaver, and Larsen. Therefore, in this chapter we shall restrict our discussion to the fields associated with internal ocean waves.

From the general solution (4.3.15), we shall derive some useful algebraic approximations which are valid under certain stated conditions. The simplified formulas so obtained are useful for discussing the physical interpretation of the general solution under relevant conditions, and will also be helpful in checking the numerical results which were obtained by programming (4.3.15) for solution on a digital computer (Appendix A).

Most of the accurate magnetometry at sea has been done with "total field" magnetometers, which record the magnetic field in the direction of the Earth's main field $\underline{F}$. Thus, in addition to $(\underline{h}_j)_x$ and $(\underline{h}_j)_z$, we shall compute the component $(\underline{h}_j)_{//}$ defined by

$$(\underline{h}_j)_{//} = (\underline{h}_j)_x C + (\underline{h}_j)_z S \qquad (5.1.1)$$

where

$$C = \cos I \cos\theta \ , \quad S = \sin I \ .$$

The components at time t and position x other than zero can be obtained by multiplying the appropriate component of $(\underline{h}_j)$ by the factor $\exp(i\omega t - imx)$.

In all the calculations we take $\alpha = 1.01$, and $F = 0.5\ G$, $I = 70^{\circ}$, which are typical values for mid-latitudes in the northern hemisphere. The curves shown are for the case $\theta = 0^{\circ}$ only, i.e. waves travelling in the direction of the magnetic north. The modified behaviour for different values of θ, and of I, will be indicated by the approximate solutions to be discussed shortly.

Figure 7, depicts graphically the relationship between wavelength and period for an internal wave under various conditions, as given by the formula (4.1.10). Note that the wavelength-period relationship is not particularly sensitive to changes in ocean depth L ; unless the wavelength is large compared with the depth.

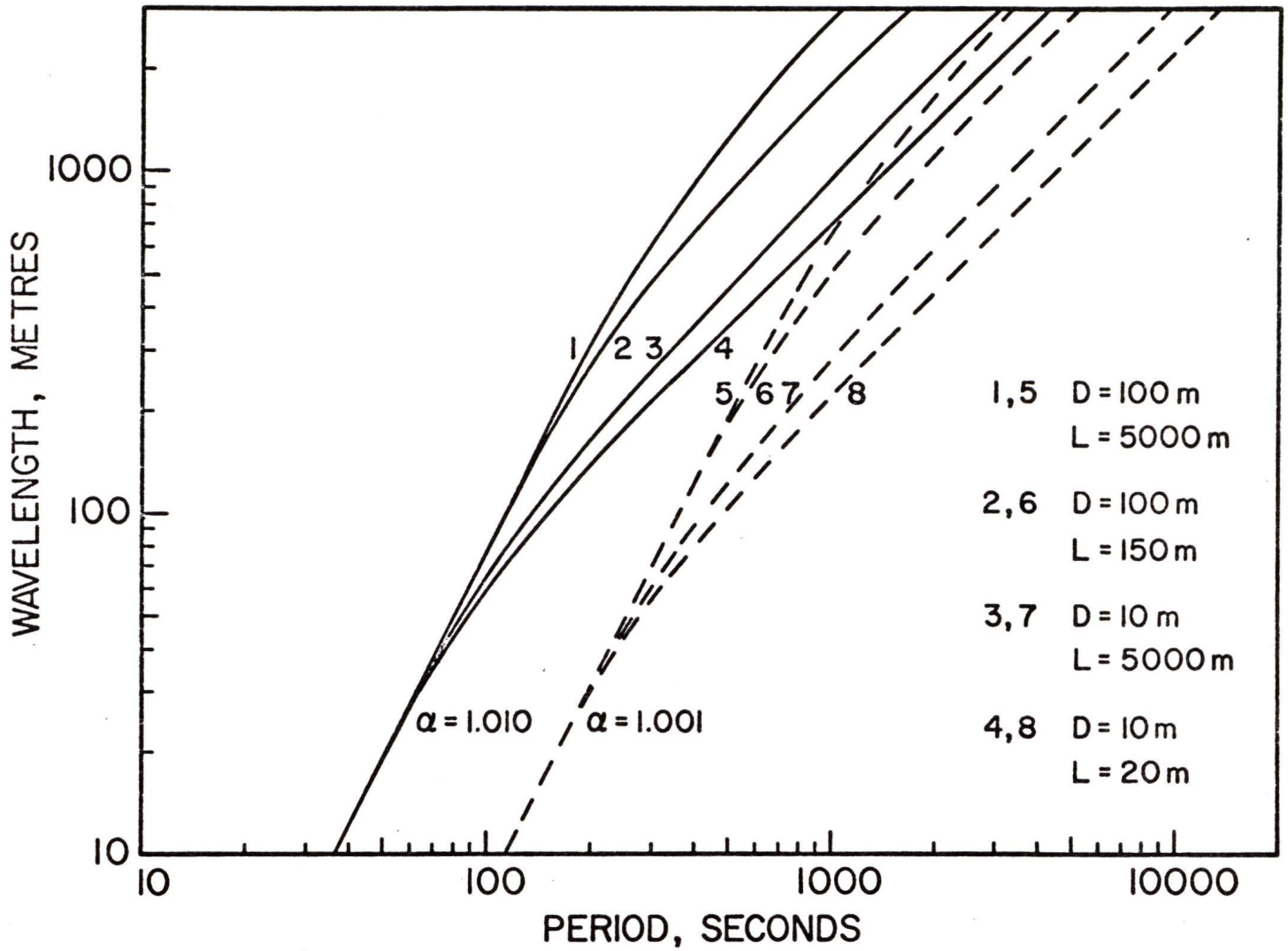

Fig. 7. Wavelength versus period for an internal wave, for various upper and lower layer depths.

5.2 The induced magnetic field in a deep ocean of constant conductivity

In this section we shall discuss a deep ocean for which $\sigma_1 = \sigma_2 = \sigma$. The numerical results were obtained for L = 5000 m and $\sigma = 4 \times 10^{-11}$ emu. Curves showing the variation of $|(\underline{h}_j)_{11}|$ with altitude and depth are shown for upper layer thicknesses of 100 m and 10 m in Figures 8 and 9 respectively. In both the figures, it is readily apparent that $|(\underline{h}_j)_{11}|$ behaves quite differently according as the wavelength is smaller or larger than the depth of the upper layer.

For wavelengths small compared to the depth of the upper layer we can use the approximate solution (4.5.16). The magnitude of the components are given by

$$
\begin{aligned}
|(\underline{h}_1)_x| &= \bar{a}_2 \{ C^2 (m\bar{z})^2 + S^2 (1 + m\bar{z})^2 \}^{\frac{1}{2}} e^{m\bar{z}} , \\
|(\underline{h}_1)_{\bar{z}}| &= \bar{a}_2 \{ S^2 (m\bar{z})^2 + C^2 (1 - m\bar{z})^2 \}^{\frac{1}{2}} e^{m\bar{z}} , \\
|(\underline{h}_2)_x| &= \bar{a}_2 \{ C^2 (m\bar{z})^2 + S^2 (1 - m\bar{z})^2 \}^{\frac{1}{2}} e^{-m\bar{z}} , \\
|(\underline{h}_2)_{\bar{z}}| &= \bar{a}_2 \{ S^2 (m\bar{z})^2 + C^2 (1 + m\bar{z})^2 \}^{\frac{1}{2}} e^{-m\bar{z}}
\end{aligned}
\qquad (5.2.1)
$$

whence, by (5.1.1),

$$
|(\underline{h}_1)_{//}| = \bar{a}_2 (C^2 + S^2) |m\bar{z}| e^{m\bar{z}} ,
$$

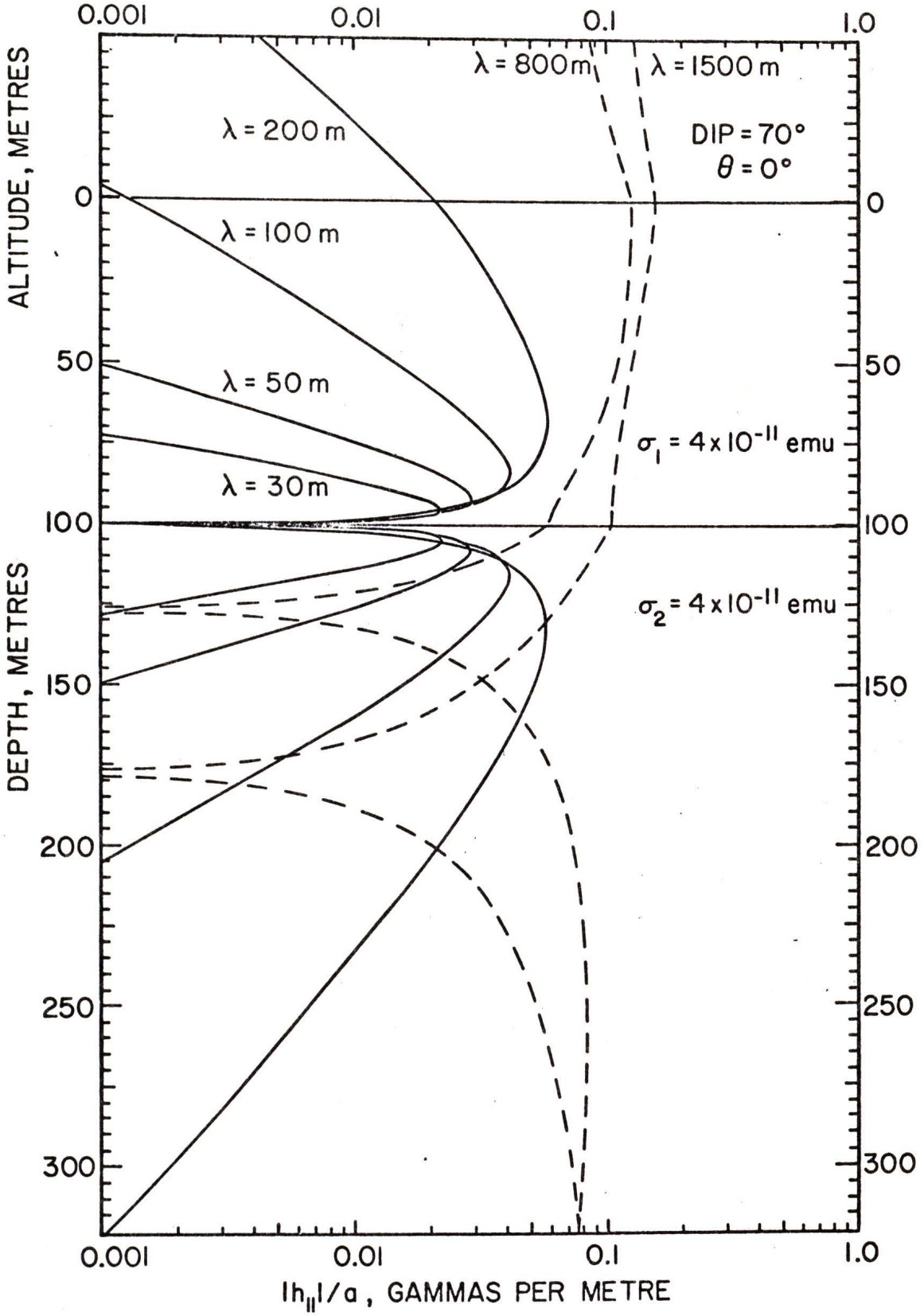

Fig. 8. The magnitude of the induced magnetic field, in an ocean of constant conductivity, per metre amplitude of an internal wave at a depth of 100 m as a function of depth and altitude, for various wavelengths.

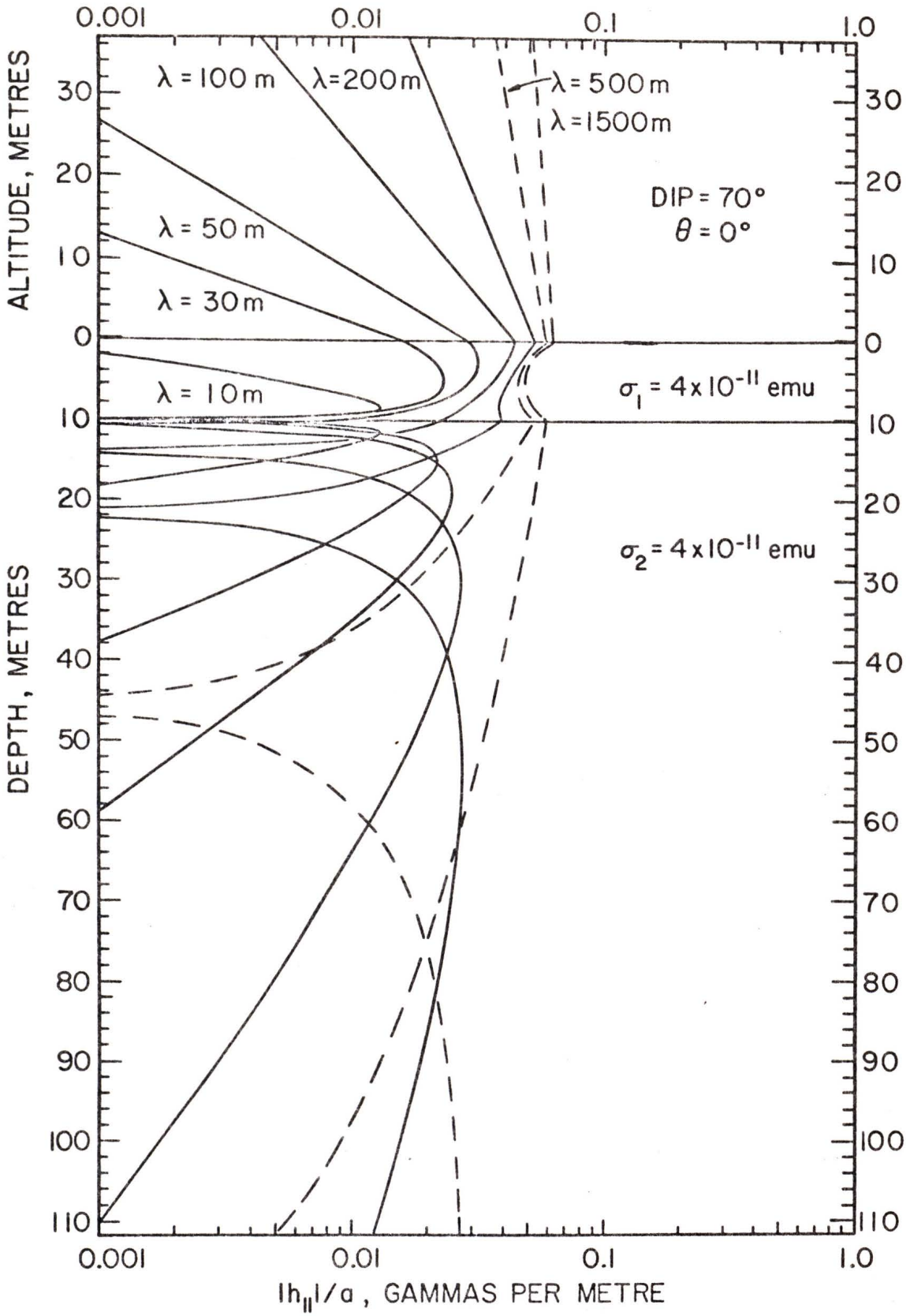

Fig. 9. The magnitude of the induced magnetic field, in an ocean of constant conductivity per metre amplitude of an internal wave at a depth of 10 m as a function of depth and altitude, for various wavelengths.

$$|(\underline{h}_2)_{11}| = \bar{a}_2 (c^2 + s^2) |m\bar{z}| \, e^{-m\bar{z}} \qquad (5.2.2)$$

where

$$\bar{z} = z - D$$

$$\bar{a}_2 = 2\pi a_2 \sigma F \{ (\alpha - 1) q / (\alpha + 1) m \}^{\frac{1}{2}} .$$

We note that the parallel component, as defined by (5.2.2), will always vanish at the interface z = D. By considering the derivative of $|(\underline{h}_j)_{11}|$ with respect to z , we can readily show that this component reaches its maximum value of

$$|(\underline{h}_j)_{11}|_{MAX} = \bar{a}_2 (c^2 + s^2) \, e^{-1} \quad , \qquad j = 1, 2 \qquad (5.2.3)$$

at $z = D \mp 1/m$. Thus a magnetometer suspended at either one of these depths will measure the largest signal. Figures 8 and 9 clearly illustrate this behaviour of $|(\underline{h}_j)_{11}|$. Furthermore, the angles I and θ are seen to only affect the magnitude and not the position of $|(\underline{h}_j)_{11}|_{MAX}$. For wavelengths less than 100 m, we see from the two figures that an amplitude of several metres is required to generate measurable signals. For example, from Figures 8 and 9 we note that at least an amplitude of 3.5 m is required to give the appreciable value of 0.1 γ for $|(\underline{h}_j)_{11}|_{MAX}$. Since amplitudes of 3 m or more are not common for short internal waves, we may conclude that these waves do not induce significant magnetic signals.

Figure 10 illustrates the variation of $|(\underline{h}_j)_x|$ and $|(\underline{h}_j)_z|$ with depth and latitude for an upper layer thickness of 100 m. We first note that above the ocean surface $|(\underline{h}_o)_x|$ and $|(\underline{h}_o)_z|$ are the same. In fact, it is immediately apparent from (4.3.15) that when $j = 0$

$$|(\underline{h}_o)_x| = |(\underline{h}_o)_z| \quad .$$

For wavelengths which are small compared with the thickness of the upper layer, it is easily established from (5.2.1) that $|(\underline{h}_j)_x|$ possesses two turning points above the density interface and two below it. The turning values are given by

$$|(\underline{h}_j)_x| = \bar{a}_2 |c| e^{-1} , \quad j = 1, 2 \qquad (5.2.4)$$

at $z = D \mp 1/m$ and

$$|(\underline{h}_j)_x| = \bar{a}_2 |s| \exp[-2s^2/(c^2 + s^2)] , \quad j = 1, 2 \qquad (5.2.5)$$

at $z = D \mp 2s^2/(c^2 + s^2)m$. The component $|(\underline{h}_j)_z|$ has one turning value

$$|(\underline{h}_1)_z| = |(\underline{h}_2)_z| = \bar{a}_2 |c| \qquad (5.2.6)$$

at the interface $z = D$, and the turning values

$$|(\underline{h}_j)_z| = \bar{a}_2 |s| \exp[-(s^2 - c^2)/(c^2 + s^2)] , \quad j = 1, 2 \qquad (5.2.7)$$

above and below the interface at $z = D \mp (s^2 - c^2)/(c^2 + s^2)m$. The above turning points, as predicted from the approximate solution (5.2.1), do indeed describe the behaviour illustrated in Figure 10 for the case $I = 70^\circ$ and $\theta = 0^\circ$. The shape of the curves for any other

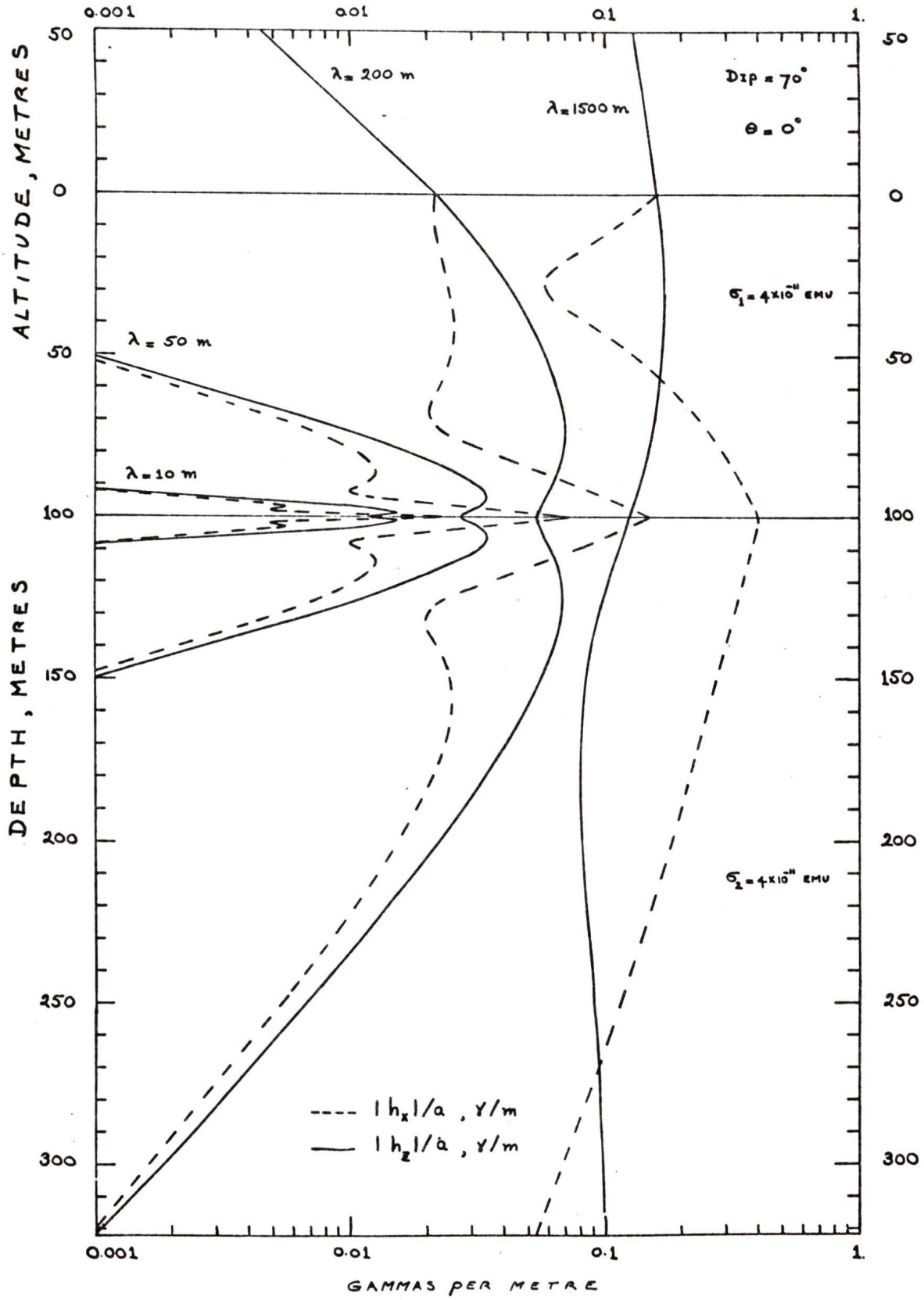

Fig. 10. A magnitude of the induced x and z components of the magnetic field, in an ocean of constant conductivity, per metre amplitude of an internal wave at a depth of 100 m as a function of depth and altitude, for various wavelengths.

values of I and θ can be predicted with the help of the above turning points. In addition, we shall find the schematic diagram shown in Figure 11 useful in explaining the physical behaviour of the field for two cases, (i) $S = 0$ ($I = 0^{\circ}$) and $C \neq 0$, and (ii) $C = 0$ ($\theta = 90^{\circ}$) and $S \neq 0$. Surface and bottom effects are neglected in Figure 11, since the wavelength is very small compared with the depth of both the upper and lower layer.

(i) When $I = 0^{\circ}$, we note that there is no z component of the Earth's field present, and hence only the vertical fluid motion will induce a magnetic field. For this situation we may deduce from Figure 11 that the magnitude of the x component should vanish at the boundary of the density discontinuity, while the z component should attain its maximum value at this boundary. This is confirmed by substituting $S = 0$ in the turning values for $|(\underline{h}_j)_x|$ and $|(\underline{h}_j)_z|$. The diagram in Figure 11 also indicates that it is not possible for $|(\underline{h}_j)_z|$ to have turning values other than its maximum at $z = D$, since the induced $(\underline{h}_j)_z$ fields are all in the same direction and diminish smoothly away from the interface. However, when $S = 0$, the locations of the turning values of $(\underline{h}_j)_z$ given by (5.2.7) reduce to $z = D \pm 1/m$, for $j = 1,2$ respectively. These positions are clearly not valid since they are not within the appropriate ranges $0 \leq z \leq D$ and $D \leq z \leq L$ for $j = 1$ and $j = 2$ respectively, and we may conclude in fact that $|(\underline{h}_j)_z|$ has only one maximum when $S = 0$.

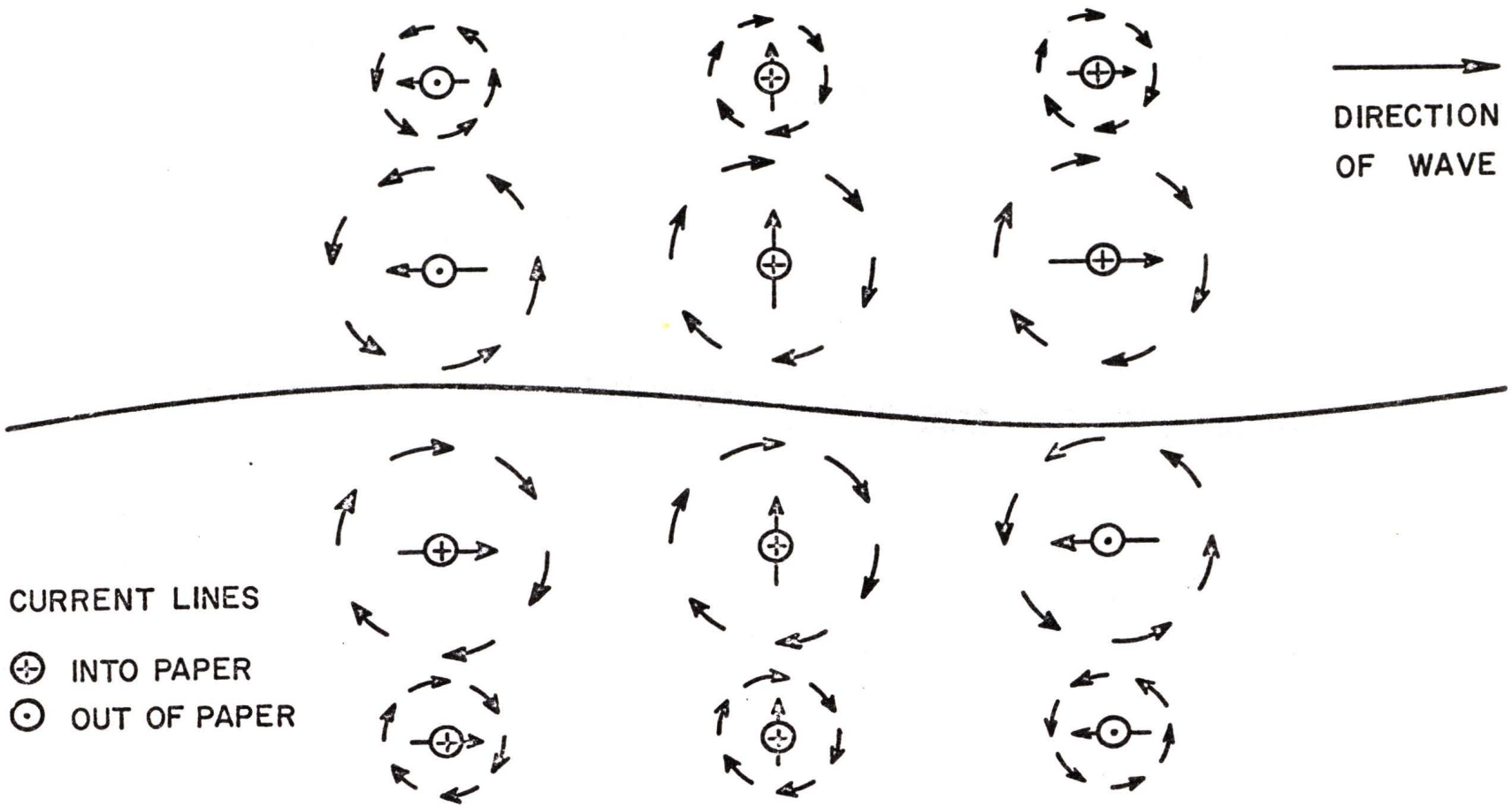

Fig. 11. A schematic diagram showing the instantaneous magnetic field loops from the elementary current lines induced by the internal wave motion across the Earth's magnetic field lines. The horizontal and vertical arrows indicate the direction of the fluid particle velocities. The fluid above and below the internal wave has the same electrical conductivity.

(ii) If $\theta = 90^{\circ}$, we note that now there is no x component of the Earth's main field present, and only the horizontal fluid motion induces the magnetic field. From Figure 11, we see that this time the x component of the induced field should attain its maximum value at the density interface, while the z component of the field should vanish at this boundary. This is easily confirmed by substituting $C = 0$ into the expression (5.2.1) for $|(\underline{h}_j)_x|$ and into the turning value (5.2.6) for $|(\underline{h}_j)_z|$. Furthermore, from Figure 11 we see that a net value of $|(\underline{h}_1)_x|$ exists just above the interface. Now the x component of the field generated by the fluid motion just below the interface is oppositely directed to the x component of the field generated by the motion just above the interface. Thus the combination of these two fields in the neighbourhood of the interface will cause $|(\underline{h}_1)_x|$ and $|(\underline{h}_2)_x|$ to pass through minimum values there. This behaviour is indeed confirmed by substituting $C = 0$ in the turning values (5.2.4) and (5.2.5).

We shall now discuss the variation of the components of $|\underline{h}_j|$ when the wavelength is very large compared with the depth of the upper layer but not so large as to invalidate the approximation of a very deep ocean. Under these conditions, this behaviour illustrated in Figures 8, 9 and 10, can be discussed in terms of some simple approximate expressions. Above the ocean surface, we have from (4.5.13) that

$$|(\underline{h}_0)_x| = |(\underline{h}_0)_z| = A\{C^2 + S^2(2\alpha-1)^2\}^{\frac{1}{2}} e^{mz}$$

whence, by (5.1.1),

$$|(\underline{h}_o)_{II}| = (c^2 + s^2)^{\frac{1}{2}} |(\underline{h}_o)_x| \qquad (5.2.8)$$

where

$$A = \pi a_2 \sigma F \{ g D (1 - 1/\alpha) \}^{\frac{1}{2}} .$$

For the components within the sea, we can obtain suitable approximate expressions by substituting (4.5.10) into the general solution (4.3.15). The resultant expressions are expanded in terms of the parameter β , and all terms $O(\beta^2)$ and $O(\beta mz)$ are neglected by a procedure analogous to the one used to derive (4.5.13). After some algebra, we obtain for $j = 1$

$$\begin{aligned}
|(\underline{h}_1)_x| &= A\{ c^2 + s^2 [(2\alpha - 1) - 4\alpha z/D]^2 \}^{\frac{1}{2}} , \\
|(\underline{h}_1)_z| &= A\{ c^2 + s^2 (2\alpha - 1)^2 \}^{\frac{1}{2}} , \\
|(\underline{h}_1)_{II}| &= A\{ (c^2 + s^2)[c^2 + s^2 (2\alpha - 1)^2] - 16\alpha^2 s^2 c^2 (1 - z/D) z/D \}^{\frac{1}{2}} ,
\end{aligned} \qquad (5.2.9)$$

and for $j = 2$

$$\begin{aligned}
|(\underline{h}_2)_x| &= A\{ c^2 + s^2 (2\alpha + 1)^2 \}^{\frac{1}{2}} \exp[-m(z - D)] , \\
|(\underline{h}_2)_z| &= A\{ c^2 + s^2 (2\alpha - 1)^2 \}^{\frac{1}{2}} \exp[-m(z - D)] , \\
|(\underline{h}_2)_{II}| &= A\{ (c^2 + s^2)[c^2 + s^2 (2\alpha - 1)^2] \}^{\frac{1}{2}} \exp[-m(z - D)] .
\end{aligned} \qquad (5.2.10)$$

The approximate expressions (5.2.10) are perfectly valid when $\beta m(z-D)$ can be neglected in comparison with unity. At the very worst, this implies that the formulas are accurate up to depths $z = 2D$.

We should note that the expressions (5.2.8) evaluated at z = 0, (5.2.9), and (5.2.10) evaluated at z = D, are all independent of the wavelength. This is a consequence of our approximation and shows that for long wavelengths the field depends only upon the fluid motion near the observation point. Again by taking the derivative of $|(\underline{h}_1)_{11}|$ with respect to z , we readily establish that this component reaches its minimum value of

$$|(\underline{h}_1)_{11}|_{MIN} = A\,|C^2 - S^2(2\alpha-1)^2| \qquad (5.2.11)$$

at z = 1/2 D. Any change in the angles I and θ only alters the value of this minimum and not its position. We also note that at the free surface and at the density interface $|(\underline{h}_1)_{11}|$ has the same magnitude, i.e.

$$|(\underline{h}_1)_{11}|_{z=0} = |(\underline{h}_1)_{11}|_{z=D} = A\{(C^2+S^2)[C^2+S^2(2\alpha-1)^2]\}^{\frac{1}{2}} \qquad (5.2.12)$$

Furthermore, in the lower layer it is seen from (5.2.10) that $|(\underline{h}_2)_{11}|$ should just decrease exponentially with depth. This behaviour of $|(\underline{h}_j)_{11}|$is best illustrated in Figure 9 with the 10 m upper layer and for the curve λ = 1500 m.

In Chapter 2, we saw that the longer internal waves (i.e. wavelengths of 200 m or more) had amplitudes of the order of 2 m and that amplitudes of 5 m were common for waves of 500 m length. Thus, we conclude immediately from Figures 8 and 9 that for these internal ocean waves the induced magnetic signals may indeed be of appreciable

strength. For instance for an upper layer of 100 m, we note from Figure 8 that an 800 m wave of amplitude 2 m induces a field of 0.16 γ and 0.2 γ at 50 m above and below the sea surface respectively, while at a depth of 300 m the field has the value 0.16 γ. Even when the upper layer is only 10 m deep, Figure 9 shows that a 500 m wave of the same amplitude still induces a field of 0.1 γ at 10 m above and below the sea surface.

Turning now to the components $|(\underline{h}_1)_x|$ and $|(\underline{h}_1)_z|$ as defined by (5.2.9), we note that the z component remains constant throughout the upper layer and that the x component possesses the minimum.

$$|(\underline{h}_1)_x|_{MIN} = A|c| \qquad (5.2.13)$$

at $z = (2\alpha - 1)\, D/4\alpha$. From (5.2.9) and (5.2.10), it is clear that the maximum values of $|(\underline{h}_1)_x|$ and $|(\underline{h}_2)_x|$, i.e.

$$|(\underline{h}_j)|_{MAX} = A\{c^2 + S^2(2\alpha+1)^2\}^{\frac{1}{2}}, \quad j = 1,2 \qquad (5.2.14)$$

coincide at the density interface z = D. In the lower layer both the x and z components decrease exponentially with depth. This behaviour is depicted in Figure 10 for an upper layer of thickness 100 m.

Figure 10 also shows quite clearly the trend in the variation of the z component of the induced magnetic field as the wavelength increases. It will be observed that when λ = 1500 m, $|(\underline{h}_1)_z|$ is fairly constant throughout the upper layer, and this variation becomes progressively smaller as the wavelength further increases. This confirms the conclusions drawn from the approximate solution.

The physical behaviour of the x and z components of the magnetic field can be understood by referring to Figure 11. Note, for example, that when C = 0 only the horizontal component of the fluid motion will contribute to the induced magnetic field. Also, since the upper layer depth is much less than one wavelength, the fluid particles there move in very long and flat elliptical orbits, whereas in the lower layer the orbits are nearly circular. Thus the horizontal motion in the upper layer is much greater than below, so that the largest magnetic field is generated above the density interface. Since the z component of the magnetic field generated by the fluid motion above the interface is oppositely directed to that generated by the motion below, we expect the resultant field $|(\underline{h}_2)_z|$ to pass through a minimum value at that depth where the fields originating above and below the interface most nearly cancel each other. Although, this minimum is not given by the approximate expression (5.2.10), this is only because it occurs outside the range for which (5.2.10) is valid. Using an argument similar to that in (ii), we can readily establish that $|(\underline{h}_1)_x|$ and $|(\underline{h}_2)_x|$ will also pass through minimum values. The minimum value of $|(\underline{h}_1)_x|$ has been predicted (5.2.13), while for $|(\underline{h}_2)_x|$ it lies outside the range for which (5.2.10) is valid.

5.3 The induced magnetic field in a deep ocean with a fresh water upper layer

In Chapter 2, we saw that a layer of nearly fresh water is often formed on the ocean surface. In this case, the conductivity of the upper layer may be much less than that of the more saline seawater below, thereby modifying the behaviour of the induced magnetic field. In this section we examine this effect.

Figure 12 shows the variation of $|(\underline{h}_j)_{11}|$ with depth and altitude for L = 5000 m, D = 100 m, $\sigma_2 = 4 \times 10^{-11}$ emu and $\sigma_1/\sigma_2 = 0.1$, and, for the same conditions Figure 13 shows the behaviour for $|(\underline{h}_j)_x|$ and $|(\underline{h}_j)_z|$. Figure 14 shows the curves of $|(\underline{h}_j)_{11}|$, for D = 10 m. If we compare Figures 12, 13 and 14 with Figures 8, 10 and 9 respectively, we see that a change in the upper layer conductivity appreciably affects the behaviour of $|(\underline{h}_j)_{11}|$, and the x and z components, within the sea. To give just one example, we note from Figure 8 ($\sigma_1 = \sigma_2$) that a magnetometer should be placed at the free surface to record the greatest signal of long internal waves at D = 100 m, while in Figure 12 ($\sigma_1 = 0.1\sigma_2$) the best position for the magnetometer is just below the density interface.

It will be noted that when $\sigma_1/\sigma_2 = 0.1$, the field displays the same general variation above and below z = D as does the field of a surface wave on a deep ocean computed by Weaver (1969) and shown in Figure 15. This strongly suggests that an upper layer conductivity

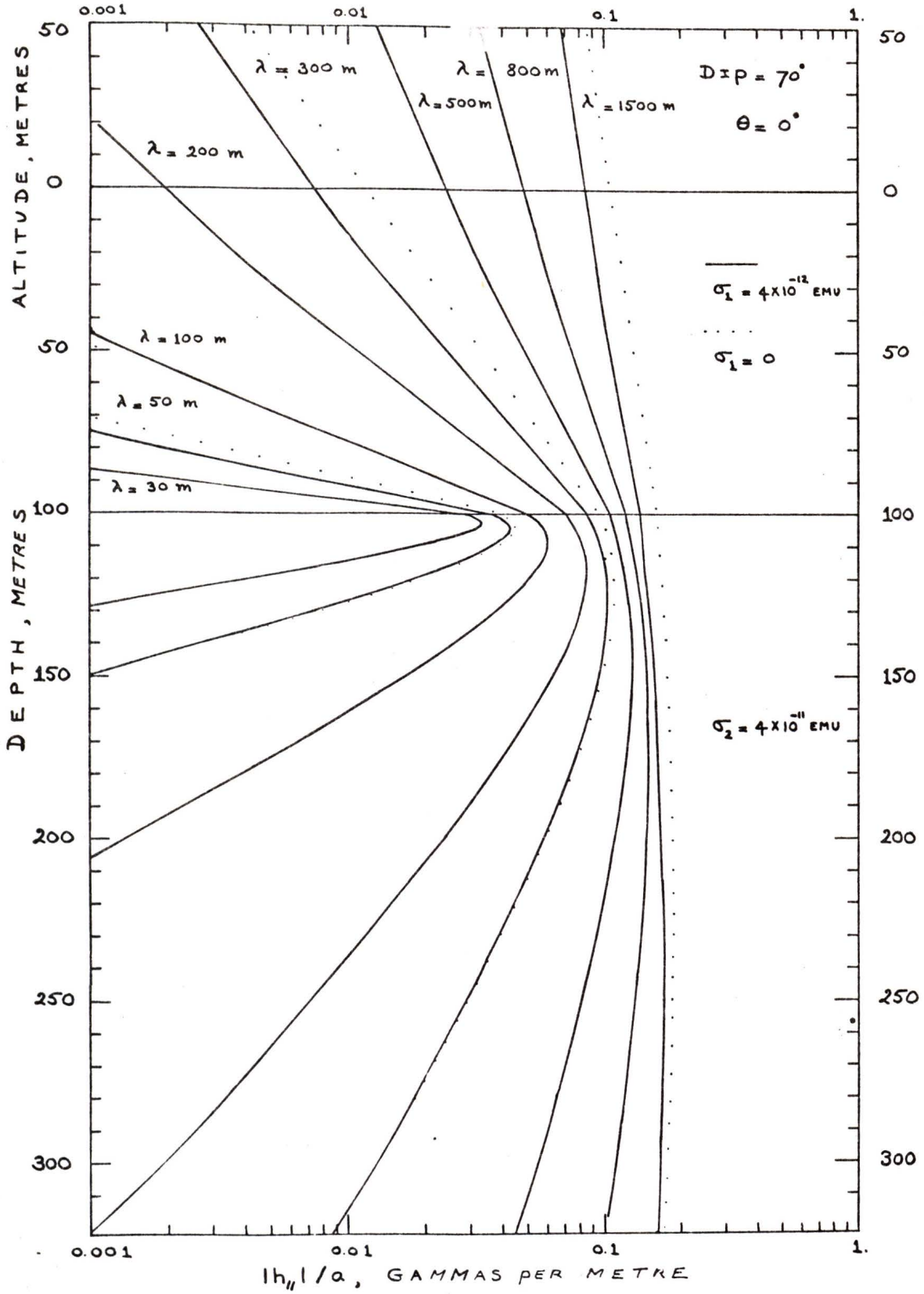

Fig. 12. The magnitude of the induced magnetic field, for two upper layer conductivities, per metre amplitude of an internal wave at a depth of 100 m as a function of depth and altitude, for various wavelengths.

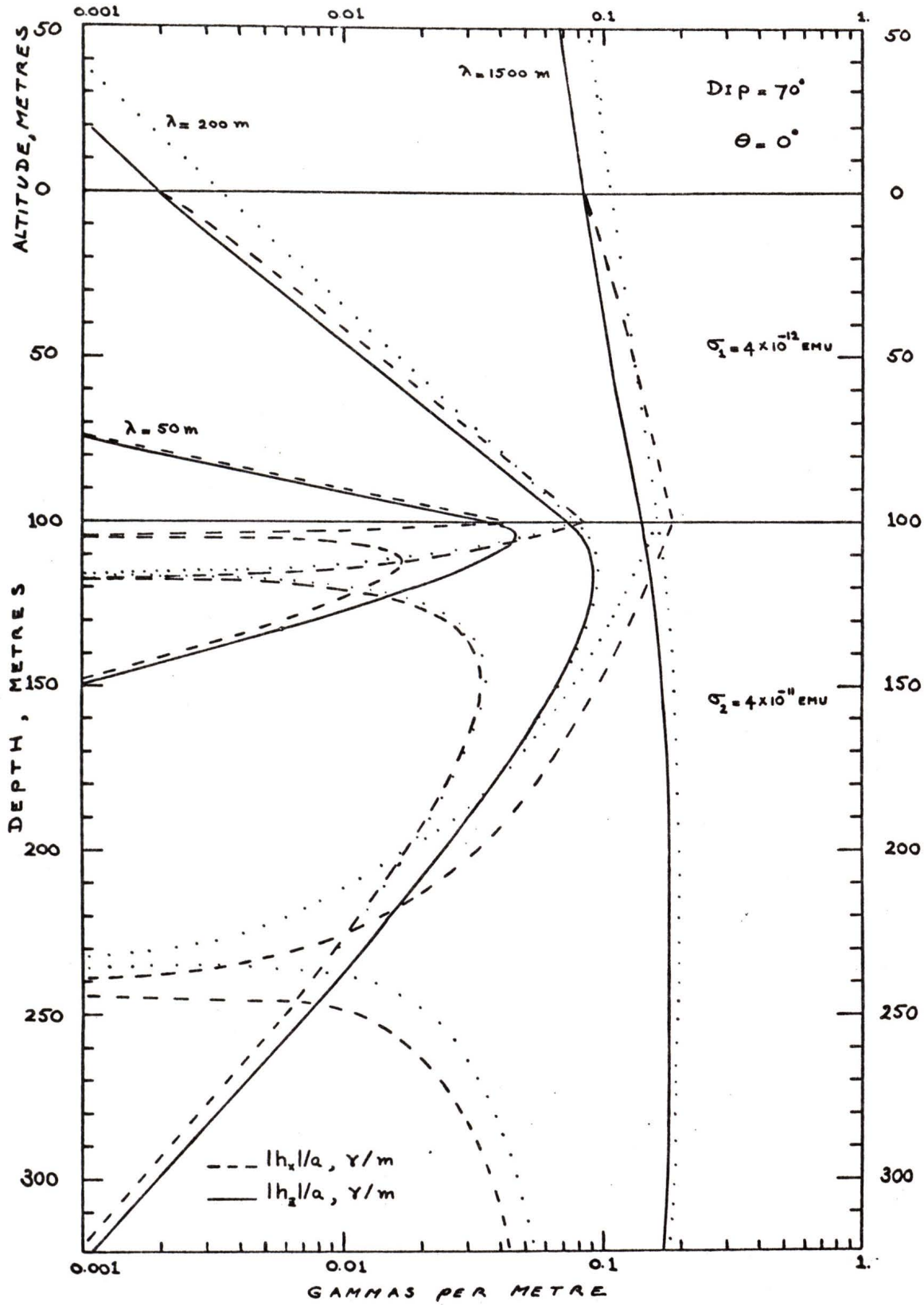

Fig. 13. The magnitude of the induced x and z components of the magnetic field, for two upper layer conductivites, per metre amplitude of an internal wave at a depth of 100 m as a function of depth and altitude, for various wavelengths. The behaviour of the x and z components for $\sigma_1 = 0$ is shown by the dotted lines.

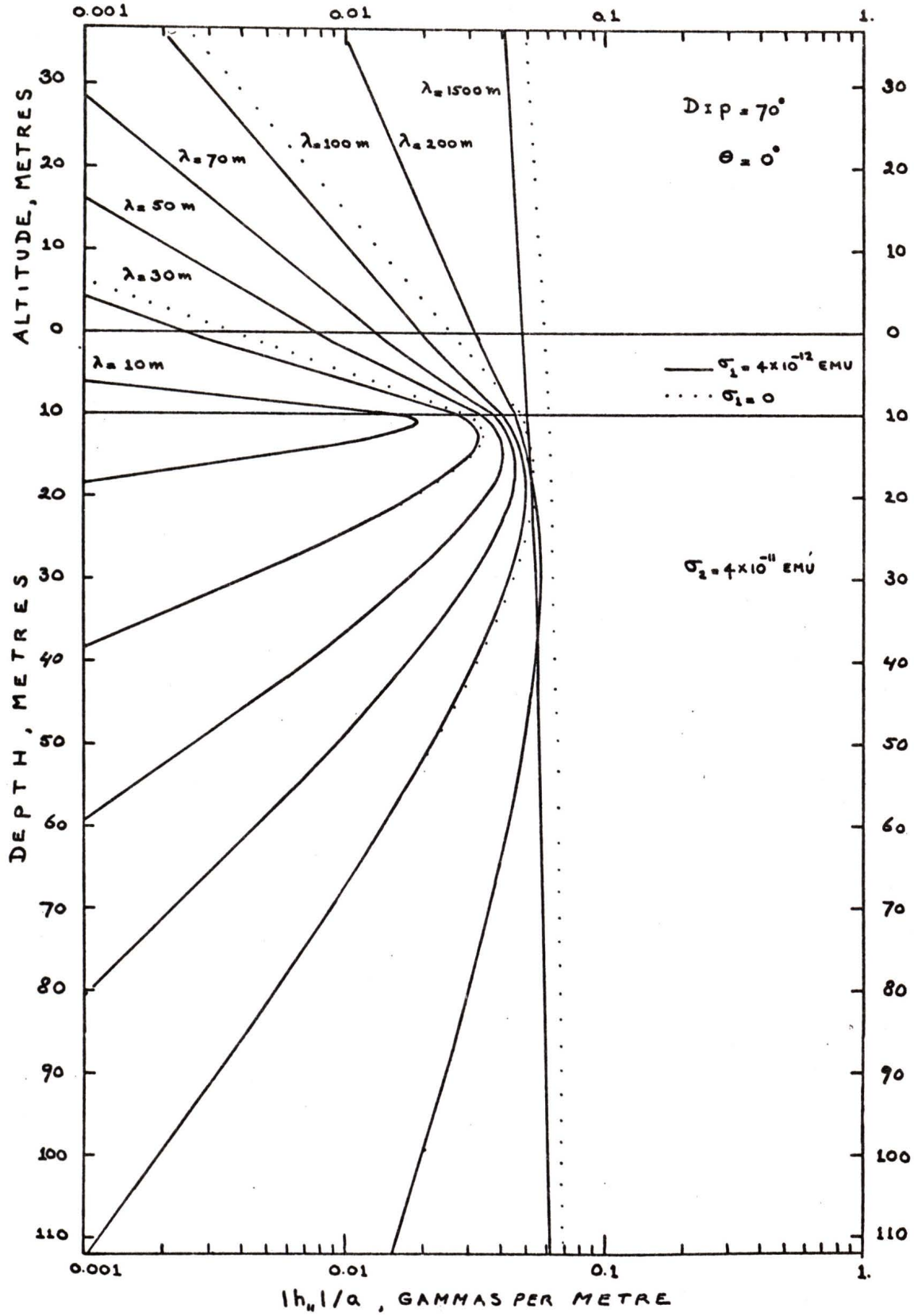

Fig. 14. The magnitude of the induced magnetic field, for two upper layer conductivities, per metre amplitude of an internal wave at a depth of 10 m as a function of depth and altitude, for various wavelengths.

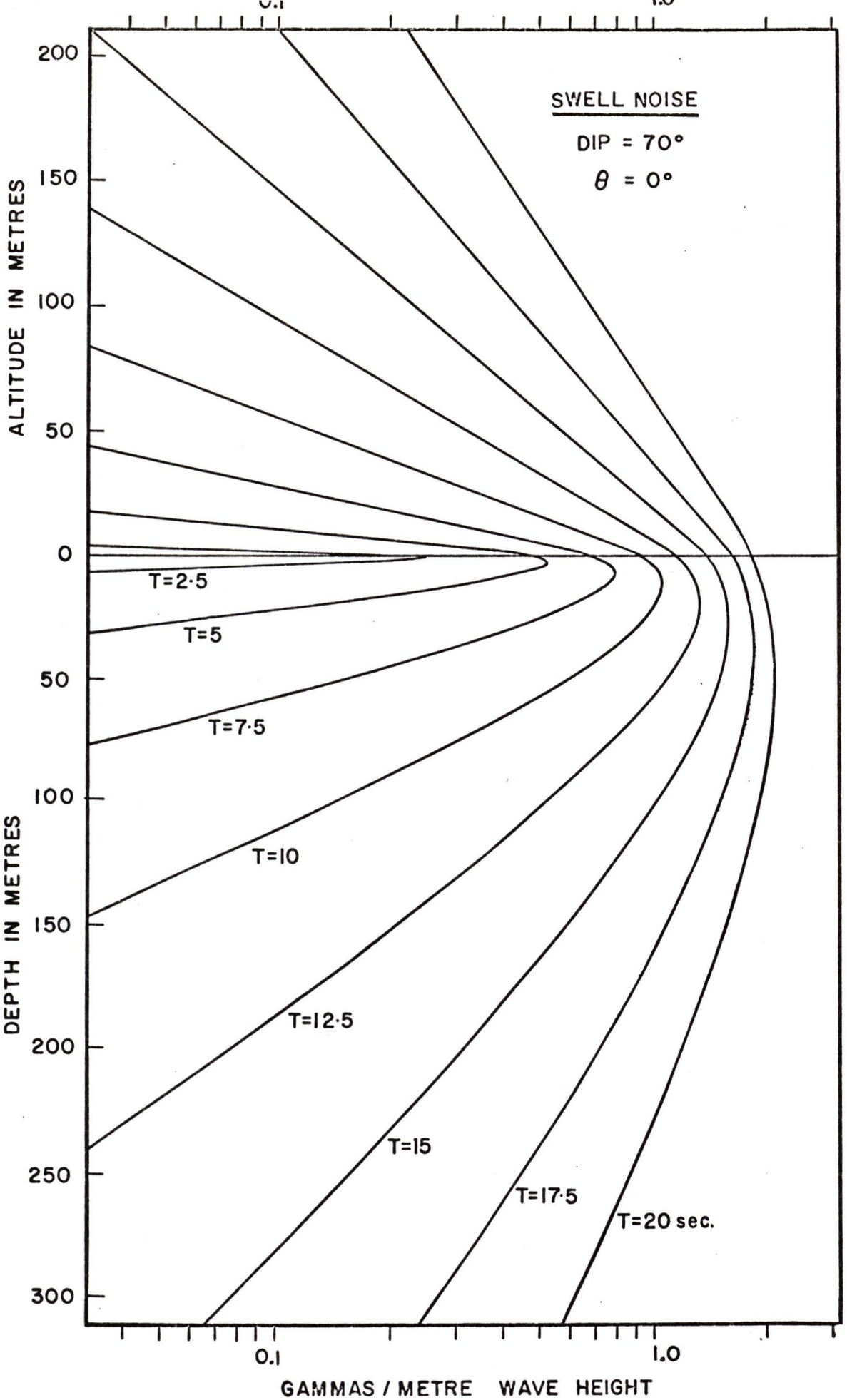

Fig. 15. The magnitude of the induced magnetic field $|h_{11}|$ per metre wave height of a surface wave as a function of depth and altitude, for various wave periods (Weaver, 1969).

of one tenth of that of the lower layer conductivity diminishes the electromagnetic screening effect of the upper layer to such an extent that it behaves almost as an insulator. In other words, as far as electromagnetic effects are concerned, the internal wave behaves as an ordinary surface wave on the "surface" z = D.

To check these conclusions, some calculations were made for the same conditions applying in Figures 12, 13 and 14 but with $\sigma_1 = 0$ i.e. the upper layer a perfect insulator. The results of these calculations are indicated by dots in Figures 12, 13 and 14. The similarity in the shapes of the graphs for the two cases $\sigma_1 = 0.1\sigma_2$ and $\sigma_1 = 0$ is readily apparent.

As a further check on the algebraic correctness of the general solution (4.3.15), the special case corresponding to $\sigma_1 = 0$ was considered. When $L = \infty$, the equations reduce to the form

$$\left.\begin{aligned}(\underline{h}_0)_x &= -i(\underline{h}_0)_{\bar{z}} \\ (\underline{h}_1)_x &= -i(\underline{h}_1)_{\bar{z}}\end{aligned}\right\} = -ia_2 mF(C-iS)(1-g)(1+g)^{-1} e^{m\bar{z}} \qquad (5.3.1)$$

$$(\underline{h}_2)_x = ia_2 mF(C-iS)\{2g(1+g)^{-1}\exp[-m(g-1)\bar{z}] - 1\}\, e^{-m\bar{z}},$$

$$(\underline{h}_2)_{\bar{z}} = a_2 mF(C-iS)\{2(1+g)^{-1}\exp[-m(g-1)\bar{z}] - 1\}\, e^{-m\bar{z}}$$

where

$$\bar{z} = z - D \quad ,$$

which are in complete agreement with the formulas giving the field induced by surface waves on an ocean whose surface is $z = 0$ (see equation (4.5.6)). Note however, that the presence of the upper layer modifies the wavelength-frequency relationship in (5.3.1) from that which applies to (4.5.6). By (4.5.2), this relationship for surface waves is

$$\omega^2/gm = 1 \ ,$$

while for internal waves it is

$$\omega^2/gm = (\alpha - 1)\tanh(mD)/[\alpha + \tanh(mD)] \ ,$$

by (4.1.10).

We may again explain the physical behaviour of the x and z components of the magnetic field by referring to Figure 11. For simplicity we will neglect the magnetic field induced by the motion of the fresh water layer above the density interface, so that we need only consider the field induced by motion of the more saline water below. It can be seen that the z components of the field associated with the current lines in one vertical plane all reinforce each other. Thus we expect $|(\underline{h}_2)_z|$ to diminish smoothly away from the interface with its largest value near the interface. Between two current lines lying in one vertical plane, the x components are seen to be oppositely directed but are unequal in magnitude. At a certain depth, the resultant x component due to all the current lines in a vertical plane above the depth will just cancel an equal but

opposite resultant x component from all current lines below it. The expected behaviour of $|(\underline{h}_2)_x|$ and $|(\underline{h}_2)_z|$ is clearly shown in Figure 13.

From Figures 12 and 14, we may conclude that the magnetic field associated with internal waves, in the presence of a relatively fresh water upper layer, has an appreciable magnitude.

5.4 The induced magnetic field in a shallow ocean

Here we shall briefly discuss the effect of a shallow ocean on the induced magnetic field. This is of some importance since the majority of internal waves which have been observed, have occurred over the continental shelves which range in depth from 20 m to 500 m. The numerical computations were made for two ocean depths with three different upper layer conductivities. Figure 16 shows the variation of $|(\underline{h}_j)_{11}|$ with depth and altitude for $\sigma_2 = 4 \times 10^{-11}$ emu, $\sigma_1/\sigma_2 = 1$, $\sigma_1/\sigma_2 = 0.1$, $\sigma_1/\sigma_2 = 0$, L = 150 m and D = 100 m. Figure 17 shows the same behaviour for L = 20 m and D = 10 m. We immediately note that when $\sigma_1/\sigma_2 = 0.1$ the field is appreciably higher than the field for the case $\sigma_1/\sigma_2 = 1$, and that in the latter case the variations of $|(\underline{h}_j)|$ again behave as though produced by an ordinary surface wave. Often in shallow depths, bottom mounted magnetometers have been used to record the induced magnetic signals. From the curves in Figures 16 and 17, it is clear that the longer internal waves of moderate amplitude can indeed be detected by bottom mounted magnetometers. For example, from Figure 16, we note that a 500 m wave of amplitude 1.5 m for the case $\sigma_1 = \sigma_2$ gives a field of order 0.1 γ at the ocean floor, while the same field is easily induced by a similar wave for the case $\sigma_1 = 0.1\sigma_2$ but of amplitude 1 m.

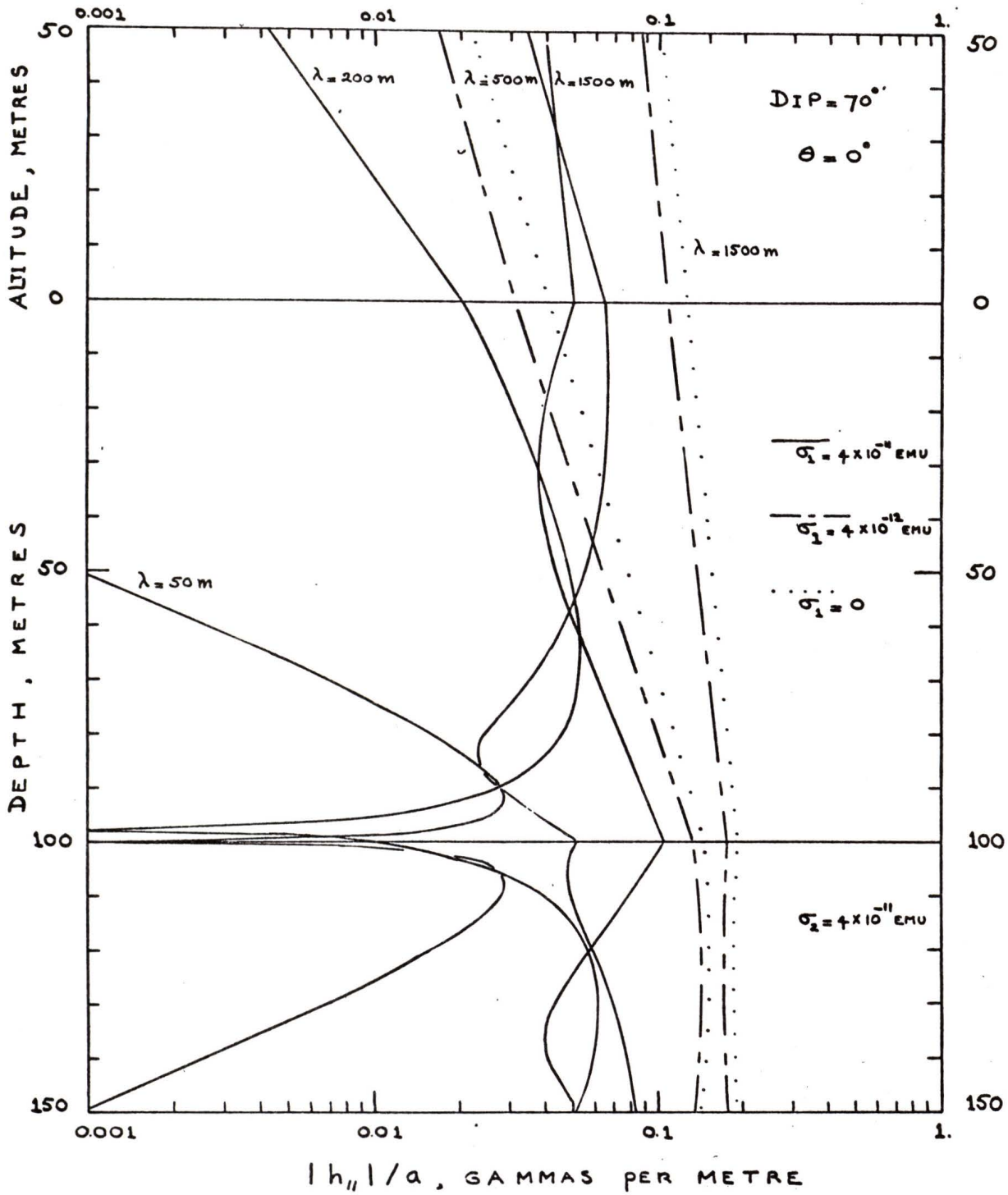

Fig. 16. The magnitude of the induced magnetic field per metre amplitude of an internal wave at a depth of 100 m, with the ocean bottom at 150 m, as a function of depth and altitude, for various wavelengths and upper layer conductivities.

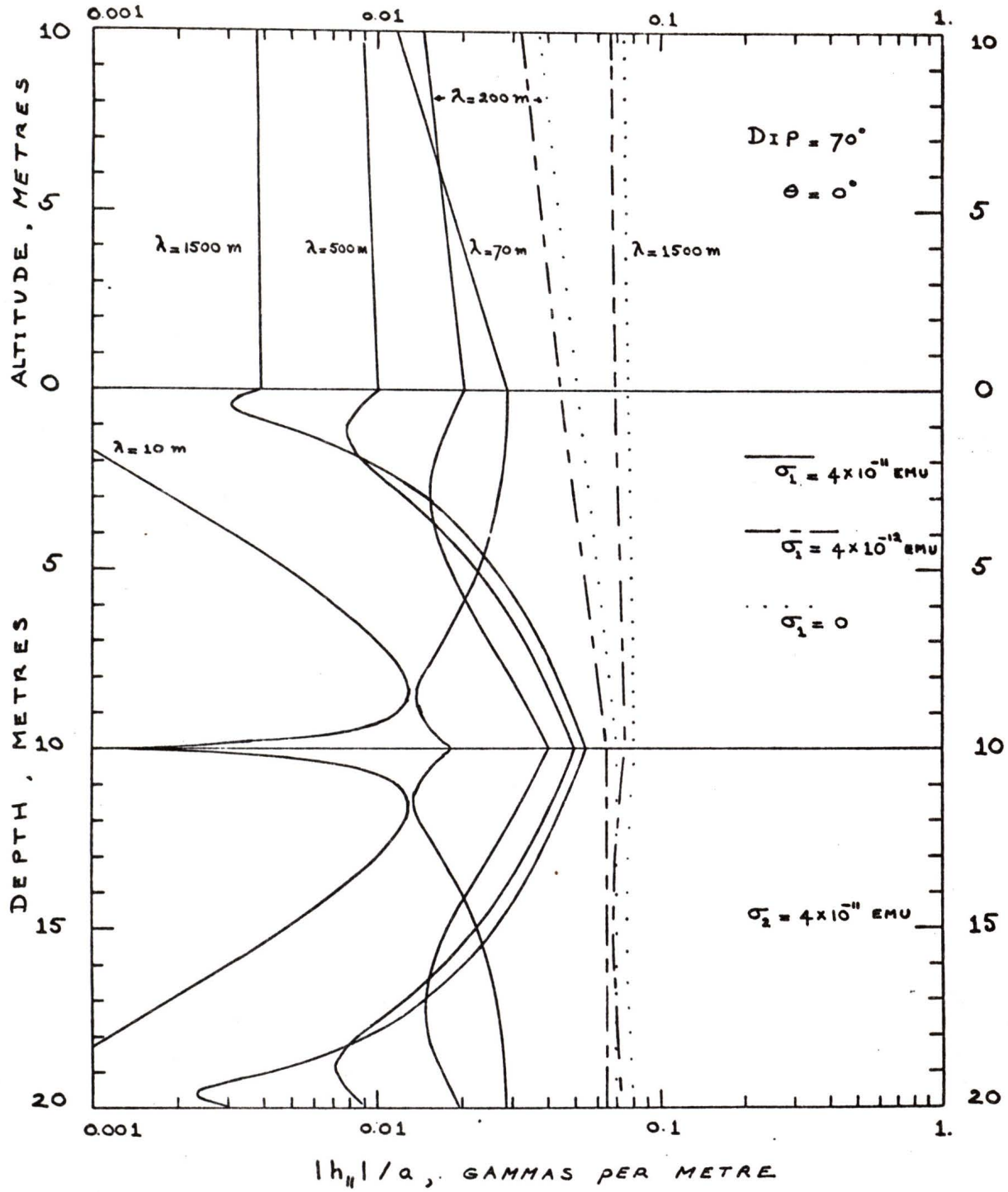

Fig. 17. The magnitude of the induced magnetic field per metre amplitude of an internal wave at a depth of 10 m, with the ocean bottom at 20 m, as a function of depth and altitude, for various wavelengths and upper layer conductivities.

5.5 Conclusions

It has been found that the magnitude of the magnetic field induced by internal ocean waves is, in general, less than that induced by surface waves. However, we have seen that for moderate periods and amplitudes of the order of 4 min and 2 m respectively the internal wave-motion can induce fields in the general neighbourhood of 0.1 γ. Fields of this magnitude can be detected by both airborne and submerged magnetometers but it seems that no such measurements have yet been reported in the literature. Because the predicted fields are of small magnitude, it is probably not worth while investigating more sophisticated ocean models (e.g. with continuously varying density) at this time.

In addition, it has been found that when the upper layer conductivity is one tenth that of the lower layer the electromagnetic screening effect of the upper layer is diminished to such an extent that it behaves almost as an insulator.

Finally, a Fortran computer programme has been written which will compute the magnetic field induced by an internal wave for a two-layer sea of any depth, conducting and density. With slight modification this programme could also compute the field induced by surface waves on a sea of any depth.

REFERENCES

Armstrong, F.A.J., and LaFond, E.C. 1966. Limnol. Oceanog. 11, 538.

Baker, R., and Graefe, P.W.U. 1968. Ocean wave profile and spectra measurement using an airborne magnetometer, Symposium on remote sensing of environment, 5th, University of Mich., Ann Arbor.

Ball, K. 1964. J. Fluid Mech. 19, 465.

Chindonova, Y.G., and Shulepov, V.A. 1965. Oceanology, 5, 78.

Cox, C.S., and Sandstrom, H. 1962. J. Ocean. Soc. Japan, 20th Ann. 449.

Cox, C.S., Filloux, J.H., and Larsen, J.C. 1970. The Sea, Vol. IV, to be published by Interscience Publishers, New York.

Crews, A., and Futterman, J. 1962. J. Geophys. Res. 67, 299.

Davis, P.A., and Patterson, A.M. 1956. The creation and propagation of internal waves a literature survey, PNL Report 56-2, Defence Research Establishment, Pacific, Victoria, British Columbia.

Ekman, V.W. 1904. Sci. Results, Norwegian North Polar Exp., 1893-1896, 5 (15).

Ewing, G.C. 1950. J. Marine Res. 9, 161.

Fairbridge, R.W. 1966, editor. The Encyclopedia of Oceanography. Reinhold Publishing Corporation, New York.

Fedosenko, V.S., and Cherkesov, L.V. 1969. Izvestiya, Atmospheric and Oceanic Physics, 4 (11), 1197.

Fraser, D.C. 1966. Geophys. J.R. Astr. Soc. 11, 507.

Gaul, R.D. 1961. J. Geophys. Res. 66, 3821.

Helland-Hansen, B. 1930. Michael Sars North Atlantic Deep-Sea Exped., 1910, Rept. Sci. Results, 1.

Hudimac, A.A. 1961. J. Fluid Mech. 11, 229.

Hutchins, R.M. 1952, Editor. Great Books of the Western World, Vol. 45, Encyclopedia Britannica, Inc., London, 286.

Kenyon, K.E. 1968. J. Marine Res. 26, 208.

Kinsman, B, 1965. Wind Waves. Prentice-Hall, Inc., New Jersey.

Knudsen, M. 1963. In American Institute of Physics Handbook, 2nd edition, edited by D.E. Gray, McGraw-Hill Book Co., Inc., Toronto, section 2, 126.

Krauss, W. 1959. Rapports et Proces-Verbaux des Reunions, 149.

LaFond, E.C. 1963. Limnol. Oceanog. 8, 417.

LaFond, E.C. 1966. In The Sea, Vol. I, edited by M.N. Hill, second printing, Interscience Publishers, New York, Chap. 22 (Part I).

Lamb, H. 1932. Hydrodynamics, 6th edition. Cambridge University Press, New York.

Larsen, J.C. 1966. Electric and magnetic fields induced by oceanic tidal motion. Ph. D. Thesis, University of California, San Diego, California.

Larsen, J.C. 1970. The electromagnetic field of long and intermediate water waves, submitted to J. Marine Res.

Long, R.R. 1953. Tellus, 5, 42.

Long, R.R. 1954. Tellus, 6, 97.

Long, R.R. 1955. Tellus, 7, 342.

Longuet-Higgins, M.S., Stern, M.E., and Stommel, H. 1954. The electrical field induced by ocean currents and waves, with application to the method of towed electrodes, Papers Phys. Oceanog. Meterorol., M.I.T. and Woods Hole Oceanog. Inst. 13, no. 1.

Maclure, K.C.,Hafer, R.A., and Weaver, J.T. 1964. Nature, 204, 1290.

Metcalf, W.G., Voorhis, A.D., and Stalcup, M.C. 1962. J. Geophys. Res. 67, 2499.

Miles, J.W. 1961. J. Fluid Mech. 10, 496.

Miles, J.W. 1963. J. Fluid Mech. 16, 209.

Milne-Thomson, L.M. 1968. Theoretical Hydrodynamics, 5th edition. MacMillan & Co. Ltd., London.

Munk, W.H., and Anderson, E.R. 1948. J. Marine Res. 7, 276.

Parker, C.A. 1968. Effect of a cold-air outbreak on the continental shelf water of the northwestern Gulf of Mexico, Texas, Agricultural and Mechanical University, College Station, Department of Oceanography, Reference 68-3T.

Perry, R.B., and Schimke, G.R. 1965. J. Geophys. Res. 70, 2319.

Phillips, O.M. 1966. The Dynamics of the Upper Ocean. Cambridge University Press, New York.

Pickard, G.L. 1954. Internal waves. Oceanography of British Columbia. Mainland inlets III, Reprint from Progress Reports of the Pacific Stations of the Fisheries Research Board of Canada, issue no. 98, 13.

Pickard, G.L. 1961. J. Fisheries Research Board of Canada, 18, (6), 907.

Proudman, J. 1953. Dynamical Oceanography. Methuen, Dover Publications Inc., New York.

Rainer, R., Munk, W., and Isaacs, J. 1967. Deep-Sea Res. 14, 117.

Rattray, M. 1960. Tellus, 12, 54.

Shand, J.A. 1953. Trans. Amer. Geophys. Union, 34, 849.

Sandstrom, H. 1966. The importance of topography in generation and propagation of internal waves. Ph. D. Thesis, University of California, San Diego, California.

Summers, H.J., and Emery, K.O. 1963. J. Geophys. Res. 68, 827.

Sverdrup, H.V., Johnson, M.W., and Fleming, R.H. 1942. The Oceans. Prentice-Hall, Inc., New Jersey.

Sverdrup, H.V., and Munk, W.H. 1947. Wind, sea and swell; theory of relations for forecasting, H.O. Publ. 601, U.S. Navy Hydorg. Off.

Tait, R.I., and Howe, M.R. 1968. Deep-Sea Res. 15, 275.

Thomas, B.D., Thomson, T.G., and Utterback, C.L. 1963. In American Institute of Physics Handbook, 2nd edition, edited by D.E. Gray, McGraw-Hill Book Co., Inc., Toronto, section 2, 126.

Thorpe, S.A. 1966. J. Fluid Mech. 24, 737.

Ufford, C.W. 1947. Trans. Amer. Geophys. Union, 28, 87.

Valdez, V. 1960. Deep-Sea Res. 7, 148.

Voorhis, A.D., and Perkins, H.T. 1966. Deep-Sea Res. 13, 641.

Warburton, F., and Caminiti, R. 1964. J. Geophys. Res. 69, 4311.

Weaver, J.T. 1965. J. Geophys. Res. 70, 1921.

Weaver, J.T. 1966. A note on the possibility of detecting the magnetic signal associated with internal waves, PNL Report 66-4, Defence Research Establishment, Pacific, Victoria, British Columbia.

Weaver, J.T. June 11, 1969. Magnetic signals associated with ocean swell, paper presented at SACLANT ASW Research Centre, La Spezia, Italy.

Weaver, J.T. and Woods, R.G. 1965. The electromagnetic field of a pressure impulse in a conducting fluid, PNL Report 65-7, Defence Research Establishment, Pacific, Victoria, British Columbia.

Wehausen, J.V., and Laitone, E.V. 1960. In Handbuch der Physik, Vol. IX, edited by S. Flügge, Springer-Verlag, Berlin, Fluid dynamics III, 446.

Weigan, J.G., Farmer, H.G. Prinsenberg, S.J., and Rattray, M., Jr. 1969. J. Marine Res. 27, 241.

Woods, R.G. 1965. Magnetic variations associated with ocean waves and swell in a shallow sea, PNL Report 65-6, Defence Research Establishment, Pacific, Victoria, British Columbia.

Wynn, M.J. 1967. The measurement of magnetic fields produced by ocean waves in three fathoms of water, U.S. Navy Symposium on Military Oceanography, 4th.

Yih, C-S. 1960. J. Fluid Mech. 8, 481.

Zalkan, R.L. 1969. J. Geophys. Res. 74, 3434.

Zeilon, N. 1913. Svensk, Hydr. Biol. Komm. Skr. 5.

Zeilon, N. 1934. Goteborgs Vetensk. Samh. Handl., Folj 5, Ser. B. 3 (10).

APPENDIX A.

THE COMPUTER PROGRAM FOR THE MAGNETIC FIELD INDUCED BY AN INTERNAL WAVE IN A TWO-LAYER OCEAN OF FINITE DEPTH.

```
      REAL*8 DISA, DISU, DISL
      REAL*8 ONE
      REAL*8  AB,AB2,EU2,EL2,TL,TF,UO,THETA,DENOL
     1,ELZ,ELZ2
      REAL*8 G,PI,ALPHA,DENSLO,DENSUP,M,LAMDA,L,D,MLD,MD,AO,BO,
     1ABA,ABB,P,ALM,FREQ,PERIOD,FL,EU,EL,EF,CONDU,CONDL,CONDF,
     2EF2,SEU,SEL,SEF,SUP,SUM,SLP,SLM,SFP,SFM,TU2,TL2,F,TF2,TU,
     3LD,Q11,Q12,Q21,Q32,Q52,UUL,FFL,Q31,Q41,Q51,Q61,DEG,RI,I,
     4RTHETA,C,S,MD2,ML2,MLD2,ED2,EL2,ELD2,DELD,DENOD,A,MZ,MZ2,
     5MLZ,MLZ2,MDZA,MDZU,MZDL,ZAIR,ZUPPER,ZLOWER,ZFLOOR,EZ,EZ2
     6 ,EDZA,EDZU,EZDL,LAM(12),ZO,AMF
      REAL*8 HXA(30,12), HZA(30,12), HPA(30,12),
     1 HXU(40,12), HZU(40,12),HPU(40,12),
     2  HXL(50,12),HPL(50,12),   HZL(50,12),
     3 HXF(2,12),HZF(2,12), HPF(2,12)
      REAL*8 ZA(30),ZUP(40),ZLOW(50),ZFLO(2)
      REAL*8 FREQ(12),PER(12)
      COMPLEX*16 ELLD2,NUPP,BR555,LT111,CISP,HXFLOR
      COMPLEX*16 NU,NL,NF,NUM,NLM,NFM,QU,QL,QF,Q1,Q2,Q3,Q4,Q5,Q6,
     1NLLDM,NLLDP,NLLD2,NUDP,NUDM,NUD2,NLLDNU,NLUD2 ,ELLDM,ELLDP,
     2EUDP,EUDM,EUD2,ELLDNU,ELUD2,BRI,BRII,TRIANG,IS,PNUP,PNUM,
     3NUPM,V1,V2,V5,V6,GAM1,GAM2,GAM3,GAM4,BR111,BR222,BR333,BR444
     4,BR666,BR777,BR888,BR999,R11,BR822,HOO,RO,HOOO,ST111,ST222,
     5LT222,IAMF,NUDZ,NUZ,NLLZ,NLZD,NFZ,EUDZ,EUZ,ELLZ,ELZD,EFZ,
     6CISM,VUZ,VPUZ,VLZ,VPLZ,HXAIR,HZAIR,HXUP,HZUP,HXLOW,HZLOW,
     7HZFLOR,HPAIR,HPUP,HPLOW,HPFLOR

      MUST READ IN THE FOLLOWING DATA.
      DENSITY,GRAMS/CUBIC CM.
      DEPTHS,AMPLITUDE,WAVELENGTHS,CM.
      DIP AND DECLINATION ANGLES,DEGREES.
      CONDUCTIVITY OF WATER,E.M.U.
      EARTH'S MAGNETIC FIELD, GAUSS.
      FIELD POINTS, CM.
      READ(5,100) (LAM(J),J=1,12)
111   READ(5,101) DENSUP,DENSLO
      IF(DENSUP.EQ.0.0.AND.DENSLO.EQ.0.0) CALL EXIT
      READ(5,102) I,THETA
      READ(5,103) CONDU,CONDL,CONDF,F
      READ(5,104) A,L,D

      READ(5,108) ZA(1), DISA,N1
      READ(5,108) ZUP(1), DISU, N2
      READ(5,108) ZLOW(1), DISL, N3
```

```
      READ(5,109) ZFLO(1), ZFLO(2)
  108 FORMAT( 2F20.0,I10)
  109 FORMAT(2F2 .0)
      N11= N1-1
      N22= N2-1
      N33= N3-1
      DO 26 J1=1,N11
      ZA(J1+1)=ZA(J1)+DISA
   26 CONTINUE
      DO 27 J2=1,N22
      ZUP(J2+1)=ZUP(J2)+DISU
   27 CONTINUE
      DO 28 J3=1,N33
      ZLOW(J3+1)=ZLOW(J3)+DISL
   28 CONTINUE
  100 FORMAT(8F10.0)
  101 FORMAT(2F20.0)
  102 FORMAT(2F20.0)
  103 FORMAT(3E10.3,F20.0)
  104 FORMAT(3F20.0)

      WRITE(6,200) DENSUP,DENSLO,I,THETA,CONDU,CONDL,CONDF,A,D,L,F

      DO 999 J=1,12
      LAMDA=LAM(J)

      FIND THE FREQUENCY,GIVEN DENSITY ANDDEPTHS AND WAVELENGTH.

      NOTE, G IS IN CM. PER SECOND PER SECOND.

      G=980.00
      ONE=1.000
      ZO=0.00
      PI=3.1415926535898
      ALPHA=DENSLO/DENSUP
      M=(2.00*PI)/LAMDA

      MLD=M*(L-D)
      MD=M*D

      AO=1.00
      BO=1.00
      IF(MLD.LT.17.0) AO=DTANH(MLD)
      IF(MD.LT.17.0) BO=DTANH(MD)

      AB=ALPHA*(AO+BO)
      AB2=AB*AB
      ABA=ALPHA+AO*BO
      ABB=4.00*AO*BO*ABA*(ALPHA-1.00)

      P=(AB-DSQRT(AB2-ABB))/(2.00*ABA)

      ALM=ALPHA-1.00
      IF(MLD.GE.17.0) P=(ALM*BO)/(ALPHA+BO)
      IF(MD.GE.17.0) P=(ALM*AO)/(ALPHA+AO)

      COMPUTE FREQUENCY AND THE PERIOD.
```

```
      FREQ(J)=( DSQRT(G*M*P))/(2.00*PI)
      PER(J)= 1.00/FREQ(J)

      COMPUTE NU,NL,AND NF.

      FL=2.00*FREQ(J)*LAMDA*LAMDA
      EU=FL*CONDU
      EL=FL*CONDL
      EF=FL*CONDF

      EU2=EU*EU
      EL2=EL*EL
      EF2=EF*EF

      SEU=DSQRT(1.00+EU2)
      SEL=DSQRT(1.00+EL2)
      SEF=DSQRT(1.00+EF2)

      SUP=DSQRT(0.500*(SEU+1.00))
      SUM=DSQRT(0.500*(SEU-1.00))
      SLP=DSQRT(0.500*(SEL+1.00))
      SLM=DSQRT(0.500*(SEL-1.00))
      SFP=DSQRT(0.500*(SEF+1.00))
      SFM=DSQRT(0.500*(SEF-1.00))

      NU=DCMPLX(SUP,SUM)
      NL=DCMPLX(SLP,SLM)
      NF=DCMPLX(SFP,SFM)

      NUM=NU-1.00
      NLM=NL-1.00
      NFM=NF-1.00

      FIND Q1,Q2,Q3,Q4,Q5,Q6.

      QU=1.00/NU
      QL=NU/NL
      QF=NF/NL

      Q1=0.500*(1.00+QU)
      Q2=0.500*(1.00-QU)
      Q3=0.500*(1.00+QL)
      Q4=0.500*(1.00-QL)
      Q5=0.500*(1.00-QF)
      Q6=0.500*(1.00+QF)

      APPROXIMATE FORM OF NU,NL, AND NF.
      TU2=EU2/8.00
      TL2=EL2/8.00
      TF2=EF2/8.00
      TU=EU/2.00
      TL=EL/2.00
      TF=EF/2.00

      IF(EU2.GE.1.0D-5) GO TO 10
      NU=DCMPLX(1.00+TU2,TU)
      NUM=DCMPLX(TU2,TU)
   10 IF(EL2.GE.1.0D-5) GO TO 11
```

```
      NL=DCMPLX(1.00+TL2,TL)
      NLM=DCMPLX(TL2,TL)
   11 IF(TF2.GE.1.0D-5) GO TO 12
      NF=DCMPLX(1.00+TF2,TF)
      NFM=DCMPLX(TF2,TF)

   12 CONTINUE

      APPROXIMATE FORM OF THE Q'S.

      IF(EU2.GE.1.0D-5.AND.EL2.GE.1.0D-5) GO TO 13
      UD=1.00+EU2/2.00
      LD=1.00+EL2/2.00

      Q11=(1.00+(5.00/16.00)*EU2)/UD
      Q12=(0.250*EU)/UD
      Q21=(3.00*EU2)/(16.00*UD)
      Q32=0.250*EL*(CONDU-CONDL)/LD
      Q52=0.250*EL*(CONDF-CONDL)/LD
      UUL=EU*(0.500*EU+EL)
      FFL=EF*(0.500*EF+EL)
      Q31=(1.00+0.125*(2.50*EL2+UUL))/LD
      Q41=0.125*(1.50*EL2-UUL)/LD
      Q51=0.125*(1.50*EL2-FFL)/LD
      Q61=(1.00+0.125*(2.50*EL2+FFL))/LD

      Q1=DCMPLX(Q11,(-Q12))
      Q2=DCMPLX(Q21,Q12)
      Q3=DCMPLX(Q31,Q32)
      Q4=DCMPLX(Q41,(-Q32))
      Q5=DCMPLX(Q51,(-Q52))
      Q6=DCMPLX(Q61,Q52)

   13 CONTINUE
      IF(CONDU.EQ.CONDL) Q3=DCMPLX(ONE,ZO)
      IF(CONDU.EQ.CONDL) Q4=DCMPLX(ZO,ZO)
      IF(CONDF.EQ.CONDL) Q5=DCMPLX(ZO,ZO)
      IF(CONDF.EQ.CONDL) Q6=DCMPLX(ONE,ZO)

      COMPUTE  C AND  S.
      READ IN I AND THETA IN DEGREES.
      MUST CONVERT TO RADIANS.

      DEG=0.01745329252
      RI=DEG*I
      RTHETA=DEG*THETA
      C=DCOS(RI)*DCOS(RTHETA)
      S=DSIN(RI)
      IF(I.EQ.90.0.OR.THETA.EQ.90.0) C=0.00

      NLLDM=MLD*NLM
      NLLDP=MLD*(NL+1.00)
      NLLD2=2.00*NL*MLD

      NUDP=MD*(NU+1.00)
      NUDM=MD*NUM
      NUD2=2.00*MD*NU
      NLLDNU=M*((NL+1.00)*(L-D)+2.00*NU*D)
```

```
      NLUD2=2.00*M*(NL*(L-D)+NU*D)

      MD2=2.00*MD
      ML2=2.00*M*L
      MLD2=2.00*MLD

      ELLDM  =DCMPLX(ZO,ZO)
      ELLDP  =DCMPLX(ZO,ZO)
      ELLD2  =DCMPLX(ZO,ZO)
      EUDP   =DCMPLX(ZO,ZO)
      EUDM   =DCMPLX(ZO,ZO)
      EUD2   =DCMPLX(ZO,ZO)
      ELLDNU =DCMPLX(ZO,ZO)
      ELUD2  =DCMPLX(ZO,ZO)

      ED2=0.00
      EL2=0.00
      ELD2=0.00

      IF(REAL(NLLDM).LE.145.0) ELLDM=CDEXP(-NLLDM)
      IF(REAL(NLLDP).LE.145.0) ELLDP=CDEXP(-NLLDP)
      IF(REAL(NLLD2).LE.145.0) ELLD2=CDEXP(-NLLD2)
      IF(REAL(NUDP).LE.145.0) EUDP=CDEXP(-NUDP)
      IF(REAL(NUDM).LE.145.0) EUDM=CDEXP(-NUDM)
      IF(REAL(NUD2).LE.145.0) EUD2=CDEXP(-NUD2)
      IF(REAL(NLLDNU).LE.145.0) ELLDNU=CDEXP(-NLLDNU)
      IF(REAL(NLUD2).LE.145.0) ELUD2=CDEXP(-NLUD2)
      IF(MD2.LE.145.0) ED2=DEXP(-MD2)
      IF(ML2.LE.145.0) EL2=DEXP(-ML2)
      IF(MLD2.LE.145.0) ELD2= DEXP(-MLD2)

      COMPUTE TRIANG.
      FIRST FIND (I) AND (II).

      BRI=Q3*Q1+Q4*Q2*EUD2
      BRII=Q4*Q1+Q3*Q2*EUD2
      IF(REAL(Q4).EQ.0.0.AND.AIMAG(Q4).EQ.0.0) GO TO 14
      TRIANG=Q5*BRII*ELLD2-Q6*BRI
      GO TO 15
   14 TRIANG=Q5*Q3*Q2*ELUD2-Q6*BRI
   15 CONTINUE

      FIND DELTA SUB ZERO.

      DELO=((P-1.00)+(P+1.00)*EL2)/((P-1.00)+(P+1.00)*ED2)
      COMPUTE THE DENOMINATORS.

      DENOD=(P-1.00)+(P+1.00)*ED2
      DENOL=1.00-ELD2

      COMPUTE V1,V2,V5 AND V6.

      IS=DCMPLX(ZO ,S)
      PNUP=P*NU+1.00
      PNUM=P*NU-1.00
      NUPP=NU+P
      NUPM=NU-P
```

```
V1=(C*PNUM-IS*NUPM)/(NU*DENOD)
V2=(C*PNUP-IS*NUPP)/(NU*DENOD)
V5=(C+IS*NL)/(NL*DENOL)
V6=(C-IS*NL)/(NL*DENOL)

DEFINE GAMMA 1,2,3 AND 4.

GAM1=Q4*V6+Q3*V5
GAM2=Q1*V2-Q2*V1
GAM3=Q3*V6+Q4*V5
GAM4=(Q5*V6+Q6*V5)*ELLDP-Q6*V5*DELO

COMPUTE THE NINE BRACKETS.

BR111=Q2*(DELO*GAM1-ELLDP*Q3*V5)
BR222=Q1*(DELO*GAM3-ELLDP*Q4*V5)
BR333=DELO*Q1*V6+Q3*GAM2*EUDP
BR444=Q6*Q4*GAM2*EUDP+Q1*GAM4
BR555=DELO*Q2*V6*EUDM-Q4*GAM2
BR666=Q2*GAM4*EUDM-Q6*Q3*GAM2
BR777=Q3*V6*(Q1*Q6*DELO-Q5*Q2*ELLDNU)-Q1*Q4*GAM4
BR888=(NU/NL)*GAM2+BR111*EUDM
BR999=DELO*(Q1*GAM3+Q2*GAM1*EUD2)+(NU/NL)*GAM2*EUDP

COMPUTE R11 AND BRACKET R22.

R11=Q5*(Q4*V1+Q3*V2*EUD2+DELO*V6*EUDM)
BRR22=Q6*(Q3*V1+Q4*V2*EUD2)+GAM4*EUDM
COMPUTE HOO.
HOO=BR888*EUDP+BR222

COMPUTE THE PRINCIPAL CONSTANTS.

RO=(R11*ELLD2-BRR22)/TRIANG
HOOO=(HOO*ELLDM-BR1*V6)/TRIANG
ST111=(Q5*BR333*ELLD2-BR444)/TRIANG
ST222=(Q5*BR555*ELLD2-BR666)/TRIANG

LT111=(Q5*BR999*ELLDM-BR1*(Q5*V6+Q6*V5))/TRIANG
LT222=(Q6*BR888*EUDP+BR777)/TRIANG

AMF=A*M*F
IAMF=DCMPLX(ZO, AMF)
CISP=DCMPLX(C,S)
CISM=DCMPLX(C,(-S))

DEFINE.

FIND MAGNETIC FIELD AMPLITUDES.
CHANGE THE ABSOLUTE VALUES TO GAMMAS


IN AIR.

DO 888 J1=1,N1
ZAIR=ZA(J1)
MDZA=M*(D-ZAIR)
EDZA=C.00
```

```
      IF(MDZA.LE.145.0) EDZA=DEXP(-MDZA)
      HXAIR=IAMF*RO*EDZA
      HZAIR=(-AMF)*RO*EDZA
      HPAIR=HXAIR*C+HZAIR*S
      HXA(J1,J)=CDABS(HXAIR) *(1.0D+5)
      HZA(J1,J)=CDABS(HZAIR)  *(1.0D+5)
      HPA(J1,J)=CDABS(HPAIR) *(1.0D+5)
  888 CONTINUE


      IN THE UPPER OCEAN LAYER.

      DO 777 J2=1,N2
      ZUPPER=ZUP(J2)
      MZ=M*ZUPPER
      MZ2=2.00*M*ZUPPER
      MDZU=M*(D-ZUPPER)
      NUDZ=NUM*MDZU
      NUZ=(NU+1.00)*MZ
      EZ=0.00
      EZ2=0.00
      EDZU=0.00
      EUDZ    =DCMPLX(Z0,Z0)
      EUZ     =DCMPLX(Z0,Z0)
      IF(MZ.LE.145.0) EZ=DEXP(-MZ)
      IF(MZ2.LE.145.0) EZ2=DEXP(-MZ2)
      IF(MDZU.LE.145.0) EDZU=DEXP(-MDZU)
      IF(REAL(NUDZ).LE.145.0)EUDZ=CDEXP(-NUDZ)
      IF(REAL(NUZ).LE.145.0) EUZ=CDEXP(-NUZ)
      VUZ=((1.00-P)*CISP-(1.00+P)*CISM*EZ2)/DENOD
      VPUZ=((1.00-P)*CISP+(1.00+P)*CISM*EZ2)/DENOD
      HXUP=IAMF*(NU*(ST111*EUDZ-ST222*EUZ)-VPUZ)*EDZU
      HZUP=(-AMF)*(ST111*EUDZ+ST222*EUZ-VUZ)*EDZU
      HPUP=HXUP*C+HZUP*S
      HXU(J2,J)=CDABS(HXUP) *(1.0D+5)
      HZU(J2,J)=CDABS(HZUP)  *(1.0D+5)
      HPU(J2,J)=CDABS(HPUP)  *(1.0D+5)
  777 CONTINUE


      IN THE LOWER OCEAN LAYER.

      DO 666 J3=1,N3
      ZLOWER=ZLOW(J3)
      MLZ=M*(L-ZLOWER)
      MLZ2=2.00*MLZ
      MZDL=M*(ZLOWER-D)
      NLLZ=(NL+1.00)*MLZ
      NLZD=NLM*MZDL
      ELZ=0.00
      ELZ2=0.00
      EZDL=0.00
      ELLZ    =DCMPLX(Z0,Z0)
      ELZD    =DCMPLX(Z0,Z0)
      IF(MLZ.LE.145.0) ELZ=DEXP(-MLZ)
      IF(MLZ2.LE.145.0) ELZ2=DEXP(-MLZ2)
      IF(MZDL.LE.145.0) EZDL=DEXP(-MZDL)
      IF(REAL(NLLZ).LE.145.0) ELLZ=CDEXP(-NLLZ)
```

```
      IF(REAL(NLZD).LE.145.0) ELZD=CDEXP(-NLZD)
      VLZ=(CISM-CISP*ELZ2)/DENOL
      VPLZ=(CISM+CISP*ELZ2)/DENOL
      HXLOW=IAMF*(NL*(LT111*ELLZ-LT222*ELZD)-VPLZ)*EZDL
      HZLOW=(-AMF)*(LT111*ELLZ+LT222*ELZD+VLZ)*EZDL
      HPLOW=HXLOW*C+HZLOW*S
      HXL(J3,J)=CDABS(HXLOW) *(1.0D+5)
      HZL(J3,J)=CDABS(HZLOW) *(1.0D+5)
      HPL(J3,J)=CDABS(HPLOW) *(1.0D+5)
666   CONTINUE

      IN THE OCEAN FLOOR.

      DO 555 J4=1,2
      ZFLOOR=ZFLO(J4)
      NFZ=(NF*(ZFLOOR-L)+(1-D))*M
      EFZ    =DCMPLX(Z0,Z0)
      IF(REAL(NFZ).LE.145.0) EFZ=CDEXP(-NFZ)
      HXFLOR=(-IAMF)*NF*HOOO*EFZ
      HZFLOR=(-AMF)*HOOO*EFZ
      HPFLOR=HXFLOR*C+HZFLOR*S
      HXF(J4,J)=CDABS(HXFLOR) *(1.0D+5)
      HZF(J4,J)=CDABS(HZFLOR)  *(1.0D+5)
      HPF(J4,J)=CDABS(HPFLOR)   *(1.0D+5)
555   CONTINUE

999   CONTINUE

      PRINT THE OUTPUT.

      WRITE(6,210)
      WRITE(6,211)  (LAM(J), J=1,12 )
      WRITE(6,212)  (ZA(J1),(HXA(J1,J),J=1,12),J1=1,N1)
      WRITE(6,212)  (ZUP(J2),(HXU(J2,J),J=1,12),J2=1,N2)
      WRITE(6,212)  (ZLOW(J3),(HXL(J3,J),J=1,12),J3=1,N3)
      WRITE(6,212)  (ZFLO(J4),(HXF(J4,J),J=1,12),J4=1,2)
      WRITE(6,213)  ( PER(J), J=1,12)
      WRITE(6,214)  ( FREQ(J), J=1,12)

      WRITE(6,215)
      WRITE(6,211)  (LAM(J), J=1,12 )
      WRITE(6,212)  (ZA(J1),(HZA(J1,J),J=1,12),J1=1,N1)
      WRITE(6,212)  (ZUP(J2),(HZU(J2,J),J=1,12),J2=1,N2)
      WRITE(6,212)  (ZLOW(J3),(HZL(J3,J),J=1,12),J3=1,N3)
      WRITE(6,212)  (ZFLO(J4),(HZF(J4,J),J=1,12),J4=1,2)
      WRITE(6,213)  ( PER(J), J=1,12)
      WRITE(6,214)  ( FREQ(J), J=1,12)

      WRITE(6,216)
      WRITE(6,211)  (LAM(J), J=1,12 )
      WRITE(6,212)  (ZA(J1),(HPA(J1,J),J=1,12),J1=1,N1)
      WRITE(6,212)  (ZUP(J2),(HPU(J2,J),J=1,12),J2=1,N2)
      WRITE(6,212)  (ZLOW(J3),(HPL(J3,J),J=1,12),J3=1,N3)
      WRITE(6,212)  (ZFLO(J4),(HPF(J4,J),J=1,12),J4=1,2)
      WRITE(6,213)  ( PER(J), J=1,12)
      WRITE(6,214)  ( FREQ(J), J=1,12)

      READ MORE DATA CARDS.
```

```
      GO TO 111
      FORMAT STATEMENTS.
  200 FORMAT('1',45X,'THE  INPUT  PARAMETERS',///
     1//' THE UPPER DENSITY =',F15.3,' GRAMS/CUBIC CM.
     2///' THE LOWER DENSITY =',F15.3,' GRAMS/CUBIC CM.
     3//////' THE DIP ANGLE =',F15.3,' DEGREES.'
     4//' THE DECLINATION ANGLE =',F15.3,' DEGREES.'
     5/////' THE CONDUCTIVITY OF UPPER LAYER=',1PE15.2,' EMU'
     6//' THE CONDUCTIVITY OF LOWER LAYER =',1PE15.2,'EMU'
     7//' THE CONDUCTIVITY OF OCEAN FLOOR=',1PE15.2,'EMU'
     8/////' THE AMPLITUDE OF INTERNAL WAVE=',0PF15.0,'CM'
     9//' THE DEPTH OF UPPER LAYER =',0PF15.0,'CM'
     1//' THE DEPTH OF THE OCEAN FLOOR =',0PF15.0,'CM'
     2/////' THE MAGNITUDE OF EARTHS FIELD=',0PF15.3,'GAUSS')
  210 FORMAT('1',' THE ABSOLUTE VALUE OF THE HORIZONTAL,X,',
     1'COMPONENT OF MAGNETIC FIELD AMPLITUDE,IN GAMMA:'///)
  211 FORMAT(' WAVE'/' LENGTH   ', 0P12F10.0/' IN CM.'//
     1' POSITION'/' IN CM.'//)
  212 FORMAT(' ',0PF9.0,1P12E10.3)
  213 FORMAT(///' PERIOD   ',0P12F10.1/' IN SEC.'/ )
  214 FORMAT(' FREQUENCY', 0P12F10.5/' IN HZ.')
  215 FORMAT('1',' THE ABSOLUTE VALUE OF THE VERTICAL,Z,',
     1'COMPONENT OF MAGNETIC FIELD AMPLITUDE,GAMMA:'///)
  216 FORMAT('1',' THE ABSOLUTE VALUE OF THE COMPONENT',
     1' OF THE MAGNETIC FIELD AMPLITUDE THAT IS ALIGNED',
     2' ALONG THE '/'   DIRECTION OF THE EARTHS MAGNETIC FIELD',
     3' VECTOR F, IN GAMMA:'///)

      END
```

Surname: BEAL Given Name: HUBERTUS THEODORUS

Place of Birth: LEIDEN, HOLLAND Date of Birth: November 22, 1944

Educational Institutions Attended, with Dates of Entering and Leaving:

UNIVERSITY OF VICTORIA, VICTORIA, CANADA 1964 to 1968

Degrees, Diplomas, Etc., Awarded, with Dates and Names of Institutions:

B.Sc. (Honours) 1968 University of Victoria, Victoria, Canada

Honours and Awards:

N.R.C. Grant, 1968/1969

Publications:

THE UNIVERSITY OF VICTORIA LIBRARY

MANUSCRIPT DISSERTATION (or THESIS)

AUTHORITY TO DISTRIBUTE

AUTHOR: This dissertation may be lent or microfilm copies made available:

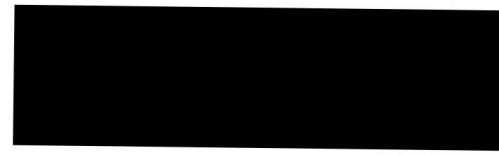

(a) Without restriction

(b) With the restriction that, for a period of five years (until)the written approval of the following is required:

(1) The Chairman, School of Graduate Studies .....

(2) The Author .....

(3) both the Chairman, School of Graduate Studies, and the Author .....

BORROWERS: The borrower undertakes, by signing below, to give proper credit for any use made of the dissertation, and to obtain the consent of the author if it is proposed to make extensive quotations, or to reproduce the dissertation in whole or in part.

Signature of Borrower	Address	Date